THE UNIVERSITY OF CHICAGO

ASSOCIATION OF METABOLIC IMPROVEMENTS FOLLOWING SLEEVE GASTRECTOMY WITH CIRCADIAN RHYTHM ALTERATIONS

A DISSERTATION SUBMITTED TO

THE FACULTY OF THE DIVISION OF THE BIOLOGICAL SCIENCES

AND THE PRITZKER SCHOOL OF MEDICINE

IN CANDIDACY FOR THE DEGREE OF

DOCTOR OF PHILOSOPHY

COMMITTEE ON MOLECULAR METABOLISM AND NUTRITION

BY

JEREMY WHITE

CHICAGO, ILLINOIS

DECEMBER 2020

Dedication

To my advisor, Matthew, who was a source of patient guidance
in the midst of uncertainty on many fronts.
To my mother, who taught me that taking a few calming breaths can
help you scale great obstacles, in time.
To my grandmother, who was our family's bedrock and exemplar
for how to live courageously and with dignity.
To my doctors, who took care of me when was in need and
without whom I could not have continued.
To Dr. Mike, who opened my eyes to the wonders and complexities
with which physiology is fraught.
And, to my wife, whose insistent love continues to give me vigor
to become more authentic, wiser, and … better.

Acknowledgements

Advisor

Matthew Brady, PhD

Thesis Committee

Ronald Cohen, MD*

Kristen Knutson, PhD

Yun Fang, PhD

*: Committee Chair

Sleep Research Group

Eve Van Cauter, PhD

Erin Hanlon, PhD

Jennifer Lee

Harry Whitmore, RPSGT

Robert Sargis, MD, PhD

Gavin Baumgart

Wajdey Nesheiwat

Stephanie Sintetas

Diana Sanchez

Numerous W-4 RAs

Current & Past Brady Lab

Matthew Piron

Paul Volden, PhD

Christopher Carmean, PhD

Sully Fernandez, PhD

Marianna Johnson, PhD

Jordan Strober

Avelino De Leon

Isabel Casimiro, MD, PhD

Ruby Ross

Amarachi Okoli

Katiannah Moise

Kyle Kunze

Bariatric Surgeons

CMMN Students

CRC Staff

Research Funding

T32 HL 007909

R01 DK103014

P30 DK020595

Table of Contents

Table of Figures

Table of Tables

Abstract

The rate of obesity increased dramatically over the course of the last half century. In the United States, non-Hispanic black women have experienced a particularly high risk to develop obesity. The consequences of the epidemic for public health are both direct, like the increased prevalence of obstructive sleep apnea, and indirect, like the increased prevalence of diabetes and cancer. Combined, obesity significantly elevates mortality risk. To reverse these risks, bariatric surgeries like sleeve gastrectomy (SG), have been effective in yielding long-term weight loss alongside substantially improved metabolic health. Yet, the specific mechanisms and specific organs that contribute to improvements in metabolic health after post-surgery are not yet clear. Nor are the changes that stall or eventually reverse the weight loss and metabolic improvements. We have evidence that there are alterations in insulin responsiveness in subcutaneous adipose tissue at two weeks post-surgery. Therefore, we became interested in creating a more detailed picture of subcutaneous adipose tissue metabolic alterations shortly after SG. We enrolled ten women who were scheduled for SG surgery following informed written consent. Despite not having diabetes, subjects did have substantial reductions in fasting serum glucose, fasting insulin, and systemic insulin sensitivity at twelve weeks following surgery. Subjects consumed roughly one-fourth of the baseline calories per day. We show upregulation of *hDBP* expression in parallel with several other elements of adipose tissue circadian clock in association with caloric restriction. Upregulation of *hNPAS2*, appeared to be associated additionally with changes to systemic insulin sensitivity. We showed phase delay of insulin signaling genes (INSR, IRS1, PIK3.CA) and lipid regulatory gene *INSIG2*. Further, we showed down regulation in adipokine genes (*LEPTIN, ADIPOQ)* and lipolysis gene (*ATGL*), and upregulation of master transcription factor genes (*SREBP1* and *PGC1α)* and insulin pathway genes (*INSR, IRS1, GLUT4, SOCS3)*. A majority of

the changes could be explained by caloric restriction with expected declines in fasting insulin and systemic insulin sensitivity. Surgery did not associate with change to *INSIG2*, but caloric restriction and associated upregulated lipolysis were associated. These changes that: 1) the adipose peripheral clock is not phase shifted but its expression is accentuated, 2) adipose tissue metabolic genes are phase delayed and their expression reflects both fasting and improved insulin sensitivity, and 3) the changes in gene expression are tightly associated with the metabolic improvements seen in systemic metabolism. Future experiments are needed to evaluate the degree of interaction between adipose tissue metabolism and circadian clock function after sleeve gastrectomy surgery.

Chapter 1: Introduction

Overview of Obesity and Metabolic Syndrome

Obesity is a medical condition that has been defined by having an abnormally high weight to height ratio called body mass index (BMI [kg/m^2]). The traditional cut-off point for Class I obesity is a BMI of above 30. The epidemic of obesity has continued to grow despite global initiatives to curb and reverse the prevalence of obesity. At the time of the first national survey of health in the US which was reported over the years 1960-1962, the self-reported rate of obesity in adults (> 20 years) was only 13.3%. (Craig M. Hales Feb 2020) Yet, in the early part of the last decade there was a period where the rate of obesity and severe obesity plateaued at around one-third of US adults (35.7% [2009-2010] and 34.9% [2011-2012]) and around one-in-sixteen adults (6.3% and 6.4%). (Flegal et al. 2012, Ogden et al. 2014) It was considered an encouraging sign because the increase in obesity year-over-year was reduced to an apparent net-zero change. As a result, the CDC Department of Health and Human Services announced a set of initiatives called Healthy People 2020, which included the goal to further lower the rate of development of obesity into a net negative to lower the rate of obesity by 4% to 30.5% of US adults. Instead, the most recent report published by the CDC over the years 2017-2018, reported that the rate of obesity had risen markedly to 42.4% of adults. (Craig M. Hales Feb 2020) And, as has been reported previously, the epidemic is substantially less prevalence for Non-Hispanic Asian (NHA) individuals (17.4% overall) while Non-Hispanic black women (NHBW) exhibit a markedly disproportionate level of risk to have obesity (56.9%). Further, the disproportionate risks for NHA individuals and NHBW are also reflected in rates of severe obesity compared with the total US population (2.0% [NHA], 13.8% [NHBW], and 9.2% [Total]). Yet, a more troubling sign was that the groups that were associated with the increase in the rate of obesity were non-Hispanic white

individuals (NHW) (34.5% [2011-2014], 42.2% [2017-2018]) and NHA individuals (11.7% [2011-2014], 17.4% [2017-2018]), which were both disproportionately less likely to have obesity in the prior reports. As of now, US adults of all races have been associated with increasing rates of obesity. In a few additional decades, obesity has become a medically-relevant health problem for everyone.

The health consequences of obesity extend far beyond the mechanical problems associated with excess weight. Obesity is also associated with increased metabolic stress and endocrine disruption. While each effect is relatively minor in a short-term scope, the cumulative effect of the annual direct and indirect economic costs of obesity rose from $78.5 billion in 1998 to an estimated $147 billion in 2008. In 2008, that would have reflected 21% of all healthcare expenditures. (Finkelstein et al. 2009, Trogdon et al. 2008)

The indirect effects of obesity are typically attributed to low grade inflammation associated with increased metabolic stress. (Monteiro and Azevedo 2010, Herder et al. 2007) Two common presentations of the early metabolic dysfunction associated with obesity are hyperglycemia and dyslipidemia. Hyperglycemia is defined as chronic high blood sugar and is the result of insufficient ability of insulin to mediate glucose removal from the blood stream. This condition can be the result of insufficient insulin production or insufficient insulin action (insulin resistance). Type II diabetes mellitus (T2DM) is the combination of these factors such that there is a lack of compensatory hyperinsulinemia to compensate for the whole-body insulin resistance. (ADA 2010) The associated risk for T2DM increases at higher classes of obesity. For Class I Obesity (BMI: 30-35) and Class II Obesity (35-40), the risk is 2.5 times and 3.5 times higher than healthy weight individuals. (Ganz et al. 2014) Dyslipidemia is a broad medical term referring to abnormally high levels of non-HDL lipoproteins (hyperlipidemia) or high amounts of free fatty acids. (Smith 2010)

Typically, dyslipidemia results from dysfunction of adipose tissue and liver lipid metabolism. (Ebbert and Jensen 2013) The consequences of dyslipidemia can initially be atherosclerosis, hypertension, and insulin resistance. Later complications of dyslipidemia can be non-alcoholic fatty liver disease and heart disease. (Singhal 2005, Wolk, Shamsuzzaman Abu and Somers Virend 2003, Miller and Cappuccio 2007)

Two significant direct consequences of obesity are obstructive sleep apnea and osteoarthritis. Obstructive sleep apnea (OSA) is the partial or complete cessation of breathing during periods of the night due to collapse of the upper airway. Major risk factors for the development of obstructive sleep apnea (OSA) are increased tissue surrounding the airway of the neck and chest. These changes are thought to increase the collapsibility of the upper airway and lead to a decrease of chest compliance, respectively. (Schwab et al. 2003, Shelton et al. 1993, Naimark and Cherniack 1960) Individuals with obesity are at nearly twice the risk of developing OSA. (Romero-Corral et al. 2010) Furthermore, the severity of OSA is able to be modulated by weight loss or gain in individuals with mild OSA. (Peppard et al. 2000) Osteoarthritis is a degenerative bone and joint disorder that is characterized by notable pain and significant loss of mobility. (King, March and Anandacoomarasamy 2013) Individuals with obesity have been reported to be at least twice the risk for developing osteoarthritis. (Blagojevic et al. 2010, Coggon et al. 2001)

The last category of obesity complications that are commonly addressed is risk of cancer. The mechanisms underlying the development of certain cancers involves more complicated descriptions of paracrine and endocrine dysfunctions arising from similar indirect perturbations of organ health. Nevertheless, there is strong evidence for obesity increasing the risk for several cancers including: endometrial, colorectal, breast, prostate, renal, and adenocarcinoma. (Pischon

and Nimptsch 2016, Avgerinos et al. 2019, De Pergola and Silvestris 2013) When all of these risks are pooled together, all-cause mortality is elevated by 29% for Class II (BMI > 35) and Class III (BMI > 40) obesity. (Flegal et al. 2013)

Overview of Metabolic Interventions

The essential challenge of combatting the obesity epidemic is that strategies to lead notable weight loss are difficult. While the strategies themselves are cheap, the level of observation required to support individuals undergoing the weight loss quickly become expensive. Traditional lifestyle modification of diet and exercise have been able to result in significant weight loss and improvements in metabolic health. (Crowe et al. 2015, Wadden, Butryn and Wilson 2007) However, long-term weight loss remains difficult to maintain. (Weiss et al. 2007, Unick et al. 2013, van Baak and Mariman 2019, Crowe et al. 2015, Wadden et al. 2007) As a result, the weight loss achieved through traditional diet and exercise intervention have not been effective enough to decrease the prevalence of obesity.

Yet, dramatic long-term improvements have been achieved in weight loss, overt measures of metabolic health, and the reduction of risk factors through bariatric surgeries including vertical sleeve gastrectomy (SG). Impressively, these effects have been shown to occur beyond the expectation by weight loss alone. (Chambers et al. 2011, Longo 2014) Bariatric surgeries have usually been described as a combination of two types of surgical modifications of the digestive tract: 1) restrictive, 2) intestinal bypass. Recently, each of the surgeries has been transitioned to a laparoscopic methodology to reduce the degree of healing following surgery, especially healing under hospital observation. Restrictive surgeries that have been widely performed have been: gastric banding to restrict the distention of the stomach, and SG to surgically remove the greater distensible portion of the stomach. Operations that involve intestinal bypass include the

gastrectomy operation, but also include an intestinal rearrangement to decrease the length of intestinal transit for food as well as the surface area of nutrient absorption.

A meta-analysis covering the results of over twelve thousand patients identified that SG led to excess weight loss of 43.9% at 12 months, 64.3% at 24 months, and 66.0% at 36 months. (Fischer et al. 2012) However, the mean excess weight loss at 12 months achieved via SG (56.1%) less than that achieved by Roux-en-Y gastric bypass (RYGB) (68.3%) in studies with direct comparisons. (Fischer et al. 2012) Studies have indicated that the more extreme the bypass, the more effective the degree of weight loss achieved. (Prachand, DaVee and Alverdy 2006) However, the rate of T2DM remission is has not been consistently different. At 36 months following surgery one study reported 80.9% remission for SG and 81.2 for RYGB. (Abbatini et al. 2010) A meta-analysis of 732 patients showed a trend for earlier remission in RYGB without a change at 12 months, 36 months, or 60 months post-surgery. (Osland et al. 2017) Using data (N = 11863) from the Scandinavian Obesity Surgery Register, bariatric surgery patients with pharmacologically-treated hypertension were able to reduce the risk for major adverse cardiovascular events by 27% and reduce risk of stroke by 48% compared to matched non-operated control subjects (N = 26,199). (Stenberg et al. 2020) Further, the rate of dyslipidemia has been shown to be decreased in prevalence at 2, 6, and 12 years post-surgery. (Adams et al. 2017) The total rate of new cancers reported 10-year follow-up examinations after bariatric surgery is significantly lower than non-surgery obese control group. (Sjöström et al. 2009) The net result of the metabolic health improvements from bariatric surgery led to a 40% reduction in all-cause mortality in US patients relative to the general population with severe obesity. (Adams et al. 2007)

There are some humoral changes that have been observed in the gut. In the hindgut, GLP1 and PYY have been shown to be substantially elevated. (Peterli et al. 2012) GLP1 is a hormone

called an incretin that increases the secretion of insulin from the pancreas after caloric intake. Contrary to expectations, the effect of GLP1 to improve insulin secretion has not been clearly evident. (Hutch and Sandoval 2017) PYY is classified as an appetite suppressing peptide. The increase in post-prandial PYY secretion has been shown to be important for post-surgery maintenance of satiety. (Mans et al. 2015, Chan et al. 2006) In the foregut, total ghrelin levels have been shown to be decreased long-term in SG and for the first year before restoration of baseline levels in bariatric surgeries involving intestinal bypass. (Peterli et al. 2012, Steinert et al. 2013) The role of ghrelin is usually considered as setting a baseline level of appetite through interaction with agouti-related peptide secreting neurons in the arcuate nucleus of the hypothalamus. (Chen et al. 2017)

The distinction on the degree of weight loss, leads to the distinction in the risks of nutritional deficiencies. Across all bariatric surgeries, the most common nutritional deficiencies are to iron and copper, folate and zinc, calcium and vitamin D, and vitamin B12. (Mahawar et al. 2017, John and Hoegerl 2009, Stroh, Manger and Benedix 2017, Emile and Elfeki 2017) Deficiencies may be worsened in gastric bypass operations as compared to restrictive procedures due to decreased intestinal surface area. (Kwon et al. 2014, Mahawar et al. 2017) However, a few other contributing factors partially explain the deficiencies: 1) chronic intolerance to meats, fish and grains, 2) reduced gastric hydrochloric acid production, and 3) dumping syndrome. (Ramadan et al. 2016, Sturniolo et al. 1991) Most individuals experience at least a period of increased gastrointestinal reflux which is worsened by consumption of foods that require more exhaustive digestion, such as: meats, fish, and grains. Moreover, there is an increased rate of partially digested food leaking into the intestines from the stomach pouch (dumping syndrome). Lastly, decreased stomach acid slows the rate of nutrient liberation and is strongly associated with gastritis.

One unexpected risk from bariatric surgery was the risk of suicidality and self-harm. In the prospective SOS study, the pooled hazard ratio of suicide and non-fatal self-harm (mean observation period of 14 years) was 3.48 for gastric bypass and 2.25 for SG compared to patients undergoing non-surgical obesity treatment. (Neovius et al. 2018) The differences were not explained by degree of weight loss achieved. (Spittal and Frühbeck 2018) A similar meta-analysis was conducted on MEDLINE and Embase databases across 148,643 bariatric subjects compared to age, sex, and BMI-matched control subjects and found the odds ratio of suicide and self-harm was 1.90.

Despite the nutritional and psychological risks, there is still consensus that the benefits outweigh the risks. Even so, there is substantial incentive to isolate the mechanisms leading to the benefits of these surgeries such that they can be replicated in a less invasive manner.

Overview on Role of Adipose Tissue in Metabolism

Adipose tissue has been defined in the past purely by the presence of adipocytes, which were thought to be most important for their role for energy storage. (Coelho, Oliveira and Fernandes 2013) However, over time there was been gradual understanding that adipose tissue is complex in terms of differences in cellular composition and increasingly complex in terms of the systemic effects of hormone secretions. (Kershaw and Flier 2004, Choe et al. 2016) Adipocytes are the largest portion of the volume of adipose tissue. (Leonhardt, Hanefeld and Haller 1978) Yet, the composition of vasculature, immune cells, dermal cells, and progenitor cells can vary considerably. (Martyniak and Masternak 2017) The differences are extremely important for the function of adipose tissue. The stark differences are reflected in distinctions between depots, between visceral and subcutaneous fat, and from adipose tissue within tumor microenvironments. (Quail and Dannenberg 2019)

An early understanding of the role of adipose tissue has been the endocrine secretion of adipokines. Two highly studied adipokines have been leptin and adiponectin. The role of leptin is primarily through its counter-regulatory role to ghrelin on neurons within the arcuate nucleus. Leptin acts on POMC neurons to activate melanocortin-4 receptors which leads to increased satiety. (Varela and Horvath 2012) Leptin is synthesized in response to insulin action, and is secreted in proportion to glucose uptake into adipose tissue. (Denroche, Huynh and Kieffer 2012) Both of these factors contribute to the increase in serum leptin in obesity. (Izquierdo et al. 2019) Adiponectin activity is exerted primarily through up-regulation of the activity of AMPK, which acts similarly to the effects of insulin. (Fiaschi 2019) Further, the AMPK-SIRT1-PGC1α axis is a key mechanism whereby adiponectin specifically feeds back to improve insulin sensitivity. (Iwabu et al. 2010)

As the study of adipose tissue has evolved there has been a breakdown of the relevant types of metabolism. Adipose tissue is effective at both the synthesis and conversion of steroid hormones. However, follow-up studies have usually confined this role to a paracrine effect. (Hetemäki et al. 2017, Rubinow 2018) Nevertheless, estrone synthesis in post-menopausal women does appear to be a relevant endocrine effect. (Hetemäki et al. 2017, Barakat et al. 2016) Plus, the proximity of adipose tissue depots to organs across the body still suggests that the paracrine effects of adipose tissue may be highly relevant. (Park, Euhus and Scherer 2011) Still, the most profound role of adipose tissue is derived from the role of energy storage. In parallel with the liver, adipose tissue is responsible for the management of whole-body lipid metabolism. (Rui 2014, Frayn, Arner and Yki-Järvinen 2006) Therefore, discussion of adipose tissue is discussed in terms of: the promotion of the number of adipocytes (adipogenesis), the rate of lipid *de novo* synthesis in adipose tissue (lipogenesis), fatty acid uptake from the blood, the lipids released from adipose

tissue (lipolysis), and to a lesser degree the energetic expenditure of adipose tissue (thermogenesis). (Hertzel et al. 2008)

The regulation of adipogenesis has been well-described. Adipocyte progenitor cells are committed to an adipocyte lineage by the concurrent upregulation of a few CCAAT/enhancer-binding protein (C/EBP) family proteins. The early up-regulation leads to the up-regulation of PPARγ and C/EBPα. Following which there is a series of positive feedback loops leading to cell differentiation. (Rosen and Spiegelman 2006, Park et al. 2012)

Lipogenesis and fatty acid uptake comprise a major role of adipose tissue in systemic lipid accumulation. The master transcriptional regulator of lipogenesis is *SREBP1* in adipose tissue. (Shimano and Sato 2017) In the endosomal membrane SREBP1 is protected from cleavage and therefore activation by interaction with INSIG2. (DeBose-Boyd and Ye 2018) Under conditions of elevated insulin action INSIG2 will be ubiquitinated and degraded, which allows for SREBP1 to become activated. (Matsuda et al. 2001) Among the gene target of SREBP1 is fatty acid synthase (FASN), which is a key protein in the synthesis of long-chain fatty acids from acetyl-CoA precursors. (Horton, Goldstein and Brown 2002) Fatty acid uptake is initially driven by lipoprotein lipase (LPL), which breaks down the triglycerides in lipoproteins, such that fatty acid uptake can be mediated by the scavenger receptor CD36 (FAT) acting in concert with acyl CoA synthetases (FATP1 and ACSL1) and endocytic vesicle formation via calveolin-1. (Goldberg, Eckel and Abumrad 2009, Wu et al. 2006, Lobo and Bernlohr 2007)

Lipolysis is the converse mechanism in adipose tissue to lipogenesis, that leads to the liberation of long-chain fatty acids and glycerol secretion into the blood. There are additional mechanisms that are responsible for the secretion of shorter chain fatty acids and keto bodies from adipose tissue that participate in paracrine signaling. (Miyamoto et al. 2019) Under conditions of

low energetic balance in the adipocyte, high sympathetic nervous system signaling, perilipin proteins become phosphorylated allowing for the exposure of the lipid droplet to intracellular lipases. (Sztalryd and Brasaemle 2017, Bartness et al. 2014) Important lipases in adipocytes are adipose triglyceride lipase (ATGL) and hormone sensitive lipase (HSL) that catalyze the triglyceride-to-diglyceride and diglyceride-to-monoglyceride steps in lipolysis, respectively. Monoacylglycerol lipase (MAGL) is considered to catalyze the last step in lipolysis to release the final fatty acid ester from the glycerol backbone. (Thomas Svava et al. 2014, Park 2014) Protein kinase A (PKA) appears to be a consensus activator of the process of lipolysis through targeted phosphorylation. Insulin activity mediates a reduction in the activation of PKA. (Duncan et al. 2007)

Adipose tissue thermogenesis in humans is less well-defined in white adipose tissue. At present there appears to be two mechanism of adipose tissue thermogenesis that have been described. Both mechanisms appear to putatively be under the control of the transcriptional co-regulator PR domain containing 16 (PRDM16) in coordination with PPARγ coactivator 1α (PGC1α). (Inagaki, Sakai and Kajimura 2016) The first mechanism is described currently as the induction of brown-like adipocytes, which are classified as beige adipocytes. These cells phenotypically appear to be brown adipocytes by exhibiting multiple smaller lipid droplets and high expression of uncoupling protein 1 (UCP1), but are not of the $Myf5^{+}$ cell lineage. (Shan et al. 2013, Ikeda, Maretich and Kajimura 2018) The second mechanism is through sarco/endoplasmic reticulum Ca^{2+}-ATPase 2B (SERCA2B) mediated calcium cycling in coordination with ryanodine receptor. (Mottillo, Ramseyer and Granneman 2018) These mechanisms produce heat through release of the mitochondrial protein gradient or the endoplasmic reticulum calcium gradient.

Respectively, they enable adipose tissue to respond to a cold challenge or as calorie clearance to prevent metabolic dysfunction. (Wu et al. 2020, Kang et al. 2016)

The other major role of adipose tissue endocrine function has been the identification cytokine secretion from adipose tissue. A few cytokines receive notable attention: tumor necrosis factor alpha (TNFα), monocyte chemoattractant protein 1 (MCP1), interleukin 6 (IL6), and plasminogen activator inhibitor 1 (PAI-1). (Coppack 2001, Makki, Froguel and Wolowczuk 2013)

Immune cells that comprise adipose tissue typically are discussed along three distinct lineages: 1) macrophages and monocytes, 2) T-helper cells and T-regulatory cells, and 3) innate lymphoid cells. Adipose tissue resident macrophages can be grouped by polarization: 1) classically activated (M1), alternatively activated (M2), or more recently 3) metabolically activated (MMe). A high ratio of M1 macrophages is described as inflammatory, and lead to high levels of secretion of adipose tissue cytokines like TNFα, IL6, and MCP-1. (Atri, Guerfali and Laouini 2018) The cytokines promote impaired insulin sensitivity and high metabolic stress in the adipose tissue and systemically. (Castoldi et al. 2015) Conversely, a high level of M2 macrophages leads to high IL10 secretion, and generally participates in tissue repair and maintenance of insulin sensitivity. Additionally, the scavenging function is thought to be important in buffering the variance in the size of adipocytes within the greater tissue architecture while limiting the degree of lipids that escape the adipose tissue microenvironment. (Flaherty et al. 2019) A high proportion of MMe macrophages is less inflammatory than M1 macrophages, but still leads to the increased secretion of inflammatory cytokine including IL6. MMe polarization is the result of excessive scavenging of fatty acids including palmitate from the extracellular fluid in adipose tissue. (Tiwari et al. 2019, Coats et al. 2017) In obesity, the predominate macrophage population may be MMe macrophages which slow the rate of systemic lipotoxicity, but also induce progressive fibrosis by initiating

apoptosis of excessively large adipocytes. (Coats et al. 2017, Muir et al. 2017) Further, a reduction in the ratio of anti-inflammatory T-regulatory cells relative to inflammatory T-helper has been observed as a precursor to increased infiltration of macrophages and macrophage polarization away from M2 polarization. (Nishimura et al. 2009, Feuerer et al. 2009, Wu et al. 2007) Lastly, a Group 1 innate lymphoid cells are shown to accumulate within adipose tissue in proportion to worsening metabolic health and lead to adipose tissue fibrosis. Further, specific attenuation of these cells in adipose tissue leads to attenuation of adipose tissue fibrosis while simultaneously improving systemic glucose tolerance. (Wang et al. 2019, O'Sullivan et al. 2016)

Insulin Signaling and Intersection with Adipose Tissue

The signaling pathway linking insulin to the downstream effects of associated with insulin is predominately through phosphorylation of Akt2. The pathway starts as insulin receptors binding to insulin at the cell membrane. Bound insulin leads to the homodimerization of the insulin receptors and subsequent tyrosine phosphorylation of the alpha-subunits of the receptors. These sites allow docking for proteins like IRS proteins (namely IRS1), which are subsequently able to be phosphorylated and activated. Activated IRS1 binds to the regulatory subunits of PI3K, leading to the activation of the catalytic subunits of PI3K. PI3K catalytic subunits are able to phosphorylate PIP_2 into PIP_3 and activate mTOR complex 2 (mTORC2). PIP_3 is able to dock PDK-1 and lead to the phosphorylation of AKT at Thr-308. mTORC2 is associated with phosphorylation of Ser473 on Akt2. Modulation of insulin action can be accomplished by SOCS3 to cap docking sites on INSR, which prevents binding by other proteins. (Saltiel and Pessin 2002)

The downstream effects of insulin can be broadly broken down into: glucose uptake, glycogen metabolism, protein synthesis, and cell survival. GLUT4 is highly associated with insulin-mediated glucose uptake through passive glucose uptake after insulin-mediated

translocation of GLUT4-containing endosomal vesicles to the plasma membrane. (Lizcano and Alessi 2002) The largest share of glucose uptake is typically associated with skeletal muscle and the brain. Yet, adipose tissue glucose uptake is integral for regulation of adipokine secretion and is necessary for *de novo* lipogenesis.(Rosen and Spiegelman 2006) Glycogen regulation by insulin is predominately via the inhibition of glycogen synthase kinase 3β (GSK3β). Inhibition of GSK3β prevents the inactivation of glycogen synthase, and allows accumulation of glycogen. (Lizcano and Alessi 2002) The liver and skeletal muscles are the major site of glycogen synthesis, but the fasting-refeeding-driven excess glycogen accumulation in adipose tissue allows short-term storage of glucose as glycogen for eventual conversion via lipogenesis. (Carmean et al. 2013) Mechanisms linking insulin to regulation of cell survival and protein synthesis are more diffuse and complex. A few defined mechanisms that encourage cells towards energy storage, cell survival, and cell growth are: 1) the activation of the MAPK cascade, activation of mTOR complex 1 (mTORC1), and the nuclear exclusion of Foxo1 by phosphorylation. (Asada et al. 2007) In adipose tissue, there is an additional role of insulin to decrease lipolysis through mTORC1 downregulation of ATGL by Egr and Akt2-mediated inactivation of HSL by phosphorylation. (Mendoza, Er and Blenis 2011, Chakrabarti et al. 2013) Further, nuclear exclusion of Foxo1 in hepatocytes inhibits gluconeogenesis by decreasing expression of the key gluconeogenesis genes: phosphoenolpyruvate carboxykinase and glucose-6-phosphatase. (Barthel and Schmoll 2003)

Termination of the insulin signaling cascade is primarily through endosomal trafficking, degradation, and phosphatase activity. Following ligand-mediated activation of INSR, a prominent step in signal termination is the onset of an INSR refractory period through endocytosis. Within an early endosome, intracellular signaling is prevented due to spatial isolation of INSR from the other signaling components. (Lizcano and Alessi 2002) INSR can be trafficked back to the

membrane surface after dephosphorylation of the phospho-tyrosine docking domains, digested, or translocated to the nucleus. (Wu, Zhu and Robertson 2012) Under normal conditions there is a small fraction of constitutive internalization (ligand-independent receptor internalization) and a small fraction of receptor degradation after internalization. (Chen et al. 2019) mTORC1 serine phosphorylation of IRS1 is major mechanism by which IRS1 can be depleted through protein degradation. (Wang, Nishina and Naggert) A few phosphatases are important to terminate insulin signaling. Phosphatase and tensin homolog (PTEN) acts to inactivate IRS1 by dephosphorylation and spatially isolates Akt2 by degradation of PIP_3 into PIP_2. (Lazar and Saltiel 2006) Further, PH domain Leucine-rich protein phosphatase (PHLPP) and protein phosphatase 2A (PP2A) are involved inactivation of Akt2 by removal of phosphorylation. (Newton and Trotman 2014)

The onset of insulin-resistance in adipose tissue has a few effects that contribute to systemic insulin resistance and dyslipidemia. In response to chronically elevated insulin levels, there is a trend to degrade more INSR. (Chen et al. 2019) Chronic insulin action also leads to gradual decrease in the protein levels of IRS1, which plays a large role in maintaining insulin resistance. (Wang et al. 2009) As a result, lipolysis and efflux of FFA is elevated. (Morigny et al. 2016) Eventually, the liver is unable to regulate the lipoprotein system to compensate for increased serum fatty acids. Ectopic deposition of lipids into the liver and skeletal muscle contributes to the systemic insulin resistance. (Angelini et al. 2019) Lipotoxicity in organs like the pancreas may contribute to the development of diabetes. (Ye, Onodera and Scherer 2019)

Sleep and Biological Rhythms in Metabolic Health

It is important to note that as the incidence of obesity rose, there was a concurrent rise in voluntary sleep restriction resulting in chronic sleep deprivation and poor sleep quality. Most recent epidemiologic statistics indicate that 35.3% of adults are sleeping less than seven hours per

day. It is notable that the most affected group is African-American women, of which 48.3% are sleeping less than seven hours per night. (Wheaton et al. 2011, Nunes et al. 2008, Bonnet and Arand 2005) From a hormonal perspective, sleep restriction of varying degrees has been consistently connected to increases in serum ghrelin and decreases in serum leptin. (Magee et al. 2009, Spiegel et al. 2004, Taheri et al. 2004) Additionally, from a chronic sleep loss perspective there have been alterations in norepinephrine, orexin, and cortisol rhythms which are indicative of loss of sleep/wake rhythms.(Kumari et al. 2009, Leproult et al. 1997, Sakurai 2007, Carter et al. 2009) Importantly, sleep restriction has been shown to have a deleterious effect on global insulin sensitivity; these changes are independent of BMI and insomnia. (Gottlieb et al. 2005, Spiegel et al. 2005)

There are well-known connections of sleep and circadian misalignments to metabolic impairment and obesity. (Knutson et al. 2007, Van Cauter et al. 2008, Hatori et al. 2012, Longo and Panda 2016) Total acute sleep restriction has been shown to decrease the leptin-to-ghrelin ratio, which associated with increased subjective hunger ratings. (SCHMID et al. 2008) Partial sleep restriction (8 days, 4h/night) has been shown to lead to reductions in glucose disposal and acute insulin release as measured by a frequently-sampled intravenous-glucose tolerance test. (Donga et al. 2010) Low average sleep duration and interrupted sleep in lean healthy individuals has been connected to decreases in leptin release, increased BMI, and increased risk of diabetes. (Taheri et al. 2004, Shan et al. 2015) Further, temporal alignment of eating with circadian rhythms through time-restricted feeding has been shown to result in resistance to the development of metabolic disease independent of caloric intake and especially under metabolic stresses like high fat diets. (Rothschild et al. 2014)

Overview of the Circadian Clock

The circadian clock is a 24-hr pacemaker that instills a temporal organization to energy-intensive metabolic processes. (Lamia, Storch and Weitz 2008, Nikolaeva et al. 2012, Zvonic et al. 2006) The baseline of these rhythms is set for all molecular clocks by the central clock in the suprachiasmatic nucleus, which is entrained to a few key signals like light. (Czeisler et al. 1999a, Berson, Dunn and Takao 2002, Radziuk 2013) Yet, the circadian clock is a cell autonomous molecular apparatus found in each cell of major peripheral organs. (Panda, Hogenesch and Kay 2002, Nikolaeva et al. 2012, Zvonic et al. 2006) This design allows for centralized control, which is decoded by the organ-specific clocks, called peripheral clocks, to affect organ-specific metabolic functions. Further, humoral signals act on specific clock components of the peripheral clocks or central clock to facilitate any necessary adjustments. (Panda et al. 2002, Dvornyk, Vinogradova and Nevo 2003, Ouyang et al. 1998, Spoelstra et al. 2016, Dodd et al. 2005) The adjustments allow for gradual realignment in response to acute time zone shifts and progressive changes like seasonal variations in daylight. The exceptional efficiency of the temporal design has allowed conservation of a circadian apparatus from organisms as simple as algae to a remarkably similarly functioning clock in plants, fruit flies, mice, and humans. (Pittendrigh 1954, Lam et al. 2018, Kaczmarek, Thompson and Holscher 2017, Cui et al. 2013, Brown, Kowalska and Dallmann 2012)

The human circadian clock is composed of a core transcription-translation loop and a few accessory transcriptional loops. The core transcriptional loop consists of the positive limb protein dimers which drive gene expression of the negative limb genes at E-box promoter regions. The negative limb protein dimers are responsible for inhibiting the transcriptional activity of the positive limb while also stabilizing the accumulation of the positive limb elements. The positive limb is driven by Brain and Muscle ARNT-Like 1 (*BMAL1*) dimerized to either Circadian

Locomotor Output Cycles Protein Kaput (*CLOCK*) or Neuronal PAS Domain Protein 2 (*NPAS2*). (Jin et al. 1999, Gekakis et al. 1998, DeBruyne et al. 2006, Debruyne 2008) The negative limb is composed of a protein dimer between period genes (*PER1, PER2, PER3*) and cryptochrome genes (*CRY1, CRY2*). (Shearman et al. 2000, Vitaterna et al. 1999, Van Der Horst et al. 1999) Rhythmicity in the expression of the positive limb is maintained by an ancillary loop that regulates the expression at REVERBA/ROR response promoter elements (RRE) found upstream of positive limb genes. (Solt, Kojetin and Burris 2011, Takeda et al. 2011) Retinoid-Related Orphan Receptors (*RORα, RORβ, RORγ*) and Rev-ErbA nuclear receptors (*REVERBα, REVERBβ*) accomplish positive and negative regulation from baseline. (Meng et al. 2008) Additionally, *PER2* is shown to be important for driving baseline transcriptional levels of *BMAL1* as well as for nuclear localization of *CRY1/2*. (Shearman et al. 2000) Further, *CRY1/2* is responsible for stabilizing *BMAL1:CLOCK* and *BMAL1:NPAS2* dimers to facilitate accumulation in the nucleus, but also for inhibiting the E-box enhancer activity. (Griffin, Staknis and Weitz 1999, Kume et al. 1999) Both positive and negative limb protein dimers require cycling between the cytosol and nucleus and are sensitive to marking by ubiquitination leading to degradation by the 26S proteasome. (Keesler et al. 2000, Vielhaber et al. 2000, Kwon et al. 2006, Zheng et al. 1999, Muratani and Tansey 2003, Camacho et al. 2001) Humoral modulation is enhanced by the other ancillary loop, which acts at D-site promoters upstream of several negative limb genes (*PER1/2/3, CRY2*). (Yamaguchi et al. 2000, Yamajuku et al. 2011) Negative regulation via nuclear factor interleukin-3 promoter transcriptional activator (*NFIL3*) and positive regulation is driven D-site-binding protein (*DBP*), a gene which contains E-box enhancer regions. (Bunger et al. 2000, Ripperger et al. 2000, Yamaguchi et al. 2000) *PER3* is not essential for the circadian clock feedback loops, but is still highly active in affecting peripheral tissue metabolism. (Bae et al. 2001)

Interaction of Circadian Clock and Metabolism

Loss-of-function mutations and gene knock-out experiment on elements of the circadian clock have provided ample evidence that systemic biological rhythms have significant interaction with the circadian clock. Loss-of-function mutation in *mCLOCK* has been associated in mice with a loss of structured diurnal-nocturnal feeding, which lead to hyperphagia-induced obesity. (Turek et al. 2005) And *mCLOCK* mutant mice have been shown to be more sensitive to both insulin-induced hypoglycemia and meal-induced hyperglycemia. (Rudic et al. 2004, Kennaway et al. 2007) Further, global BMAL1$^{-/-}$ mice have been shown to have attenuated rhythms in glucose and triglycerides. (Lamia et al. 2008) Global *mPER2*$^{-/-}$ mice have exhibited a loss of glucocorticoid rhythm associated with sleep. (Yang et al. 2006) And, surprisingly, BMAL1 LOF studies have suggested that baseline expression of the circadian clock genes is determined by non-clock elements.(Bunger et al. 2000)

Yet, there is a documented role of an interaction of the circadian clock with normal physiological function. Absolute energetic state of cells has a protracted effect on activity and transcription of the circadian clock. cAMP is an independent mechanism to regulate the basal levels of *mPER1* and *mPER2*, but not of *mPER3*. (Travnickova-Bendova et al. 2002) Modulation of total NAD levels is responsible for increasing the levels of BMAL1 transcriptional activity via a decreased transcriptional repression by PER2 due to increased PER2 interaction with NAD-dependent SIRT1. (Strzyz 2020) SIRT1 is also a histone deacetylase that will act on BMAL1 and PER2 to prevent PER2-CRY1 interaction and increase BMAL1-CLOCK interaction (Asher et al. 2008, Nakahata et al. 2008) The DNA-binding activity is increased in during periods when the NAD+/NADH ratio is lowered. (Rutter et al. 2001) The post-translational changes of CLOCK/NPAS2 are important in the difference in the binding affinity, namely phosphorylation

and acetylation. (Dardente et al. 2007) The contribution of these interactions was outlined above in the CRY1-mediated stabilization of BMAL1-CLOCK during accumulation of the positive arm elements. During which, CRY1 prevents transcriptional activity at E-box promoter regions. The dissociation and degradation of CRY1 allows for the restart of the clock transcriptional cycle with E-box mediated promotion of transcription.

Caloric balance can also have effects through AMPK. AMPK is a kinase that has many potential protein targets as a central regulator of energy homeostasis, and is activated by a low energetic state in cells reflected by elevated AMP levels. (Steinberg and Carling 2019) AMPK activity leads to difference in the phosphorylation of period and cryptochrome genes, which leads to protein instability through ubiquitination and increased transcriptional repressive activity of steroid receptors function. (Lamia et al. 2009) The effects can be direct like those to CRY1 or indirect through activation of casein kinase I epsilon which can phosphorylate PER2. (Um et al. 2007) Physiologically, it has been noted that AMPK is important for the transition to a decreased respiratory exchange ratio during the night. (Vieira et al. 2008)

A major mechanism explaining the role of circadian clock elements effect on metabolism is through tissue specific interactions with steroid receptors. (Duez and Staels 2010, Zhao et al. 2014, Hatcher, Royston and Mahoney 2020) Co-immunoprecipitation experiments has indicated that as much as 37% of nuclear receptor binding sites are also genomic binding sites of mCRY1 and mCRY2. Strong interactions were discovered with nuclear receptors including: glucocorticoid receptor, peroxisome proliferator-activated receptor (PPAR) α and PPARγ, liver x receptors (LXR) α and β, and androgen receptor. (Kriebs et al. 2017) The interactions of CRY1/2 with nuclear receptor has been mostly co-repression of transcription. (Jordan et al. 2017) CLOCK and NPAS2 have been shown to interact strongly with RARα and RXRα in vasculature. (McNamara

et al. 2001) RORα, β, δ and REVERBα, β receptors exert prominent effects to integrate metabolism through the ability to heterodimerize with steroid receptors to promote or repress transcription, respectively. (Yang et al. 2006)

The aim of this thesis was to provide insight into the interaction of adipose tissue with systemic metabolism shortly after surgery. We choose twelve weeks after surgery to allow for an interrogation of the association of both weight and metabolic parameters with changes to metabolic health. We were interested in understanding how overt measures of metabolic risk like fasting glucose and fasting free fatty acids aligned with sleep metrics and the physiologic alterations of endocrine hormones. We then characterized the phase of and overall gene expression of essential genes involved in regulating adipose tissue metabolic function as well as the elements of the circadian clock. Lastly, we associated the changes at the gene expression level back to the systemic metabolic changes. Collectively, we provided insight into the contribution of adipose tissue metabolism to systemic metabolism in the period twelve weeks after vertical SG in women with morbid obesity.

Chapter 2: Characterization of Metabolic Outcomes Twelve Weeks Following Sleeve Gastrectomy in Women with Morbid Obesity

Abstract

Sleeve gastrectomy (SG) surgery is known to lead to profound weight loss and substantial metabolic improvements by one year following surgery. While the primary intervention performed was a removal of the greater distensible portion of the stomach, there appear to be complex networks of compensatory physiological and endocrine alterations. However, it is not yet clear which organs, and at what times, are responsible for the changes that occur after surgery. This study was designed to evaluate the effect of SG twelve weeks after surgery. We show that subjects have lost a substantial amount of weight, leading to significantly lower adiposity and BMI. Subjects also experienced notable declines in fasting insulin and fasting glucose levels as well as an increase in insulin sensitivity. At this point, the degree of caloric restriction closely predicts the degree of weight loss that subjects achieved. In response to the caloric restriction, there is the observation of a higher ratio of active ghrelin and substantially decreased serum leptin levels. There is evidence that the adipose tissue is also exhibiting more lipolysis that would underlie reduced fat mass and weight loss. However, the serum free fatty acid levels are unchanged. Most notably, we report that global appetite is decreased and hunger is unchanged after surgery.

Introduction

The epidemic of obesity has continued to grow despite global initiatives to curb and reverse the prevalence of obesity. In 1960-1962, only 13% of the US population had obesity. (Craig M. Hales Feb 2020) In 2011-2014, the prevalence of obesity had risen to roughly one-third of the US adults (>20 years). (Flegal et al. 2012, Ogden et al. 2014) In 2017-2018, 42.4% of the US population had acquired obesity and 9% had acquired severe obesity. (Craig M. Hales Feb 2020) The health consequences of obesity extend far beyond the mechanical problems associated with excess weight. Two significant direct consequences of obesity are obstructive sleep apnea (OSA) and osteoarthritis. (Schwab et al. 2003, Shelton et al. 1993, Naimark and Cherniack 1960) Further, individuals with obesity are at nearly twice the risk of developing OSA. (Romero-Corral et al. 2010) Individuals with obesity have been reported to be at least twice the risk for developing osteoarthritis. (Blagojevic et al. 2010, Coggon et al. 2001) For Class I Obesity (BMI: 30-35) and Class II Obesity (35-40), the risk is 2.5 times and 3.5 times higher than healthy weight individuals. (Ganz et al. 2014) There is strong evidence obesity increasing the risk for several cancers including: endometrial, colorectal, breast, prostate, renal, and adenocarcinoma. (Pischon and Nimptsch 2016, Avgerinos et al. 2019, De Pergola and Silvestris 2013)

Bariatric surgery was one class of interventions that was identified early as a powerful tool to induce gradual long-term weight loss with significant improvement to metabolic health. A meta-analysis covering the results of over twelve thousand patients identified that SG led to excess weight loss of 43.9% at 12 months, 64.3% at 24 months, and 66.0% at 36 months. (Fischer et al. 2012) At 36 months following SG surgery, one study reported 80.9% diabetes remission for SG. (Abbatini et al. 2010) Additionally, bariatric surgery patients with pharmacologically-treated hypertension were able to reduce the risk for major adverse

cardiovascular events by 27% and reduce risk of stroke by 48% compared to matched non-operated control subjects (N = 26,199). (Stenberg et al. 2020) The net result of bariatric surgery is a 40% reduction in all-cause mortality in US patients relative to the general population with severe obesity. (Adams et al. 2007)

We were interested in observing the role of humoral regulation of appetite alongside subjective hunger and appetite during the period of greater weight loss following surgery. We choose to study SG in women due to purely restrictive nature of the procedure and due to that women stably comprise 80% of patients on whom bariatric surgeries are performed. We hypothesize that the decline in plasma leptin will still be associated with increase appetite and hunger, but that despite the caloric restriction subjective hunger and appetite will not be altered.

Materials and Methods

Subject characteristics

Pre-menopausal women with morbid obesity were voluntarily enrolled with informed written consent in the clinical research study (University of Chicago IRB 14-0984) following approval and scheduling for laparoscopic SG (LSG) surgery. A summary of subject characteristics was reported (Table 2.1). Subjects did not exhibit irregular lifestyles or irregular menstrual cycles, or have diabetes managed with medication (HbA1c: 5.6± 0.6). No malignant diseases were identified by complete blood count nor was pregnancy detected via urine. Additionally, patients were monitored by a registered polysomnographic technologist during a full polysomnography recording to ensure the absence of sleep-related disorders. Subjects with obstructive sleep apnea

met inclusion criteria with documented compliance using a continuous positive airway pressure machine.

Laboratory Sessions

Identical sessions were conducted at baseline one-to-two weeks prior to the scheduled surgery date and twelve-to-thirteen weeks following the surgery date. The duration of each session was two evenings and one day (Figure 2.1). Metabolic characterization was reported in Table 2.3. Four isocaloric macrocalorie-matched mini-meals were administered per day. After each meal,

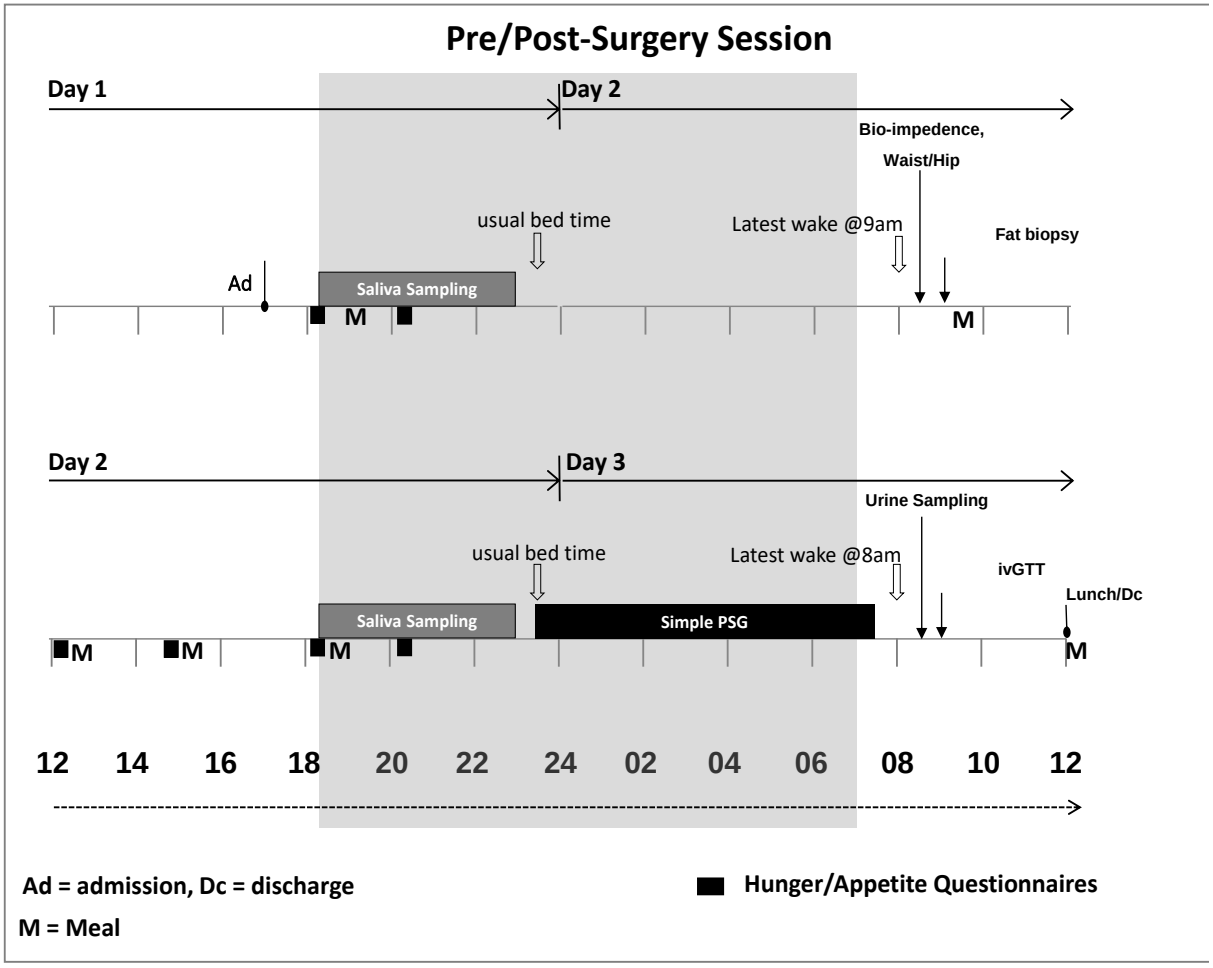

Figure 2.1: Structure of in-laboratory sessions. Subjects were scheduled for two identical laboratory sessions at baseline one week prior to surgery and at twelve weeks following surgery.

remaining food was weighed and recorded by CRC nutrition staff. To regulate evening light exposure, ambient light was lowered three hours preceding the scheduled subject sleep start. Saliva was collected by cotton salivette, from which melatonin and cortisol were measured by ELISA. No changes in evening cortisol or melatonin were found. An aspiratory subcutaneous peri-umbilical fat biopsy was conducted on one of the mornings of the laboratory session. (Broussard et al. 2012) On the other morning, a frequently-sampled intravenous glucose test (fsIV-GTT) was conducted. Outcome variables of glucose management were calculated using MINMOD Millenium software (Pacini and Bergman 1986, Boston et al. 2003). Individual non-invasive body composition measures have well known pitfalls, but collectively can provide robust indications of the success of bariatric surgery. We collected from each subject at each laboratory session: BMI, body weight, adiposity, and waist-to-hip ratio. Adiposity was determined by CRC staff using full-body bioimpedance.

Biopsy Processing

The processing of the tissue was a modification of the Fried Protocol. *(Carswell, Lee and Fried 2012)* (Figure 2.2) A laminar flow hood was used to wash tissue with sterile M199 media (Gibco cat# 12350-039, +1% low endotoxin BSA, +200 nM N6-Rphenylisopropyladenosine) and mince it into approximately five milligram segments. These steps removed blood clots and balanced cellular hypoxia while maintaining tissue architecture that facilitated conventional paracrine signaling. Following initial processing, the tissue was washed once in BSA-free media and rested for four hours in a cell incubator (37 °C, 5% CO_2) in ten volumes of sterile culture media (Gibco cat # 12350-059, 1 nM insulin, 40 nM dexamethasone). Then, one hundred microliters of packed tissue (± 5%) was aliquoted and measured volumetrically from a 40 μm cell strainer (CellTreat cat # 229481) into one milliliter of culture media (1:10 by volume) per well

into a twenty-four well tissue culture plate (Falcon cat# 353047). The first collection was approximately twelve hours following the biopsy in an effort to allow for the majority of cytokine secretion and acute inflammation to abate. Subsequently, a well of tissue and respective media were collected separately every three hours, weighed, and snap frozen in liquid nitrogen before storage at -80°C. Similar protocols have shown that human adipose tissue circadian clock gene and clock-controlled gene rhythms can be maintained without direct SCN signal. (Fain et al. 2003, Phillips et al. 2008, Rogers et al. 2008, Garaulet et al. 2011, Gómez-Abellán et al. 2012, Gómez-Santos et al. 2009, Aubin et al. 2015, Wang et al. 2015) Yet, to preserve the SCN-mediated imprint

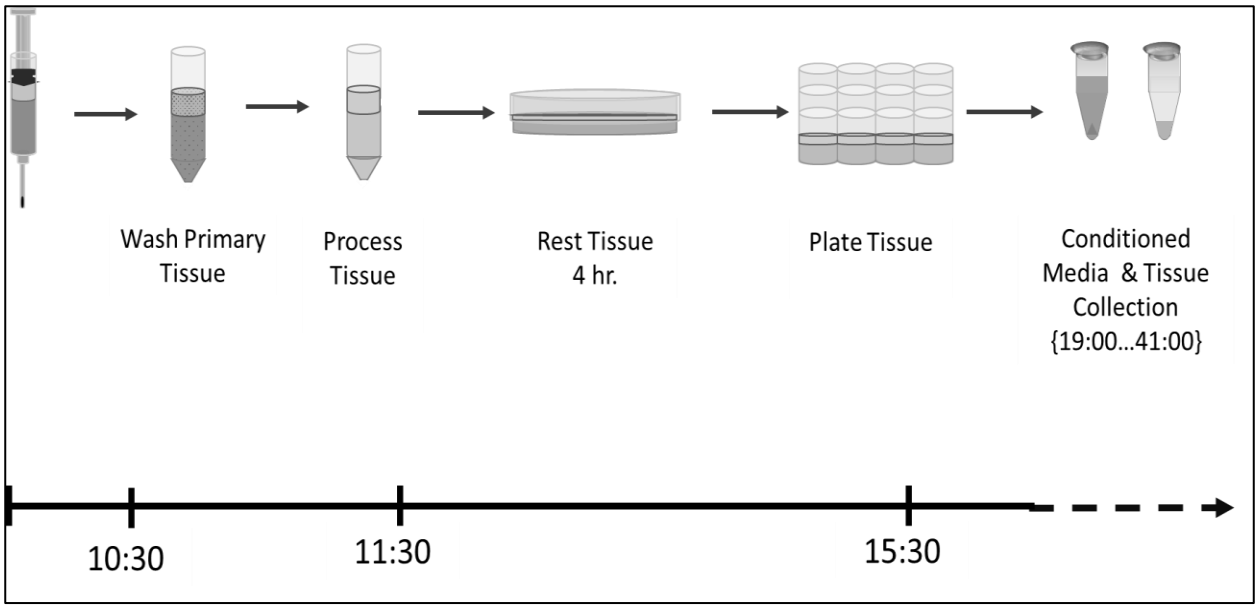

Figure 2.2: Flowchart of adipose tissue *ex vivo* time series tissue culture experiment. Subjects were scheduled for two identical laboratory sessions at baseline one week prior to surgery and at twelve weeks following surgery.

of endogenous entrainment of the peripheral circadian clock, the tissue was not serum shocked.

Polysomnography Recording

Simple polysomnography recording was performed at baseline and post-surgery. Electrodes were placed, recording monitored, and grading completed by registered sleep technologist. Each epoch was assigned as a twenty second window. The reported generated

included the total recording time, the total sleep time, the time spent in each sleep stage, sleep efficiency, and time spent awake after sleep onset.

Conditioned Media Analysis

Culture media was thawed and time series accumulation of glycerol was measured in technical duplicates according to kit instructions (Millipore Sigma MAK117). Glycerol secretion rate was calculated as the average increase in glycerol in media across time series experiment when calibrated to standard curve.

Fasting Serum and Plasma Hormone Levels

Serum and plasma samples were prepared from samples collected by nursing staff prior to start of fs-IVGTT. Each were prepared as directed by kit. Acylated ghrelin and total ghrelin were measured via ELISA (Millipore Sigma EZGRT-89K, EZGRA-88K). Leptin was measured via radioimmunoassay (Millipore Sigma HL-81K).

Hunger and Appetite Questionnaires

Questionnaires were administered to subjects electronically through ASWIN software on laboratory laptop computers. Subjects were asked to rate answers to each question by marking along the visual scale of a 10 cm horizontal black line. Surveys were administered before and after each meal of the first full day of each laboratory session. Hunger appetite questions were: 1) “How hungry do you feel right now?”; “How thirsty do you feel right now?”; 3) “How satiated do you feel right now?”; 4) “How strong is your desire to eat right now?”; 5) “How much food do you think you could eat right now?”, 6) “How nauseated do you feel right now?”. Appetite Questionnaire questions were: 1) ‘What is your appetite for fruits right now?”; 2) “What is your appetite for sweets right now?”; 3) “What is your appetite for starchy foods right now?”; 4) “What

is your appetite for salty foods right now?"; 5) "What is your appetite for dairy right now?"; 6) "What is your appetite for protein right now?"; and 7) "What is your appetite for vegetables right now?". Composite appetite results were computed arithmetically by summation of respective simple appetites. Computed appetites results were: 1) Global Appetite, 2) High-Carb, High-Fat, 3) High-Carb, Low-Fat, 4) Sweets & Starchy, and 5) High Protein.

Mixed Model Construction

Mixed modeling was utilized to estimate the degree of difference in gene expression levels between baseline and post-surgery. Model fitting was conducted by R package (lme4). In order to ensure that the dependence derived from time series collection was accounted for in the statistics, the random vector was a simple intercept set as the subject identification number (SID). Experimental ratings were unaltered at entry into the data set.

The surgery-associated parsimonious model was calculated by using surgery as a binomial variable (Pre [0], Post [1]) and iterative inclusion of factors representing potential corrections for: 1) age (integer, years), 2) pre-surgery weight loss, 3) post-surgery weight loss, or 4) time of day. Given the known effect of meals to affect hunger and appetite, we represented time of day as the best combination of factors including 1) prandial (binomial, pre-meal [0], post-meal [1]); and 2) time point (integer, {1,2, ..., 8}), meal (integer, {1,2,3,4}), latter part of day (binomial, first half [0], latter half [1]). To allow for correction by weight loss, it was held constant for all respective points of a given subject. An enhanced model was chosen by: 1) an improved Akaike Information Criterion of the N+1 model (compared to N model without the addition of the factor), 2) each factor effect has low Type S error rate ($p < 0.05$), and low inflation of standard error of estimation (< 50%).

Results

Weight loss and Body Composition

Subjects exhibited significant weight loss compared to baseline during the week prior to surgery (1.7 kg, 1.3%WL, p = 0.004) and in the twelve weeks following surgery (20.6 kg, 15.5% WL, 38.5 %EWL, p = 1.5e-8). These changes resulted in a markedly decreased BMI (6.7, 32.5% EBMIL, p = 2.6e-7). Full-body bioimpedance confirmed that adiposity also decreased (4.5%, p = 2.2e-4). This decrease in adiposity would indicate that 79.0% of the weight that was lost was from adipose tissue. Waist-to-hip ratio was unchanged at post-surgery (-0.03 ± 0.03, p = 0.23).

Table 2.1: De-identified subject characteristics.

Subjects	N=10	
Race	8 AA, 2 NHW	
Age (yr.)	36.1 ± 2.3	
Height (cm)	168.2 ± 1.9	
BMI (kg/m^2) , Baseline	45.6 ± 1.4	
BMI (kg/m^2) , Post-surgery	38.9 ± 1.8	2.60E-07
Weight (kg), Baseline	128.6 ± 4.3	a) 4.0e-3
Weight (kg), Surgical Intake	126.9 ± 4.5	b) 6.0e-10
Weight (kg), Post-surgery	106.3 ± 4.5	c) 1.5e-8
Calories Eaten, Baseline	2,189 ± 93	
Calories Eaten, Post-surgery	681 ± 57	7.1e-3
Adiposity (%), Baseline	51.5% ± 1.7%	
Adiposity (%), Post-surgery	47.0% ± 1.5%	2.20E-04
Waist:Hip Ratio, Baseline	0.88 ± 0.02	
Waist:Hip Ratio, Post-surgery	0.85 ± 0.03	0.23

All subjects self-identified as non-Hispanic. Weight was measured with subject vitals at each of three intake appointments. Values in third column represent the paired t-test values comparing measurements of: a) baseline to surgical intake, b) baseline to post-surgery, and c) surgical intake to post-surgery. BMI, adiposity, and waist:hip ratio were measured by CRC staff during the morning for baseline and post-surgery laboratory sessions. Four meal average for calories eaten was weighed and measured by CRC nutrition staff. P-values represent paired t-tests comparing baseline to post-surgery measurements.

Polysomnography:

Polysomnography sleep profiles did not exhibit significant differences between baseline and post-surgery. Yet, there were trends for decreased wake after sleep onset, increased total sleep time, and increased sleep efficiency at post-surgery (Table 2.2). Subjects averaged over seven hours of sleep in the eight-hour recording window; no subject exhibited markedly different total sleep or slow wave sleep (N3) between baseline and post-surgery. However, one subject did exhibit markedly low N3 sleep at both baseline and post-surgery.

Table 2.2: Polysomnography recording results

Total Recording Time (min)	Baseline	482.0	±	3.1	0.48
	Post-surgery	480.1	±	0.6	
Total Sleep Time (min)	Baseline	431.0	±	10.4	0.11
	Post-surgery	447.7	±	6.0	
Sleep Efficiency (%)	Baseline	89.4	±	1.9	0.08
	Post-surgery	93.1	±	1.2	
N1 Sleep Latency (min)	Baseline	8.1	±	1.8	0.90
	Post-surgery	7.8	±	1.3	
Wake after Sleep Onset (min)	Baseline	50.9	±	8.9	0.08
	Post-surgery	33.1	±	5.9	
N1 (min)	Baseline	32.8	±	3.7	0.59
	Post-surgery	34.5	±	3.7	
N2 (min)	Baseline	225.2	±	14.9	0.23
	Post-surgery	234.8	±	13.1	
N3 (min)	Baseline	76.9	±	10.8	0.85
	Post-surgery	78.5	±	15.8	
REM (min)	Baseline	96.2	±	6.4	0.68
	Post-surgery	100.0	±	4.2	

Subjects had a simple polysomnography recording conducted during the first night of each laboratory session at baseline and post-surgery (N = 10). A registered sleep technologist analyzed the raw recordings in epochs of twenty seconds to denote transitions and maintenance of each sleep stage. Significance of difference in sleep were calculated by two-tailed paired t-tests.

Glucose Regulation

A subset of seven subjects completed both a fsIV-GTT and had laboratory meal data available at baseline and post-surgery. At post-surgery, subjects consumed substantially less calories (2223 ± 168, 591 ± 90, p = 2.7e-6). Additionally, fasting glucose (-4.18 mg/dL, p = 0.01) and fasting insulin levels (-6.62 mU/L, p = 3.8e-5) were substantially lower than baseline. Systemic insulin sensitivity was improved (0.85, 0.02). Acute insulin response to glucose and glucose disposal rate were unchanged from baseline. Beta-cell function, which weights first and second phase insulin secretion, was decreased (-20.13 mU/mM, p = 0.01). Despite an increased glycerol secretion rate (p = 0.04) which suggests elevated lipolysis, there was no measured change

Table 2.3: Summary of metabolic parameters

Calories Eaten (kcal)	Baseline	2223	±	168	2.7E-06
	Post-surgery	591	±	90	
Fasting Glucose (mg/dL)	Baseline	82.55	±	1.78	0.01
	Post-surgery	78.37	±	1.93	
Fasting Insulin (mU/L)	Baseline	14.09	±	2.92	3.8E-05
	Post-surgery	8.47	±	2.27	
Insulin Sensitivity (mU/L*min^-2)	Baseline	1.76	±	0.19	0.02
	Post-surgery	2.61	±	0.38	
Beta Cell Function (mU/mM)	Baseline	315.5	±	74.7	0.01
	Post-surgery	294.4	±	97.8	
Disposition Index (AU)	Baseline	1579	±	270	0.11
	Post-surgery	1460	±	334	
Glycerol Secretion Rate (ng/hr)	Baseline	30.7	±	5.0	0.04
	Post-surgery	51.4	±	8.5	

Four meal average for calories eaten (N = 7) was weight and measured by CRC nutrition staff. Subjects (N = 7) had a frequently sampled intravenous glucose tolerance test (fsIV-GTT) conducted during the morning before the first meal of the laboratory session at baseline and at post-surgery. fasting values were calculated from blood collected before start of fsIVGTT, outcome measures were calculated using MINMOD software based on the respective IV-GTT results. Glycerol secretion rate (N = 6) was calculated from culture media collected across time series experiment normalized to 100 mg adipose tissue. Statistics were calculated by two-tailed t-tests.

in the serum free fatty acids levels. Incredibly, the trend for fasting free fatty acids is a decrease, which suggests that the lipids are effectively cleared from the blood.

Blood Hormone Levels

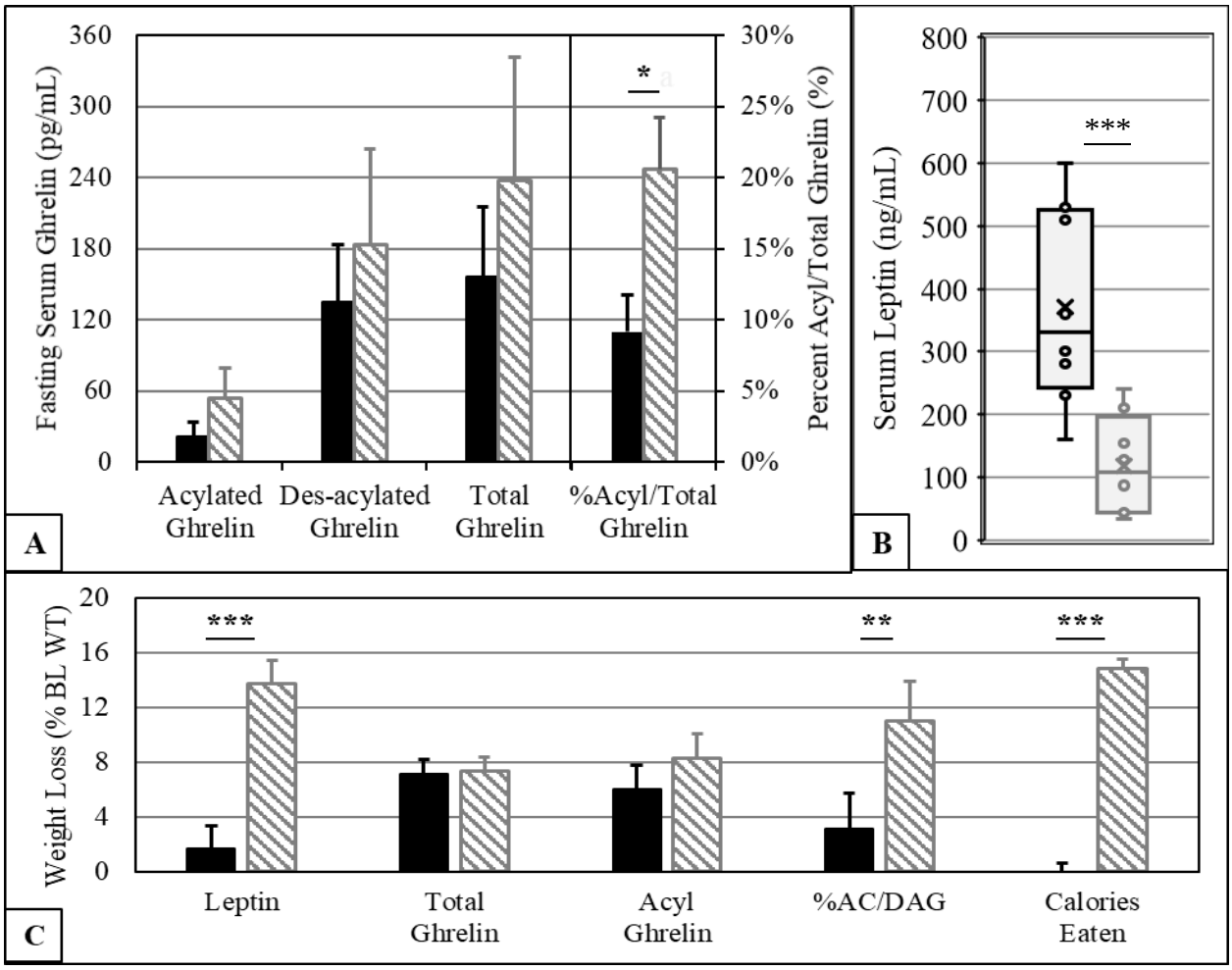

Figure 2.3: Serum ghrelin and leptin and respective associations to weight loss. Fasting serum was collected (N = 8) during the morning prior to the first meal at baseline and at twelve weeks post-surgery. Hormones measured were: A) acylated ghrelin and total ghrelin via ELISA (Millipore Sigma EZGRT-89K, EZGRA-88K), and leptin via radioimmunoassay (Millipore Sigma HL-81K). A&B) serum hormone levels at baseline (black), or post-surgery (grey). C) Linear modeling to estimate percent weight lost using respective single fixed factor of respective hormone levels, the ratio of acyl-ghrelin to total ghrelin, or calories eaten across four meals of laboratory session at baseline (black) or post-surgery (grey). P-values were, respectively: * < 0.05, ** < 0.01 and *** < 0.001.

Plasma ghrelin levels, acyl and des-acyl, were not significantly changed from baseline, respectively ($p = 0.14$, $p = 0.49$) (Figure 2.3A). However, the percent of acyl-ghrelin-to-total-

ghrelin was markedly elevated (9.1% [BL], 20.6% [PS], p = 0.014). Serum leptin levels were markedly decreased at post-surgery (371 [BL], 118 ng/mL, p = 6.7e-4) (Figure 2.3B).

Association of blood hormone levels and weight loss

Unsurprisingly, the decrease in calories eaten associates almost perfectly to the experimental percent weight loss after surgery (Figure 2.3C). Additionally, there is a clear association linking greater declines in serum leptin and greater increases in percent active ghrelin with increased weight loss attained.

Hunger and Appetite Survey Ratings

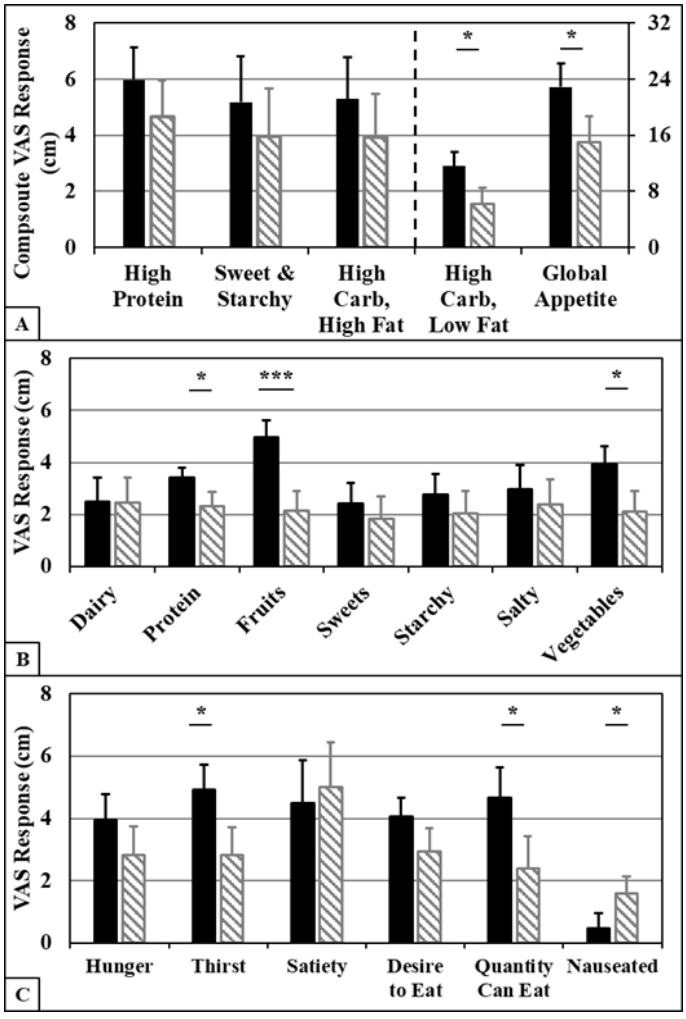

Figure 2.4: Hunger and appetite ratings at baseline and at post-surgery. Survey responses were collected before and after each of four isocaloric mini-meals at baseline (black) and twelve weeks following surgery (grey) for each subject (n=10). Average estimated survey responses for each survey question were estimated through mixed linear modeling with subject ID as the random intercept and the effect of surgery assigned as a fixed binomial parameter. Models corrected for effects of age, weight loss before or after surgery, and time of day relative to meals if present. Composite appetite ratings were summated, and then modelled separately. Significance of differences were determined by two-sided t-tests with propagated parameter uncertainties. P-values were, respectively: * < 0.05, ** < 0.01 and *** < 0.001.

There is a trend for decreased rating for hunger and appetite (Figure 2.4). Global appetite is significantly decreased (22.9 [BL], 15.0 [PS], p = 0.04). There is also a decrease in appetite for fruits (5.0 [BL], 2.1 [PS], p = 2.7e-4), protein (3.4 [BL], 2.3 [PS], p = 0.047), vegetables (3.9 [BL], 2.1 [PS], p = 0.02), and high-carb, low-fat foods (11.6 [BL], 6.3 [PS], p = 0.02). Subjects also rated less thirst (4.9 [BL], 2.8 [PS], p = 0.02), quantity subject felt they could eat (4.7 [BL], 2.4 [PS], p = 0.03), and slightly higher rating for nausea (0.5 [BL], 1.6 [PS], p = 0.046). Hunger is not substantially changed after surgery.

Discussion

The goal of this study was to identify is there were alterations in systemic metabolic function or sleep-related health parameters following SG. At twelve weeks following surgery, weight loss was evident. However, there was not a measured change in waist-to-hip ratio in this study. Yet, the degree of weight loss was approximately in range with prior reports at around twenty kilograms. It may be surprising that 79.0% of the weight loss was estimated to have come from adipose tissue. The lack of change to the waist-to-hip ratio could be explained by the adipose tissue depots responsible for the weight loss. (Galanakis et al. 2015, Garrido-Sanchez et al. 2012) There are conflicting reports about whether the weight loss from adipose tissue shortly after surgery is from subcutaneous or visceral fat. The degree of android or gynoid fat loss was not measured.

It is also clear that there is a caloric restriction element to the weight loss. The differences in the four-meal average calories consumed in laboratory sessions between baseline and post-surgery convincingly estimates the degree of weight loss achieved by each subject. And, the

decline in the fasting leptin in accordance without a change to ghrelin levels, would suggest that there would be a shift towards increased hunger and appetite. However, this does not align with the hunger and appetite rating of the subjects. Firstly, global appetite is significantly reduced. And, secondly, hunger does not show evidence of a change. While nausea was shown to be increased after surgery, the degree of nausea did not associate with the degree of weight loss. This would suggest that there are factors outside of ghrelin and leptin that are largely responsible for the decreased appetite despite significant caloric restriction.

We were surprised to find that the ghrelin levels were not depressed. The traditional paradigm asserts that SG involves the removal of a large portion of the ghrelin-secreting cells within the stomach. Several reports have supported the premise, including shortly after surgery. It is possible that in this study, the remaining ghrelin cells in the proximal duodenum were able to compensate for the loss of the gastric secretion of ghrelin. If this were the case, then the dramatically lower caloric consumption would be expected to induced higher ghrelin secretion, and a higher percent of active ghrelin. It would be unsurprising if cell fatigue eventually resulted in the decreased ghrelin levels usually present following SG.

The results of the fsIVGTT indicated that there was less decline to fasting glucose, fasting insulin, and beta cell function, while there was an increase to systemic insulin sensitivity. Since the cute insulin response to glucose was unchanged following surgery, it would suggest that there is a decline the second phase of insulin secretion from beta cells. These results are consistent with prior results of SG surgeries in patients without Type II Diabetes. (Basso et al. 2011, Min et al. 2020)

While none of the measurements from polysomnography were altered following surgery, there were trends for improved wake-after-sleep-onset and sleep efficiency. It is important to note

that subjects that used a continuous-positive-air-pressure machine at baseline also utilized the machine at post-surgery. Further, a full-polysomnography recording session was conducted prior to baseline and post-surgery sessions, which should reduce the risk of spurious differences due to first exposure to the protocol.

Chapter 3: Evaluation of Reference Gene Suitability for Serial qRT-PCR Measurements of Human Adipose Tissue from Obese Women Undergoing Sleeve Gastrectomy Surgery

Abstract

A hallmark of biology is the cyclical nature of organismal physiology driven by networks of biological, including circadian, rhythms. Quantitative reverse transcriptase polymerase chain reaction (qRT-PCR) has been a fundamental method to measure oscillation in messenger RNA expression, which is an essential foundation for the study of the physiological circadian regulatory network. Adjustment of raw qRT-PCR outputs to enable the detection of rhythmic oscillations has involved the use of reference gene normalization. However, the validation and identification of suitable reference genes is a significant challenge across different biological systems. Therefore, to ensure consistent normalization conditions, we identified a well calibrated reference gene set. This study focuses on subcutaneous adipose tissue of premenopausal, otherwise healthy, women with morbid obesity. Tissue was collected longitudinally by primary biopsy at baseline one week before surgery and twelve weeks following surgery. Further tissue was cultured *ex vivo* and serially collected every four hours across a thirty-six-hour time series experiment. Candidate reference genes were: *18S rRNA, GAPDH, HPRT1, RPII, RPL13α, and YWHAZ*. Three analytic tools were used to test suitability, and the candidate reference genes were used to measure oscillation in expression of known circadian clock elements (*hDBP* and *hBMAL1*). No gene was deemed suitable as an individual reference gene control, which indicated that the optimal reference gene set was the geometrically averaged 3-gene panel composed of *YWHAZ, RPL13α,* and *GAPDH*. These methods can be employed to identify optimal reference genes in other systems.

Introduction

A hallmark of biology is the cyclical nature of organismal physiology, which is driven by networks of biological rhythms. These rhythms are remarkable for their breadth throughout biology as showcased by their observation across the phylogenetic tree from bacteria, fungi, plants, and animals that include fruit flies and mammals. (Pittendrigh 1954, Lam et al. 2018, Kaczmarek et al. 2017, Cui et al. 2013). Further investigation into the biological rhythms has revealed a major role of a molecular apparatus composed of a hierarchical set of transcription factors called the circadian clock, which enables fine-tuning of physiological function to meet the multitude of constantly changing conditions and demands. (Czeisler et al. 1999b)

A large portion of the molecular basis of central and peripheral circadian rhythms has been examined via quantitative reverse transcriptase polymerase chain reaction (qRT-PCR), which has served as the gold-standard method to measure individual mRNA species. In this period, reproducibility and comparability of qRT-PCR experiments has been bolstered by establishment of the MIQE guidelines, which are the minimum information for publication of quantitative RT-PCR experiments. (Bustin et al. 2009) However, all potential reference genes have conditions whereby expression has been shown to deviate significantly. For circadian rhythms, the adjustment step may either accentuate, or attenuate, circadian gene expression differences across the 24-hour period. The consequence is that we need a library of conditions whereby reference genes or sets of reference genes have been identified as suitable for normalization. (Bustin et al. 2013) The primary goal of this study was to characterize the consistency of candidate reference genes for repeated measurements of circadian gene expression in the context of obesity and bariatric surgery. We were unable to identify a single gene, but were able to identify a reference gene set that was suitable.

Materials and Methods

Study Design

As previously reported, pre-menopausal women with morbid obesity were voluntarily enrolled with informed written consent in the clinical research study (University of Chicago IRB 09-337-B) following approval and scheduling for laparoscopic sleeve gastrectomy (LSG) surgery. A subset of four subject were used for the analysis supplied herein. There were no differences in criteria applied for medical or lifestyle requirements. Nor were there differences in the design or timing of the baseline and post-surgery sessions. One of the four subject utilized continuous positive airway pressure machine both the baseline and post-surgery session.

Biopsy Processing

There are no differences in the protocol used for processing the primary tissue biopsy nor were there differences in the design of the time series tissue culture experiment. The tissue was washed, minced finely, and rested. Following which, the tissue was volumetrically plated into separate wells in a 1:10 ratio to minimal M199 media for the tissue culture. Every three hours, a well of minced adipose tissue was collected and flash-frozen for storage in a -80°C manual thaw freezer.

Recombinant DNA Sample Preparation

Tissue was homogenized by two ten-second-pulses using a dispersion-based homogenizer (VWR VDI 12). RNA was isolated from the tissue homogenate using a cold phenol-chloroform-isoamyl-alcohol liquid-liquid separation followed by acid guanidinium-ethanol mini-column isolation and final elution with 1 µM sodium citrate (Omega cat # R68300). RNA purity was verified and concentration determined by Nanodrop UV-spectroscopy. For reverse transcription

step of cDNA synthesis, 500 ng sample RNA per 20 µL was converted using Quanta Qscript Master Mix (cat # 95048) chemistry in a standard thermocycler (Applied Biosystems GeneAmp PCR System 9700). RNA integrity was conducted using a 5'-3' primer assay on the reference gene: YWHAZ; all samples were assessed to have high integrity (1.00 ± 0.72).

Primer Validation

Efficiency and dynamic range were collected via the gold-standard method of a dilution curve. Maximal cDNA template concentration was a ten-fold dilution from the completed cDNA synthesis thermocycler reaction volume; successive serial dilutions were eight-fold. The slope of the line (m) was calculated by a trendline from three or more consecutive dilutions. Efficiency was calculated using the equation below with m as the slope and d as the dilution:

$$E = d\text{^}\frac{1}{m} - 1$$

Perfect efficiency was 100%. According to MIQE guidelines, primer efficiency estimated above 0.9 can presumed to be perfect efficiency for ΔΔCq relative quantification. Primer sets with lesser efficiency are suggested to use the Pfaffl correction to adjust raw Cq values to be as if the primer set had optimal efficiency. RPII was the only gene that required a Pfaffl correction (E = 0.89), the formula for which is listed below:

$$C_{q,adj} = C_{q,raw} + \log_2\left(\frac{2^{-C_{q,raw}}}{(E+1)^{-C_{q,raw}}}\right)$$

Dynamic range was experimentally defined by the template concentrations used to calculate efficiency. Within this concentration range, no extrapolation is needed to confirm high efficiency amplification. No raw Cq values obtained fell outside the dynamic ranges calculated from the dilution curves.

qRT-PCR

Hypoxia & Differentiation	Hormonal Milieu Changes	Visceral & Subcutaneous adipocytes from Lean & Obese Subjects
1. YWHAZ	**1. HPRT1**	**1. HPRT1**
2. TBP	2. ACTB	2. HMBS
3. GUSB	**3. GAPDH**	**3. RPL13α**
4. GAPDH	**4. RPII**	**5. GAPDH**
5. ACTB	**5. YWHAZ**	**6. YWHAZ**
6. *18S rRNA*	> 8. B2M	8. ACTB
	18S rRNA	*9. 18S rRNA*

Figure 3.1: Experimental conditions that informed selection of candidate reference genes. Columns represent ranked stability of reference genes under each different experimental manipulation from previous studies. The thick black dividing line indicated genes that were considered unsuitable for use as reference genes. Bolded genes indicated the reference genes chosen as candidate reference genes.

The selected screen for effective reference genes was limited to the bolded genes in Figure 3.1, which illustrated reference gene suitability from previously published experimental manipulations. (Fink et al. 2008, Foldager et al. 2009, Curtis et al. 2010, del Pozo et al. 2010, Mehta et al. 2010, Amable et al. 2013, Jacob et al. 2013) The primer sequences are listed in Table 3.1. (Radonić et al. 2004, Curtis et al. 2010, Valadan et al. 2015) *hDBP* and *hBMAL1* primers (Qiagen cat# PPH19697A & PPH06229F) were purchased with a documented guarantee for high efficiency and broad dynamic range but without a precise sequence. To prepare the qRT-PCR experiment, all equipment was thoroughly cleaned with 70% ethanol. Only autoclaved tubes and unopened pipette tip boxes were utilized. Per well, the total reaction volume was 10 µL which consisted of: 4 µL cDNA template, 5 µL SYBR green master mix (Quantabio cat# 95071), and 0.5 µL of each forward and reverse primers. Template concentration of cDNA was 1:100 relative to the reverse-transcription-reaction-derived cDNA. One plate was used per gene per subject with three technical replicates, three positive controls to serve as inter-plate calibration, and three no-template negative controls. Loading was completed over ice before plates were sealed (BioRad cat

MSB1001) and centrifuged (1000 xg, 1 min) to eliminate any bubbles. Running conditions on the CFX Connect Real-time PCR Detection system was: (40 cycles, 60°C annealing temperature). A melt curve was collected for each plate; no contamination or primer dimers were found.

Table 3.1: Summary table of candidate reference gene primer nucleotide sequences with efficiency (E) and source of prior publication.

Gene List	Nucleotide Sequence	E	Source
18S	F: 5'- CGG CTA CCA CAT CCAA AGG A -3' R: 5'- GCT GGA ATT ACC GCG GCT -3'	1.00	
YWHAZ	F: 5'- TGC TTG CATCCC ACA GAC TA-3' R: 5'- AGGCAGACAATGACAGACCA-3'	1.00	(Curtis et al., 2010)
RPL13α	F: 5'- AAG GTC GTG CGT CTG AAG-3' R: 5'- GAG TCC GTG GGT CTT GAG-3'	0.94	(Radonić et al., 2004)
RPII	F: 5'- GCA CCA CGT CCA ATG ACA T-3' R: 5'- GTG CGG CTG CTT CCA TAA-3'	0.89	(Radonić et al., 2004)
GAPDH	F: 5'- TGC ACC ACC AAC TGC TTA GC-3' R: 5'- GGC ATG GAC TGT GGT CAT GAG-3'	0.96	(Curtis et al., 2010)
HPRT1	F: 5'- GGA CTA ATT ATG GAC AGG ACT G -3' R: 5'- GCT CTT CAG TCT GAT AAA ATC TAC -3'	1.00	(Valadan et al., 2015)

Results

BestKeeper

Four subjects were utilized for the sub-study. The total data set was composed of approximately one hundred points, which is high enough resolution to visualize the distribution of the expression levels of each potential reference gene (Figure 3.2). A quantile-quantile plot was constructed to identify whether the relative expression levels was approximately normal. To prepare the data, raw Cq values were converted to the relative quantities. Secondly, the mean and standard error was calculated using the relative quantities. Next, estimated data points were produced from a normal distribution with a mean and standard deviation equivalent to the

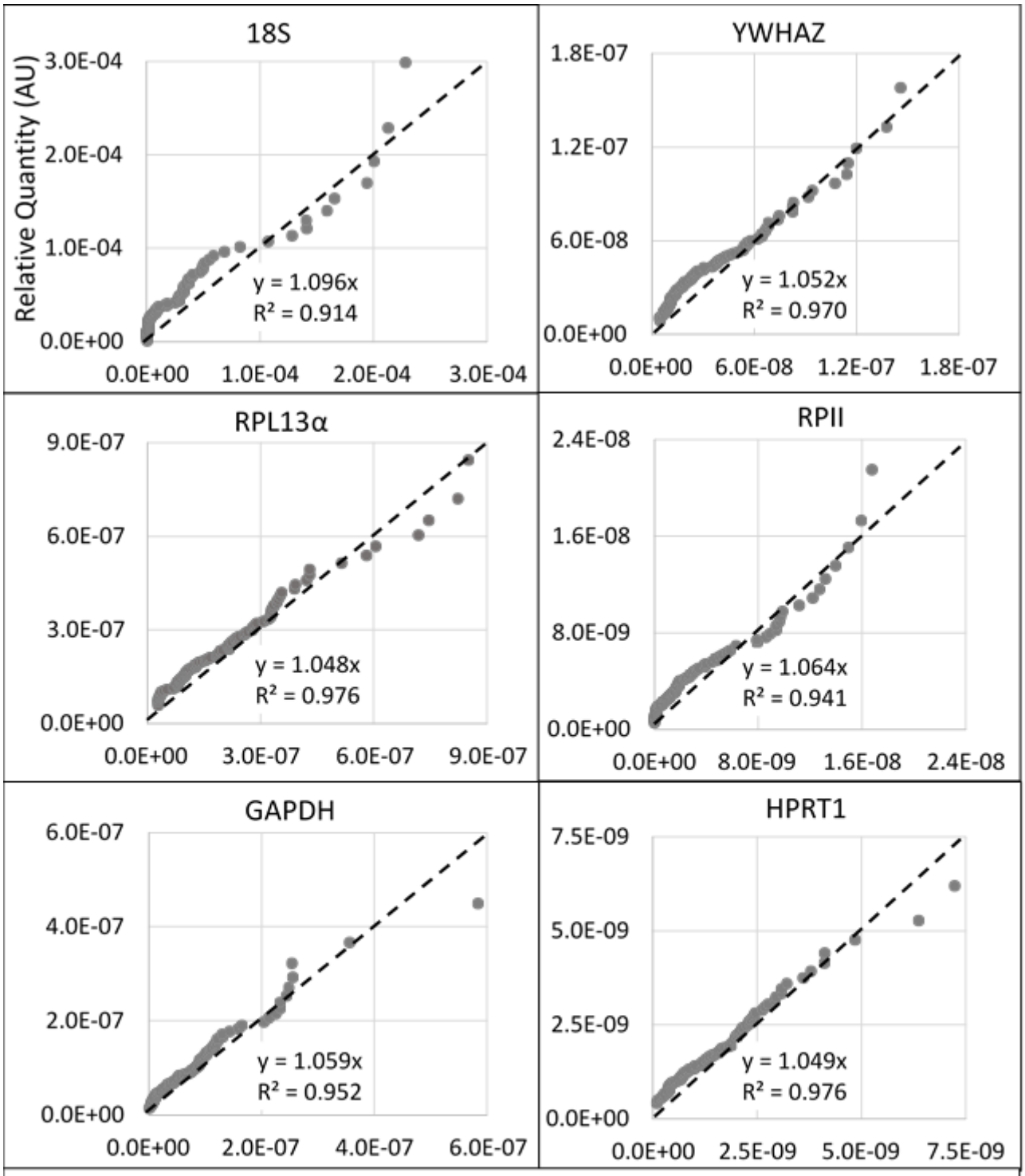

Figure 3.2: Quantile-Quantile plot of the distributions of mRNA transcript expression imputed from the raw fluorescence data of candidate reference gene runs. Horizontal axis represented the linearly-transformed experimental data (2^{-Cq}). Vertical axis represented the imputed quantile from a normal distribution with mean and standard error imputed from linearly-transformed experimental data. Normality was indicated by adherence to the black dotted line.

calculated sample mean and sample standard error. The values of the estimated data points were calculated from the normal distribution at z-scores that reflected the percentile of the rank-ordered data set. The rank-ordered experimental data set was then plotted against the estimated data set in a quantile-quantile plot (Figure 3.2). If the experimental data set was perfectly normal, this plot would reflect a line with slope of one. The plots were approximately linear for each of the candidate reference genes with each gene suggesting a slightly higher dispersion (slope > 1) than standard for a normal distribution.

Given acceptable data distributions, general measures of each distribution were calculated using the Microsoft Excel Add-in BestKeeper. Statistics that provided a general idea of the suitability of the candidate reference genes were: mean Cq, and standard error. Mean raw Cq is probative, or qualitative, evidence of stability. Extremely high or low mean Cq (above/below the range of 20-30) suggested potential for instability in future experiments. Two explanations inform this general property: 1) the technical limitations of a qRT-PCR assay, and 2) the dynamic range of each primer set. High Cq, which reflected low transcript copy number, did warrant greater concern for failed wells and randomness-induced Cq variability. Mean Cq values for each gene were calculated arithmetically, geometrically, or logarithmically by relative quantities (Figure 3.3). The mean Cq value for 18S was higher than the optimal range (geo μ= 16.77). Additionally, RPII and HPRT1 had mean Cq values near the upper boundary (respective geo μ = 29.41; 29.65). The three that were in the middle of the range were YWHAZ, RPL13α, and GAPDH. The respective geometric mean Cq for these genes were 25.19, 22.5, and 24.35. These results suggested that using three of the six genes (RPII, HPRT1, or 18S) may add experimental difficulty to potential future experiments.

The second statistic used within the software was standard error of the raw Cq values (Figure 3.3). Given the normality of the sample distributions, a minimized standard error strongly suggested superior reference gene stability. The suggested cut-off points for individual reference gene suitability (± Cq) have been recommended to be 0.5 for genetically homogenous data sets and 1.0 for heterogeneous data sets. For three genes (18S, RPII, and GAPDH), respective standard error was markedly elevated (2.37, 1.94, and 1.46) from the recommended standard. F-test

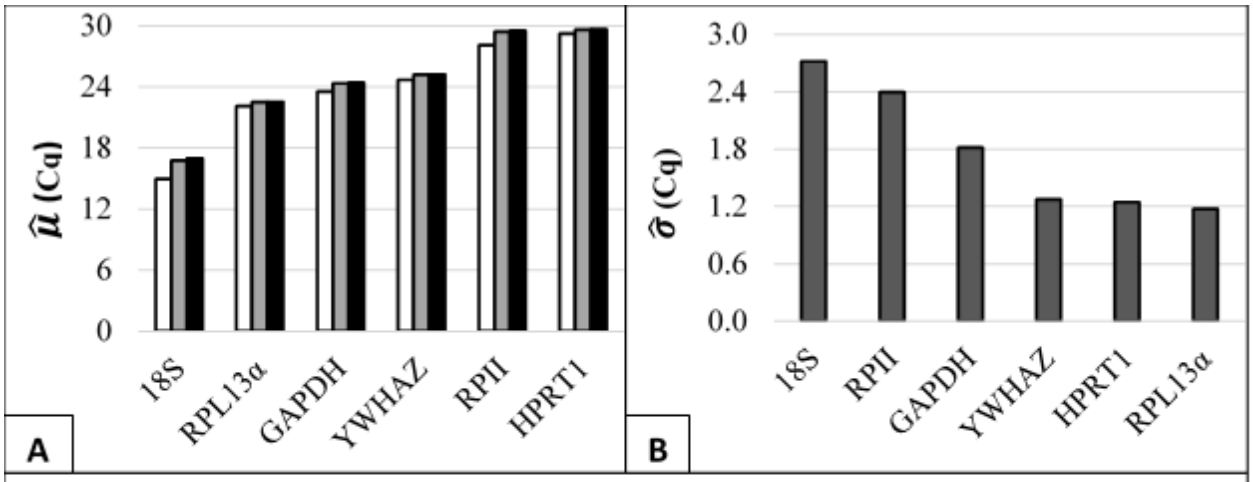

Figure 3.3: General characteristics of candidate reference gene sample Cq distributions. **(A)** Respective estimates of mean Cq ($\hat{\mu}$) were calculated for sample Cq values using [white] relative transcript quantities, [grey] geometric averaging, and [black] arithmetic averaging. **(B)** Estimates of standard deviation ($\hat{\sigma}$) were calculated from sample Cq values.

	18S	YWHAZ	RPL13a	RPII	GAPDH	HPRT1
18S	--	2.87E-12	1.67E-14	0.22054	1.26E-04	6.39E-13
YWHAZ	2.87E-12	--	0.42866	4.05E-09	7.40E-04	0.81273
RPL13a	1.67E-14	0.42866	--	4.17E-11	3.52E-05	0.57899
RPII	0.22054	4.05E-09	4.17E-11	--	8.26E-03	1.07E-09
GAPDH	1.26E-04	7.40E-04	3.52E-05	8.26E-03	--	3.14E-04
HPRT1	6.39E-13	0.81273	0.57899	1.07E-09	3.14E-04	--

Figure 3.4: Significance of differences in estimations of variance between candidate reference genes. Significance of estimated standard deviations was calculated by an F-test on the raw Cq values for all samples. White indicated comparable experimental variance. Dark grey indicated statistically significant differences in the estimations of experimental variance.

comparison of variances indicated that 18S rRNA and RPII had comparable variances (0.22), while GAPDH had different variance from either (1.3e-4 and 8.3e-3, respectively) (Figure 3.4). For the remaining three genes tested (YWHAZ, HPRT1, and RPL13α), comparable standard error was found (1.08, 0.96, 1.01). Yet, it is notable that none of the reference genes exhibited standard error that was clearly below the heterogeneous data set standard.

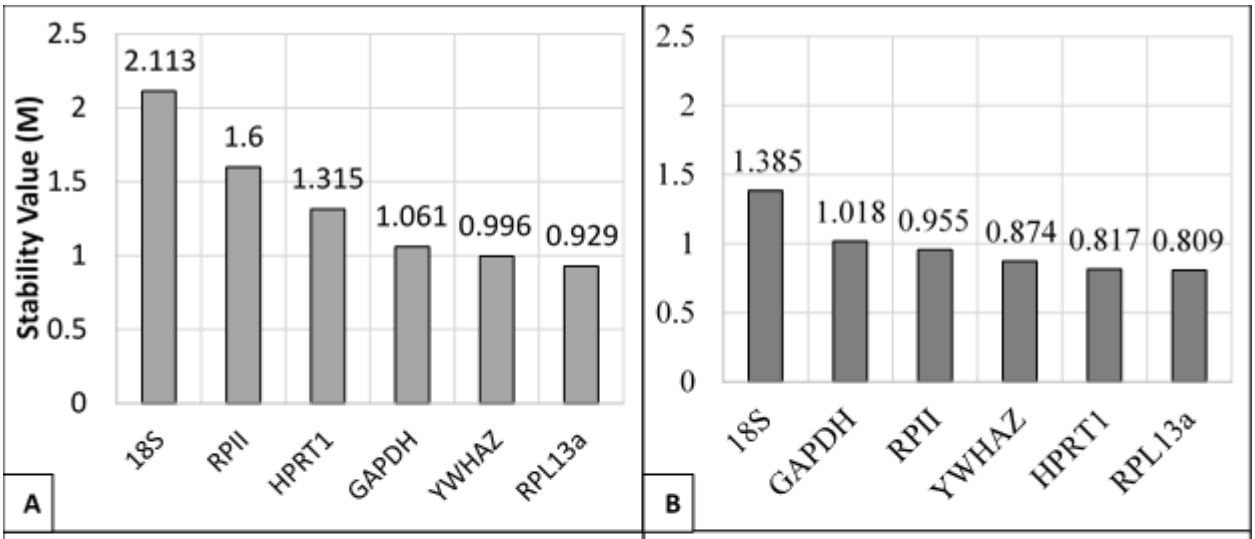

Figure 3.5: Stability values for each candidate reference gene by biopsy as calculated using qBase+ software. To illustrate data leverage for respective composite stability values, respective stability values were calculated for data from each included biopsy. Smaller values indicated better suitability. **(A)** subcutaneous adipose tissue, one-to-two weeks prior to surgery. **(B)** mesenteric adipose tissue, immediately prior to surgery. **(C)** subcutaneous adipose tissue, twelve-to-thirteen weeks following surgery.

GeNorm

The module geNorm within the subscription software qBase+ was next used to assess stability by a proprietarily determined variable (M). Under optimal suitability M is minimized to

zero. Similar to the prior analysis, the cut-off for suitable genes was 0.5 for genetically homogenous data sets and 1.0 for heterogeneous data sets. Due to the software adjusting for input sample size, this software was used to look at overall stability of the genes and also stability of the genes when segregated by biopsy collection. Given that there were three biopsies collected with identical collection times, the size of the data sets for the individual biopsy experiments are one-third the size of the cumulative data set.

For each gene, it was clear that one-to-two weeks prior to surgery exhibited the highest M, and therefore the worst stability (Figure 3.5). However, twelve-to-thirteen weeks following surgery was more stable for three genes (GAPDH, YWHAZ, and RPL13α) and less stable for three genes (18S, RPII, and HPRT1) as compared to immediately prior to surgery. As a result of these

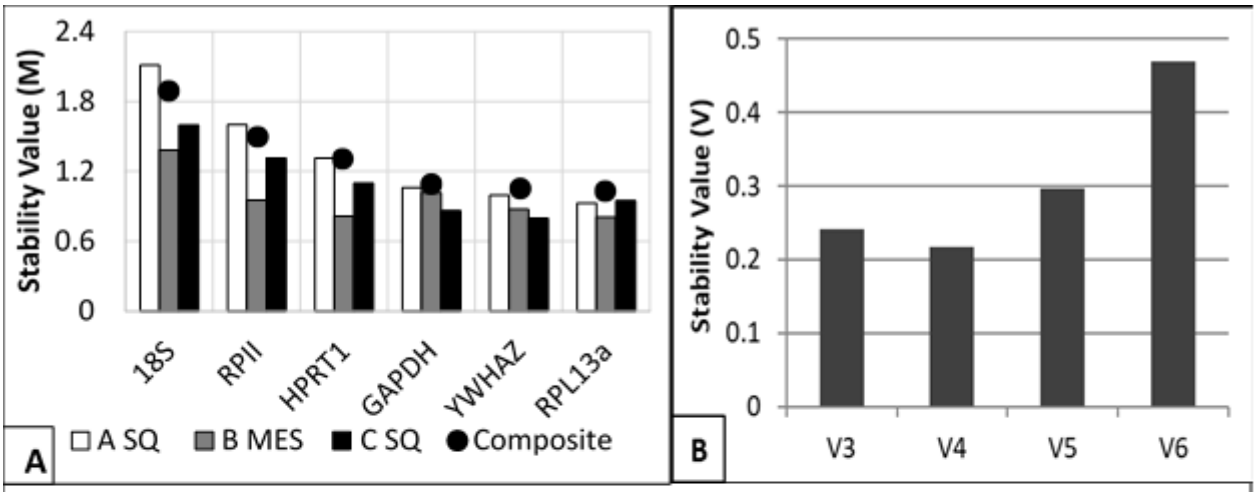

Figure 3.6: Stability values calculated using qBase+ software. A) Stability values for each candidate reference gene by biopsy. Smaller values indicated better suitability (suitable for homogenous data < 0.5; suitable for heterogeneous data < 1.0). Data set was partitioned and analyzed separately by biopsy: (white) subcutaneous adipose tissue, one-to-two weeks prior to bariatric surgery [A SQ]; (grey) mesenteric adipose tissue, immediately prior to surgery [B MES]; (black) subcutaneous adipose tissue, twelve-to-thirteen weeks following surgery [C SQ]. The plotted points represented the data analyzed as one set. **B) Output from geNorm V panel in qBase+ software.** Panel suggested the optimal number of genes to include in the reference gene set. Columns represented stability value associated with geometrically-averaged top three gene Cq values (V3 = YWHAZ, RPL13a, GAPDH), and then the successive stability values that included HPRT1, then RPII, and lastly 18S.

findings, the cumulative data set closely paralleled the stability value of the biopsy obtained one-to-two weeks prior to surgery.

As an overall ranking, three genes exhibited comparable stability values (GAPDH, YWHAZ, and RPL13α) at respective M: 1.09, 1.051, and 1.03 (Figure 3.6). HPRT1, despite indicating higher stability in the previous analysis, was indicated to have notably lower stability (1.307). RPII and 18S rRNA exhibited M values of 1.60 and 2.11, respectively. As individual reference genes, none of the genes exhibited overall stability values below one. Yet, the three highest rated genes were, again, only slightly offset from the soft cut-off point.

Normfinder

In the Normfinder algorithm, stability values were not independently determined for each candidate gene. Rather, each candidate reference gene was given a stability value estimating the instability that it provided to the ordered set of geometrically-averaged relative quantities (2-Cq). As designed, the dependency was to facilitate construction of candidate reference gene sets, which will be discussed later. As a result of the program design, suitability in this program was qualitative and was relative to the other genes in the set. For clarity, reported stability values were calculated including each of the six candidate genes (Figure 3.7). As the last parameter, the

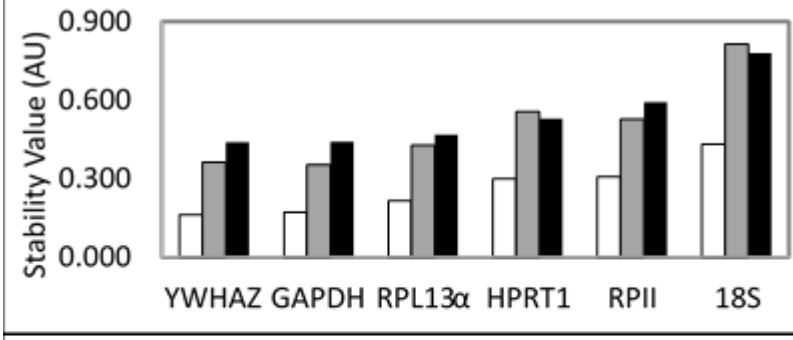

Figure 3.7: Stability values as calculated by Normfinder Excel Add-in with explanatory variable grouping. Increased suitability of respective reference genes was qualitatively indicated by lower stability values. Measurements were grouped to define an explanatory variable for relative quantity variation. Group were defined as: (white) collection times, (grey) biopsies, or (black) both biopsies and collection times.

program allowed explicit grouping of samples to explain a portion of the variation. In Figure 3.7, three different sample groupings were used: 1) collection time, 2) biopsy, or 3) both collection time and biopsy.

For each of the ways to group samples, the genes measured to be the most stable were: YWHAZ, GAPDH, and RPL13α. 18S, again, was assessed to be the least stable candidate reference gene irrespective of sample grouping. HPRT1 was ranked to be more stable than RPII under two groupings, but worse when grouping samples by biopsy. Grouping by collection time did result in lower stability values compared to the other groupings, which suggested that more variation could be explained by collection time.

BestKeeper, Composite

Since no individual reference gene was definitively sufficient to serve as the internal reference, the analysis shifted to identifying the suitable composite reference gene set. (Vandesompele et al. 2002b) The procedural definition was that, upon geometric-averaging of multiple reference gene Cq values, the composite Cq for the derived standard will exhibit minimal standard error across samples. Improved stability has been accomplished through deconstructed stochastic variation resulting from opposing biological regulation which should be tangential to the experimental manipulation. However, this effect was balanced by retention of more individually unsuitable genes in the reference gene set.

Three statistics were used to conduct the analysis: 1) individual gene standard error, 2) correlation between the genes, and 3) the composite standard error. The process of finding the optimal set was to, until the composite standard error increased, to iteratively remove the: 1) the gene with highest remaining standard error, or 2) given similar standard errors, the gene with the

highest correlation to remaining genes. This iterative progression enabled the most stable genes to be retained and to maximize the deconstructive variation. The two worst genes were removed from the model leading to the overall variance to decrease markedly. The complete model had a total standard error across samples of 1.480. By the removal of 18S the standard error decreased to 1.256; the subsequent removal of RPII decreased the standard error to 1.074. Following the three individual analyses, it was not clear whether HPRT1 or GAPDH was less suitable.

To gauge the potential consequences of including GAPDH or HPRT1 in the reference gene set, estimated of Pearson correlation were used to estimate covariation between candidate reference genes. Contextually, low covariation suggested that geometric averaging would have an effect to lower experimental variance in future experiments. In this data set, all remaining genes had significant positive correlation with the other genes except GAPDH and HPRT1 ($\rho = 0.166$, $p = 0.11$) (Table 3.2). HPRT1, while significantly related to both YWHAZ ($\rho = 0.266$, $p = 0.009$) and RPL13α ($\rho = 0.275$, $p = 0.007$), the correlation is notably less than GAPDH for the same. Therefore, it was expected that inclusion of HPRT1 would improve future stability of a composite reference set that included YWHAZ, RPL13α, and/or GAPDH.

Table 3.2: Experimental estimation of Pearson correlation between candidate reference gene Cq values. Correlation coefficients were calculated from respective Cq values of all samples. P-values represented the probability that the correlation coefficient resulted from random chance.

		18S	YWHAZ	RPL13a	RPII	GAPDH	HPRT1
18S	$\hat{\rho}$	--	0.4376	0.3531	0.5646	0.5627	0.6119
	p-value	--	1.0 E-05	4.8 E-04	3.1 E-09	3.6 E-09	5.69E-11
YWHAZ	$\hat{\rho}$	0.4376	--	0.5630	0.7670	0.7148	0.2663
	p-value	1.0 E-05	--	3.5 E-09	2.0 E-19	5.9 E-16	0.00947
RPL13α	$\hat{\rho}$	0.3531	0.5630	--	0.8328	0.6134	0.275
	p-value	4.8 E-04	3.5 E-09	--	2.3 E-25	4.9 E-11	0.00726
RPII	$\hat{\rho}$	0.5646	0.7670	0.8328	--	0.8605	0.1917
	p-value	3.1 E-09	2.0 E-19	2.3 E-25	--	1.1 E-28	0.0642
GAPDH	$\hat{\rho}$	0.5627	0.7148	0.6134	0.8605	--	0.1659
	p-value	3.6 E-09	5.9 E-16	4.9 E-11	1.1 E-28	--	0.1101
HPRT1	$\hat{\rho}$	0.6119	0.2663	0.2752	0.1917	0.1659	--
	p-value	5.7 E-11	0.0095	0.0073	0.0642	0.1101	--

To test the prescription, a table was constructed with all permutations of the four most suitable genes (Figure 3.8). When looking at the standard error of gene sets (2 or 3 total) including these genes, the only sets of genes that were overall more stable included HPRT1. YWHAZ and RPL13α had almost no difference in effect on overall stability. And, due to the higher estimate of standard deviation and high covariation with YWHAZ and RPL13α the overall effect of GAPDH was to increase the reference gene set estimates of standard deviation. The suggestion from this analysis was HPRT1 inclusion would improve future composite stability.

Figure 3.8: Standard deviation of geometrically-averaged reference gene set. Excluding RPII and 18S, all possible permutations of multiple genes were tested. First, each sample was geometrically-averaged for included genes. Then, an estimate of standard deviation was calculated for the resulting data set.

Reference Genes				$\widehat{\sigma}$ of $\bar{x}$
YWHAZ	RPL13a	GAPDH	HPRT1	
×	×	--	×	0.946
--	×	--	×	0.971
×	--	--	×	1.005
×	×	×	×	1.074
×	×	--	--	1.081
--	×	×	×	1.096
×	--	×	×	1.149
--	--	×	×	1.215
×	×	×	--	1.237
--	×	×	--	1.336
×	--	×	--	1.436
Mean $\widehat{\sigma}$ for each gene				
1.133	1.106	1.220	1.065	

Table 3.3: Single exclusion analysis conducted through Normfinder Add-in. To identify the best three-gene-set, each gene was iteratively excluded from the reference set, and the stability values were estimated from the remaining genes. Higher stability was evidenced by lower stability values. Additionally, the stability values of the set of the four best suited genes were reported. Lastly, estimated mean stability values ($\hat{\mu}$) were calculated for each gene and reference gene set.

	Best Four	(-) GAPDH	(-) HPRT1	(-) RPL13a	(-) YWHAZ	$\hat{\mu}$, gene
GAPDH	0.535	--	0.369	0.532	0.608	0.511
HPRT1	0.515	0.549	--	0.555	0.523	0.535
RPL13α	0.377	0.468	0.365	--	0.398	0.402
YWHAZ	0.364	0.507	0.230	0.387	--	0.372
$\hat{\mu}$, set	0.448	0.508	0.321	0.492	0.509	

Normfinder, Composite

RPII and 18S were excluded from this analysis due to two variables: 1) previously established poor performance of each in all three analyses, and 2) dependent calculation of each reference gene stability in the analysis module. Similar to the prior test, a selective exclusion was conducted (Table 3.3). Yet, since three genes are needed for the macro to function, the analysis only included the differential effect of a single gene exclusion. Similar to the preliminary analysis, YWHAZ and RPL13a did not notably change the overall data set. However, the effect of GAPDH and HPRT1 on the stability of the reference gene set was reversed in effect compared to the preliminary analysis. Exclusion of GAPDH led to a reduction in average stability of 10-15%, which was commensurate with the effect of excluding YWHAZ and RPL13a. And, exclusion of HPRT1 led to a 30% improvement in reference gene stability. These results suggested that the HPRT1 was the least suited remaining gene for the model. It is notable that this is the opposite recommendation from the BestKeeper analysis.

GeNorm V

In addition to stability value estimates, qBase+ contains a panel, geNorm V, that conducted a selective inclusion analysis. Genes with higher calculated M were iteratively included into the reference gene set. Similar to the earlier stability value, the lower the resulting output the more stable the reference gene set. The goal output for homogeneous data sets is 0.10, and for heterogeneous data sets the output is optimally 0.15. The result of the analysis was to indicate that at least three genes ought to be included in the optimal reference set and that there was evidence to support the inclusion of four genes (Figure 3.6B). The relative improvement from three genes to four genes was a decrease from 0.24 to 0.21. Addition of RPII and 18S into the gene set decreased the relative stability, which agrees with the other analyses that were conducted.

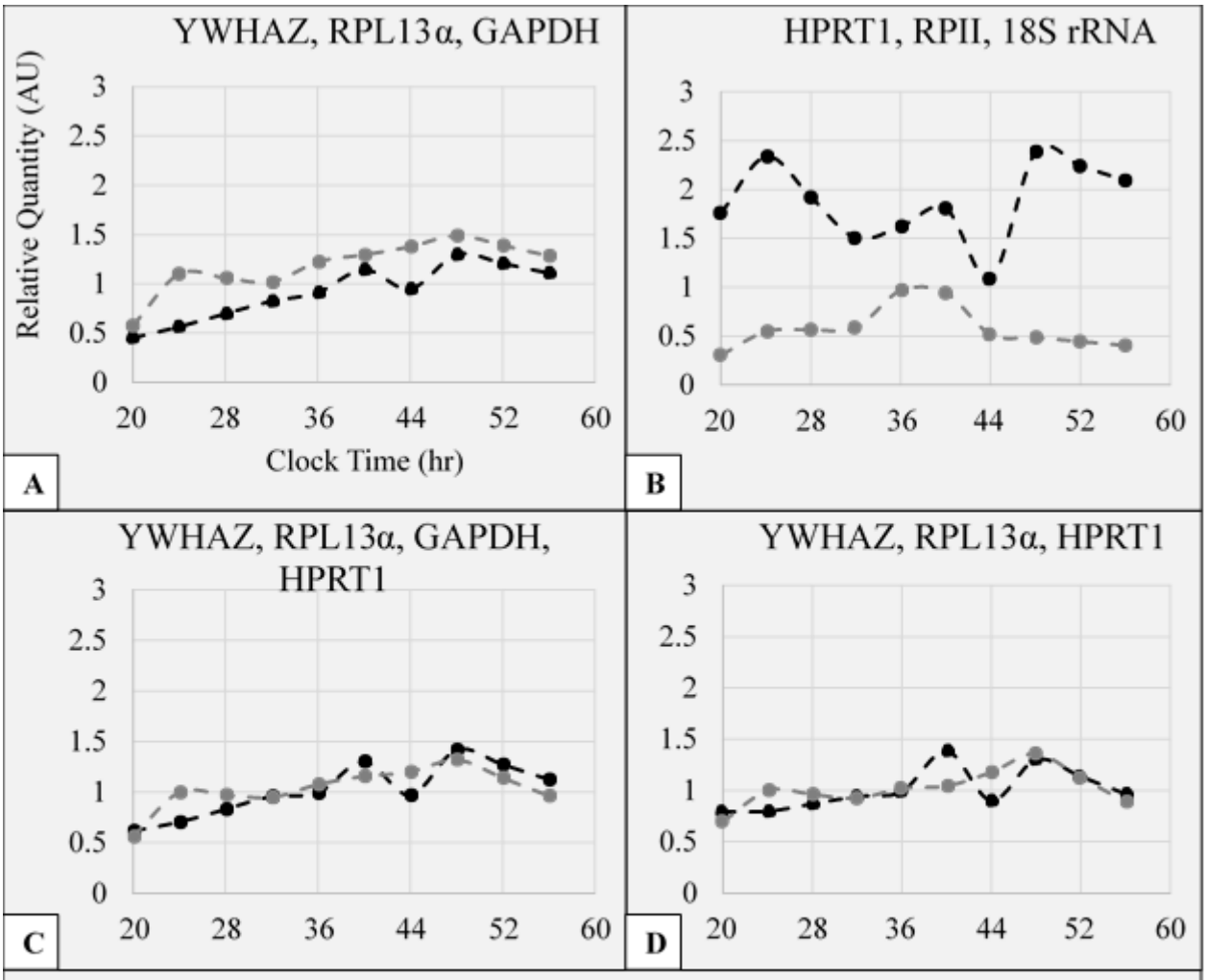

Figure 3.9: Profiles of relative quantities for geometrically-averaged reference gene sets. Sample Cq values for each included gene were geometrically averaged together then were calibrated to the mean Cq values of both included biopsy data sets, which were: (black) one-to-two weeks prior to surgery and (grey) twelve-to-thirteen weeks following surgery. Clock time is counting up from day 0, which included the initial biopsy collection in the morning (20 CT = Day 0, 8 PM).

Circadian Gene Normalization

At the completion of the above analysis, it was concluded that YWHAZ and RPL13α were optimally included in the reference gene set with GAPDH. There is an argument for HPRT1 to be included instead of GAPDH. Yet, it presents increased technical challenges due to high raw Cq

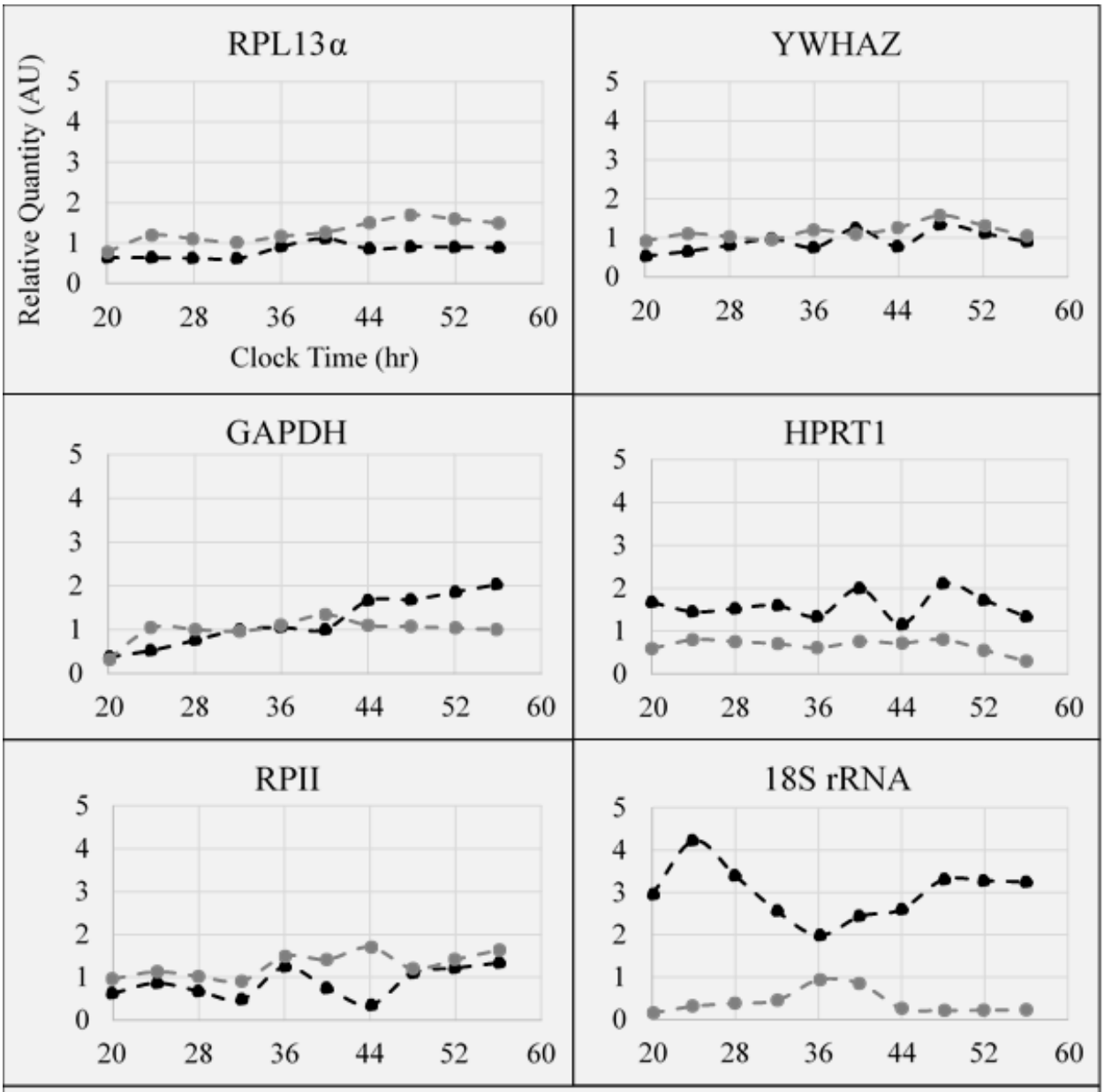

Figure 3.10: **Relative quantity of transcript across time for candidate reference genes.** Time series data were used from biopsies: (black) one-to-two weeks prior to surgery or (grey) twelve-to-thirteen weeks following surgery. Respective relative quantities were calibrated to the arithmetic average Cq of both included biopsy data sets. Clock time is the hour of day starting from day 0, which included the biopsy in the morning (20 = Day 0, 8 PM).

that could overshadow the benefit of greater coverage of stochastic variation due to lower correlation to the other genes in the panel. The disputed suggestion was addressed thusly: 1) illustrating the geometrically averaged relative quantities with four different combinations of

reference gene sets (Figure 3.9), and 2) one subject had mRNA expression measured for Dbp, a circadian clock gene, from samples derived from the biopsies prior to and following surgery normalized by the same four reference gene sets (Figure 3.10). For the latter, reported fold changes are relative to the biopsy from which the samples were derived. Lastly, the relative quantities for each candidate reference gene were plotted across time after calibration to the experimental average Cq for the data collected from the biopsies: 1) one-to-two weeks prior to surgery, and 2) twelve-to-thirteen weeks following surgery (Figure 3.9).For Figure 3.9, the four reference gene sets were: 1) YWHAZ, RPL13α, and GAPDH; 2) YWHAZ, RPL13α, and HPRT1; 3) YWHAZ, RPL13α, GAPDH, and HPRT1; and 4) HPRT1, RPII, and 18S rRNA. The first three reference gene sets corresponded to the suggested options remaining after the conclusion of the rhythm-blind analysis. The fourth reference gene set corresponded to the geometric average of the three worst individually suitable genes (Figure 3.9B). For three potential reference gene sets (Figure 3.9A, C, and D), there was fluctuation across the time series (between 0.5 and 1.5 relative quantity). For the post-surgery biopsy, there were minor peaks that occurred at midnight (24 and 48 clock time). For the pre-surgery biopsy, there were minor peaks at 4 PM of day 1 and 12 AM of day 2. In Figure 3.9B, the pre-surgery biopsy additionally had a peak at midnight of day 1 and the post-surgery biopsy only had a peak between noon and 4 PM of day 1. Lastly, the difference in relative quantity was of a greater magnitude than other panels (Figure 3.9A, C, D) and in a reverse direction. The individual reference gene relative quantity plots were represented in Figure 3.10.

The circadian clock genes, *hBMAL1* and *hDBP*, were measured for the post-surgery biopsy of three subjects. The normalizations were to each reference gene set previously shown in Figure 3.9. These data sets were used to conduct a least-squares cosinor analysis using the method

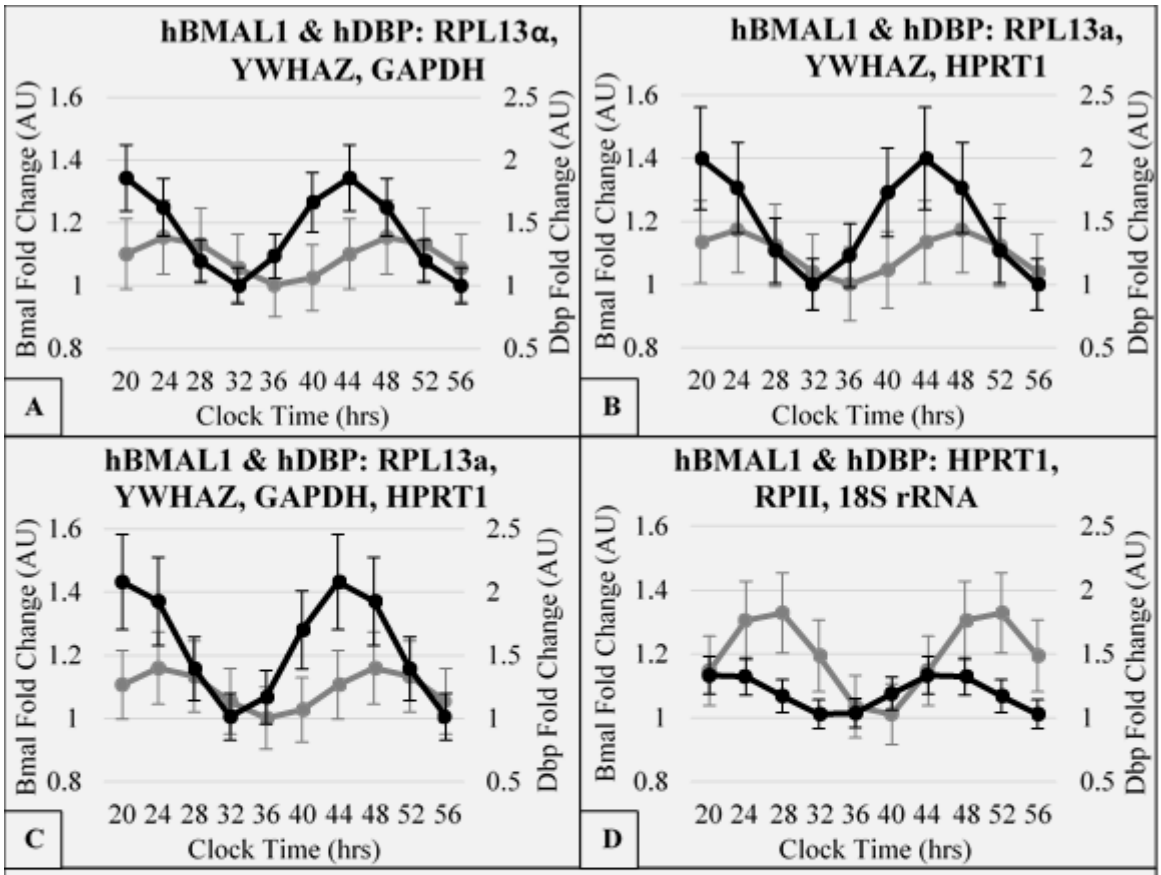

Figure 3.11: Rhythmic gene expression of clock genes, Dbp and Bmal1, as output from least squares cosinor analysis following normalization. Each gene was measured (n = 3) across the time series experiment for *hBMAL1* (grey) and *hDBP* (black) at: twelve-to-thirteen weeks following surgery. Gene expression was normalized to one of four geometrically-averaged reference gene sets. Fold change was calibrated to maximal ΔCq of each gene's normalized data set. Time is clock time relative to day 0, which had the biopsy during the morning (20 CT = Day 0, 8 PM). Cosinor analysis was conducted using R project package: ***cosinor2***.

cosinor.lm from R-project package *cosinor2*. For each gene, cycle length was set to twenty-four hours and time was the only explanatory variable used for the output variable: fold change. The object output from *cosinor.lm* had defined acrophase and amplitude, which were used to calculate the modeled data set for each normalization condition (Figure 3.11). The curves were calibrated such that the minimal data point was set to one. The calculated amplitudes for hDBP were, respectively: 0.43, 0.50, 0.55, and 0.18. The calculated amplitudes for Bmal1 were, respectively:

0.08, 0.09, 0.08, and 0.17. In each panel, the acrophase of hDBP was calculated to be prior to hBMAL1 in agreement with previous work in mice. (Takahashi 2017) The range for acrophase differences was between 3:47 and 5:19 hours (Figure 3.11A, 3.11B, and Figure 3.12). For hBMAL1, the calculated acrophases were, respectively: 0:54, 23:46, 0:43, and 2:39. In contrast, prior reports of hBMAL1 acrophase preceded our report. (Gómez-Abellán et al. 2012, Gómez-Santos et al. 2009) However, in our current study we: 1) utilized no FBS serum shock, which allowed us to maintain the endogenous rhythmicity from each subject; 2) utilized base media of M199 instead of DMEM; and 3) utilized, in media, low insulin (1 nM) and very low dexamethasone treatment (40 nM) to support cell viability. For hDBP, the calculated acrophases were, respectively: 19:36, 19:58, 20:46, and 21:42 (Figure 3.12). Thus, the optimization of reference genes used to normalize the data affect both the amplitude of gene rhythms of circadian genes as well as the phase relationship between the two clock genes.

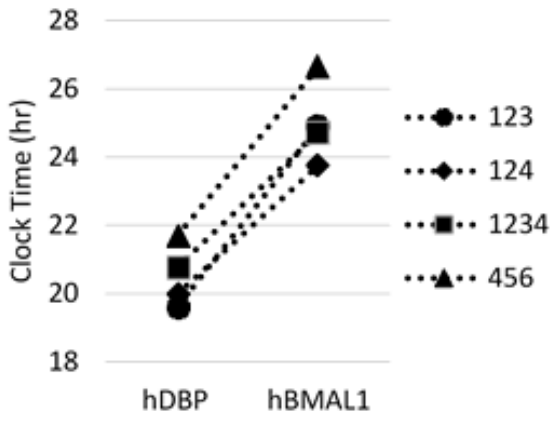

Legend	Reference Gene Set	Bmal Acrophase	Dbp Acrophase	Offset
123	RPL13α, YWHAZ, GAPDH	0:54	19:36	5:19
124	RPL13α, YWHAZ, HPRT1	23:46	19:58	3:47
1234	RPL13α, YWHAZ, GAPDH, HPRT1	0:43	20:46	3:57
456	HPRT1, RPII, 18S rRNA	2:39	21:42	4:57

Figure 3.12: Acrophase for hBMAL1 and hDBP calculated through cosinor analysis. Cosinor analysis was conducted through use of R-project package: ***cosinor2.*** Acrophase is a calculated variable of linear modeling object produced through cosinor.lm() method. Data set for each gene (n = 3), *hDBP* and *hBMAL1*, was from biopsies obtained: twelve-to-thirteen weeks following surgery.

Discussion

Circadian rhythms are indispensable for understanding of normal physiology, and for research addressing the transition into pathophysiology. This is made clear in studies that have examined the disruption of circadian rhythms by sleep curtailment or shift work, and the resulting positive association with obesity, insulin resistance, and diabetes. Improving precision of the assays that observe circadian rhythms is still on-going. This work is meant to add to this knowledge, particularly, in this context, qRT-PCR assays for measuring target gene expression.

To accomplish this goal, primary subcutaneous human adipose tissue was *ex vivo* cultured and periodically harvested. Previous literature documented that these culture conditions allowed for the preservation of circadian patterns of gene expression in primary adipose tissue, and the results shown in Figure 3.12 support this conclusion. These conditions were utilized to allow for a complex example of adipose tissue health and endocrine regulation on circadian rhythmicity. With this data, we were able to analyze the proof-of-concept differences in circadian rhythmicity, and assess how suitable previously verified reference genes were under the tested experimental conditions.

The aim of this study was to assess whether any of the candidate genes were sufficient to function individually as reference genes, a practice widely employed in research. Despite vetting by other papers assessing that the genes used were stable under hormonal treatment, BMI-variation, and in adipose tissue, in our hands under the experimental conditions and human subjects used, none of the genes resulted in sufficient stability to function across these conditions. Yet, even under these extremely heterogeneous conditions it was possible to create a reference gene set (YWHAZ, RPL13α, and GAPDH) that was most advantageous to interpret experimental results. At the least, these results strongly suggest that more attention is owed to verifying that the

reference standard is sufficiently stable for any given experiment. It is plausible to create a system with an unwieldy oversight burden for disseminating qRT-PCR results. Yet, the process is not sufficiently transparent regarding the effect of normalization on experimental results. This critique either overtly or implicitly undermines the confidence in a technique that is still widely relied upon.

Each method to determine the stability of the reference genes relied on different assumptions of what was required for an acceptable reference gene standard. Use of more than one method is encouraged to verify the provisional stability assessment offered by a single method. The overlap for genes that performed well or poorly did agree between the methods utilized in this study. However, the suitability became more muddled between the approaches if under the experimental conditions there was no gene that clearly performed well. In this case, using the multiple analytic tools offers two options: 1) finer distinctions between suitability of the individual genes, or 2) incorporation of multiple genes into a reference gene set. Since the genes that are being considered are likely to be nearer to the border of acceptability, use of multiple methods fosters a more balanced understanding how each gene could serve within the reference gene set.

There were two genes that deserved to be discussed in particular. Despite still being widely used, 18S rRNA performed the worst of the six genes tested in the study. This provides increasing evidence that 18S rRNA has certain experimental conditions that lead to notably high variation. Since this is the case, this study shows evidence that corroborates that 18S rRNA should be rigorously tested before acceptance as a reference gene, particularly in regards to circadian clock genes assayed over a period of time. The other gene of note was HPRT1. As would be expected with the previously noted high average Cq, there were a high rate of failed qRT-PCR runs. Yet, also supporting previous literature is that re-running the failed wells did result in an average Cq

across conditions that was near to the stability of the best performing genes. It remains uncertain whether the stability is due to actual gene expression or manipulation of stability by the rejection of any results that fall out of the narrow acceptable range.

This current study does rely on the fundamental assumption that random enrollment yields representative subject selection. More subjects are always advantageous for suitable representative of subject populations, and there were a comparatively small number of subjects included in this analysis. However, the paired aspect of the study design enabled a more thorough interrogation of the stability of the genes in these individuals. It is true that individual time course measurements were not entirely independent of the other measurements, but there is not consensus of how dependency should be effectively controlled given that biological rhythm research already involves one layer of linear modeling. This study instead made more measurements to account for the stated dependency.

In the tool BestKeeper, there is explicit regard for the concern of co-regulation of reference genes and target genes. The conceptual risk is that since neither reference genes nor target genes operate outside the cellular regulatory mechanisms, there exists the possibility that the experimental manipulation will be reflected in both the reference gene and target gene expression. The downside of this result is that the ΔCq normalization step will eliminate, or dampen, the actual change in target gene expression. This is an example of a false negative error. Therefore, care should be taken in the selection of candidate reference genes. Yet, there is no firm guideline as to what constitutes unacceptable co-regulation. So, instead, it is suggested that this error is conceptually and experimentally addressed by considering and measuring covariance of a number of potential reference genes for each set of experimental protocol used to obtain the greatest fidelity in these critical tools for data normalization.

Chapter 4: Adipose Tissue Circadian Clock Upregulation is Highly Associated with the Degree of Weight Loss Twelve Weeks following Sleeve Gastrectomy

Abstract

In humans with morbid obesity, there is a significant trend for the attenuation of systemic circadian rhythms and a deterioration of metabolic health. Bariatric surgery has been shown to improve several systemic and adipose tissue metabolic health parameters. We tested the hypothesis that bariatric surgery would accentuate the cycling of the adipose tissue circadian clock. We recruited ten women with morbid obesity who had been scheduled for laparoscopic sleeve gastrectomy (LSG). We collected a peri-umbilical fat biopsy at baseline and twelve weeks following surgery. The tissue was minced and sterile cultured in separate wells for approximately twenty-four hours. A well of fat was collected every three hours and flash frozen. To assess changes in gene expression of components of the circadian clock, reverse-transcriptase qPCR was conducted from each tissue section on twelve genes. Fourier-based bimodal cosinor regression was conducted (CircWave) to estimate parameters of the respective biological rhythm profiles assuming 24-hr phase duration. The amplitude of the *hBMAL1* profile was accentuated after surgery. No phase shifts were detected. To assess the changes to average expression, a parsimonious mixed effect models were built from expression data from each circadian clock gene. Expression was increased for seven genes (hNPAS2, hDBP, hCRY1/2, hPER1/2/3) and decreased for two genes (*hNFIL3*, *hREVERBα*). Changes to hDBP expression were highly associated with changes to several clock elements (*hCRY2*, *hPER1/2/3*). Changes to *hNPAS2* expression were associated with changes to *hCRY1*, *hPER2/3*. The degree of these changes was associated with improved weight loss and decreased calories consumed post-surgery. Therefore, in adipose tissue, the short-term effect of

LSG appears influence accentuation of rhythmicity driven by greater overall expression favoring expression of positive regulatory elements for *hDBP* and *hNPAS2*.

Introduction

Despite lesser contribution to overall glucose disposal, adipose tissue has been shown to have a profound impact on systemic metabolic function. (Fu et al. 2005, Salans, Knittle and Hirsch 1968, Li et al. 2011, Cao 2013, Kershaw and Flier 2004, Kohlgruber and Lynch 2015, McGown, Birerdinc and Younossi 2014, Manna and Jain 2015) Traditional lifestyle modification can result in improvements in metabolic syndrome, but weight loss remains difficult to maintain. (Weiss et al. 2007, Unick et al. 2013, van Baak and Mariman 2019, Crowe et al. 2015, Wadden et al. 2007) Yet, dramatic long-term improvements have been achieved in weight loss, overt measures of metabolic health, and the reduction of risk factors through bariatric surgeries including LSG. (Fischer et al. 2012, Shi et al. 2010, Albers et al. 2015, Adams et al. 2007, Basso et al. 2011, Ashrafian et al. 2011, Bohdjalian et al. 2010, Casella et al. 2016, Castagneto-Gissey and Mingrone 2012) Impressively, these effects have been shown to occur beyond the expectation by weight loss alone. (Chambers et al. 2011, Longo 2014)

The circadian clock is a 24-hr pacemaker that instills a temporal organization to energy-intensive metabolic processes. (Lamia et al. 2008, Nikolaeva et al. 2012, Zvonic et al. 2006) The baseline of these rhythms is set for all molecular clocks by the central clock in the suprachiasmatic nucleus, which is entrained to a few key signals like light. (Czeisler et al. 1999a, Berson et al. 2002, Radziuk 2013) Yet, the circadian clock is a cell autonomous molecular apparatus found in each cell of major peripheral organs. (Panda et al. 2002, Nikolaeva et al. 2012, Zvonic et al. 2006) This design allows for centralized control, which is decoded by the organ-specific clocks, called

peripheral clocks, to affect organ-specific metabolic functions. Further, humoral signals act on specific clock components of the peripheral clocks or central clock to facilitate any necessary adjustments. (Panda et al. 2002, Dvornyk et al. 2003, Ouyang et al. 1998, Spoelstra et al. 2016, Dodd et al. 2005)

Our inquiry was focused on the human subcutaneous adipose tissue clock in time-relation to LSG surgery. We conducted time-series experiments on sterile-cultured adipose tissue derived from peri-umbilical aspiratory biopsies at baseline prior to surgery and at twelve weeks following surgery from women with morbid obesity. At this time following surgery, reports indicate that weight loss and metabolic improvements have begun but have yet to stabilize. Our hypothesis is that the circadian clock activity and organization would be improved following LSG surgery. The particular effects will provide insight into how adipose tissue is involved in the systemic metabolic changes. We show an apparent upregulation in the E-box and D-box ancillary axes that was associated with increased negative arm clock expression. The observed changes were associated strongly with metabolic alterations consistent with negative caloric balance with E-box-associated connection to improved insulin sensitivity.

Materials and Methods

Subject characteristics

Screening of potential subjects and the process of enrollment into the clinical study was conducted as previously described (University of Chicago IRB 14-0984). (White et al. 2020) Ten women with morbid obesity were voluntarily enrolled with informed, written consent following approval and scheduling for LSG surgery.

Laboratory Sessions

In-laboratory sessions were structured as previously reported. (White et al. 2020) Identical sessions were conducted at baseline one-to-two weeks prior to the scheduled surgery date and twelve-to-thirteen weeks following the surgery date.

qRT-PCR

Experimental design and execution of qRT-PCR runs were as previously described. (White et al. 2020) The runs were prepared on ice with SYBR green chemistry in low-profile 96-well plates with melt curve calculation, three technical replicates, and inter-plate calibration on CFX Connect Real-time PCR Detection systems (40 cycles, 1000 fixed fluorescent unit threshold). Reference gene normalization was conducted as previously described with three reference genes using geometrically-averaged Cq, as previously described. (Vandesompele et al. 2002a, White et al. 2020) Circadian clock gene primers were purchased from Qiagen with a documented guarantee for high efficiency and broad dynamic range but without a precise sequence. The list of primers used were: *hBMAL1* (PPH06229F), *hCLOCK* (PPH06233A), *hNPAS2* (PPH06232A), *human D-box binding protein* (*hDBP*) (PPH19697A), *hNFIL3* (PPH00415E), *hRORα* (PPH02373A), *hREVERBα* (PPH02259A), *hPER1* (PPH02075A), *hPER2* (PPH06234E), *hPER3* (PPH19810B), *hCRY1* (PPH06231B), and *hCRY2* (PPH06235A).

Rhythm and Expression Analysis

To robustly identify alterations in gene expression of the circadian clock a time series experiment was conducted on minced sterile-cultured peri-umbilical subcutaneous adipose tissue at baseline and post-surgery as previously described. (White et al. 2020) This experimental design allows the ability to interrogate alterations in both the twenty-four-hour rhythms in time proximity

to surgery and to leverage the power of the repeated measures design of the time series experiment to increase confidence of overall gene expression levels.

Quantitative characteristics of each circadian clock gene rhythm were obtained from parameter estimation of Fourier-based cosinor regression software (CircWave version 1.4). (Costa et al. 2013) One harmonic was utilized with phase set to twenty-four hours to allow for testing and regression to a circadian profile. The experimental delta Cq measurements were formatted in two steps: 1) conversion to relative expression, and 2) average twenty-four-hour expression for each subject was adjusted to one. The second adjustment was necessary to treat each subject identically for the regression, which was conducted once including all ten subject profiles. The set of estimated parameters were used to create a profile for a twenty-four-hour rhythm with a data interval of three minutes. The estimated rhythm profile was created for both the baseline measurements and the post-surgery measurements. The acrophase was the estimated clock time of maximal expression. The amplitude was defined as half the difference between the point of lowest expression, the nadir, and the point of maximal expression, the peak. Significance of difference in profiles were compared using two-tailed t-tests.

Mixed Model Construction

Mixed modeling was utilized to estimate the degree of difference in gene expression levels between baseline and post-surgery. Each model required that subjects have at least seventy-five percent of the potential collection samples at both baseline and post-surgery. Model fitting was conducted by R package (lme4). In order to ensure that the dependence derived from time series collection was accounted for in the statistics, the random vector was a simple intercept set as the subject identification number (SID). Experimental expression level was prepared according to the equation below:

$$E_{SID,\ TP} = 2^{-\Delta C_{q,TP}} \div R_{CT}$$

Relative expression (2^-ΔCq) was adjusted for estimated circadian rhythm (R_{CT}) at the clock time (CT) corresponding to that time point to yield gene expression estimates specific for each subject (SID) and time point (TP). The sinusoidal 24-hr rhythms would have violated the linearity assumed in the modeling leading to distorted estimated factor effects and increased variance.

The surgery-associated parsimonious model was calculated by using surgery as a binomial variable (Pre [0], Post [1]) and iterative inclusion of factors representing potential corrections for: 1) age (integer, years), 2) pre-surgery weight loss, 3) post-surgery weight loss, or 4) expression drift across time (time point = integer: $\{1, 2, \ldots, n\}$). This was enabled by holding each potential correction factor constant for all respective points of a given subject. An enhanced model was chosen by: 1) an improved Akaike Information Criterion of the N+1 model (compared to N model without the addition of the factor), 2) each factor effect has low Type S error rate ($p < 0.05$), and low inflation of standard error of estimation (< 50%).

Additional models were made to identify any associations of gene expression with the changes to metabolic parameters. Weight loss after surgery is a primary outcome variable that is collected. Therefore, given that there is weight loss after surgery, we constructed a univariate fixed model to estimate the weight loss after surgery (float, 5 digits) given no change in gene expression (float, 5 digits) from baseline or the average change in gene expression observed in this study from baseline to post-surgery. Yet, we also wanted to provide insight into which metabolic changes were associated with the changes to clock gene expression. Therefore, we estimated baseline and post-surgery gene expression (float, 4 digits) by: 1) fasting glucose (float, 0.01 mg/dL precision),

2) fasting insulin (float, 0.01 mU/L precision), insulin sensitivity (float, 0.01 mU/L*min^-2 precision), four meal laboratory session calories consumed (float, 1e-4 [kCal] precision), glycerol secretion rate (float, 0.01 ng/hr precision), fasting serum FFA (float, 0.001 [100 μM] precision). Disposition Index and beta cell function were run in models, but yielded no significant associations.

Lastly, models were set up to identify whether the changes in one clock gene was associated with the change to other clock genes. A complete model was formed to explain the expression of each gene. Clock elements were excluded that notably increased unexplained variance and that did not notably decrease AIC. Multiple negative arm clock elements (*hPER1/2/3, hCRY1/2*) were not included in the same model due to collinearity of regulation. A parsimonious model was completed when there was at least one D-box acting, E-box acting, and RRE-acting element as well as a negative arm element. This allowed comparison of the degree of association between changes to each element and the association with internal clock transcriptional regulation.

Results

Surgery Effect on Body Composition

A summary of the deidentified subject characteristics is found in Table 2.1. From baseline to post-surgery, subjects lost on-average $7.4 \pm 0.4\ \mathrm{kg/m^2}$ (BMI) (p = 2.6e-7), which was reflected in weight loss of 21.1 ± 0.9 kg (p = 6.0e-10) and 16.7 ± 0.8 % baseline weight loss (p = 1.8e-10). Further, waist-to-hip ratio (unitless) decreased 0.03 ± 0.03 (p = 0.23) while adiposity declined 4.6 ± 0.7% (p = 2.2e-4). These changes reflect profound weight loss and notable improvements in body composition shortly following LSG. Subjects from baseline until preparation for surgery

experienced in 1.7 ± 0.4 kg (p = 3.4e-3) weight loss corresponding to 1.3 ± 0.4 % percent baseline weight loss (p = 3.5e-3) due to pre-surgery-mandated diet.

Surgery Effect on Metabolic Parameters

A summary of changes to metabolic parameters is found in Table 2.3. The four-meal average of calories eaten during laboratory sessions decreased 72.3 ± 4.0% (p = 2.7e-6) from baseline at post-surgery. Fasting plasma glucose (-7.3 ± 2.6%) (p = 0.01), fasting plasma insulin (-50.4 ± 8.8%) (p = 3.8e-5), and beta cell function (-28.7 ± 9.7%) (p = 0.01) decreased from baseline. Insulin sensitivity (57.2 ± 20.9%) (p = 0.02) and glycerol secretion rate (67.4 ± 25.6%) (p = 0.04) increased while disposition index (178 ± 104%) (p = 0.11) trended toward an increase at post-surgery. Serum free fatty acid levels were unchanged after surgery.

Twenty-four-hour Rhythm Analysis

To analyze the twenty-four-hour profiles, we utilized a unimodal cosinor regression algorithm to create an estimated profile of gene expression for each circadian clock gene (CircWave). Each of the genes that were measured has been previously shown to exhibit robust circadian profiles in healthy individuals, which supported the assumption of a twenty-four-hour phase. For each profile, the regression fit was evaluated for suitability by the algorithm and found

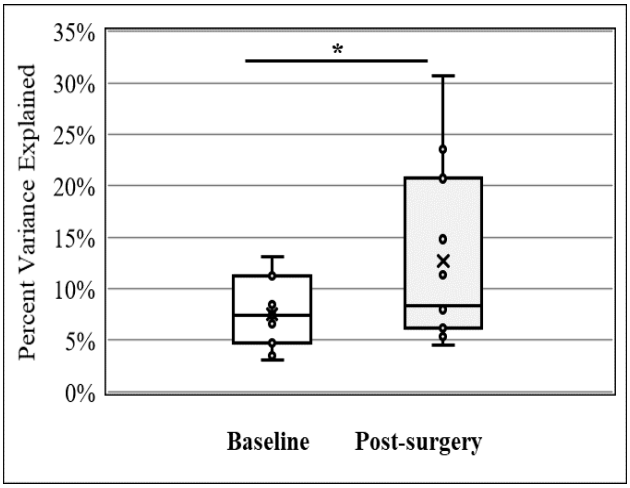

Figure 1: Explained variance of cosinor regression for clock gene expression levels. **S**terile cultured adipose tissue was collected (N=10) at baseline (black) and post-surgery. The gene expression profiles of clock genes were analyzed for circadian rhythmicity using cosinor program CIRCWAVE. Significance was determined by two-tailed t-test. P-value was: * < 0.05.

to have a statistically significant fit ($p < 0.05$). The ability of the program to assign the variance to the regression algorithm was increased at post-surgery as compared to pre-surgery (Figure 4.1). The across-subject average experimental expression before and after surgery was co-plotted with

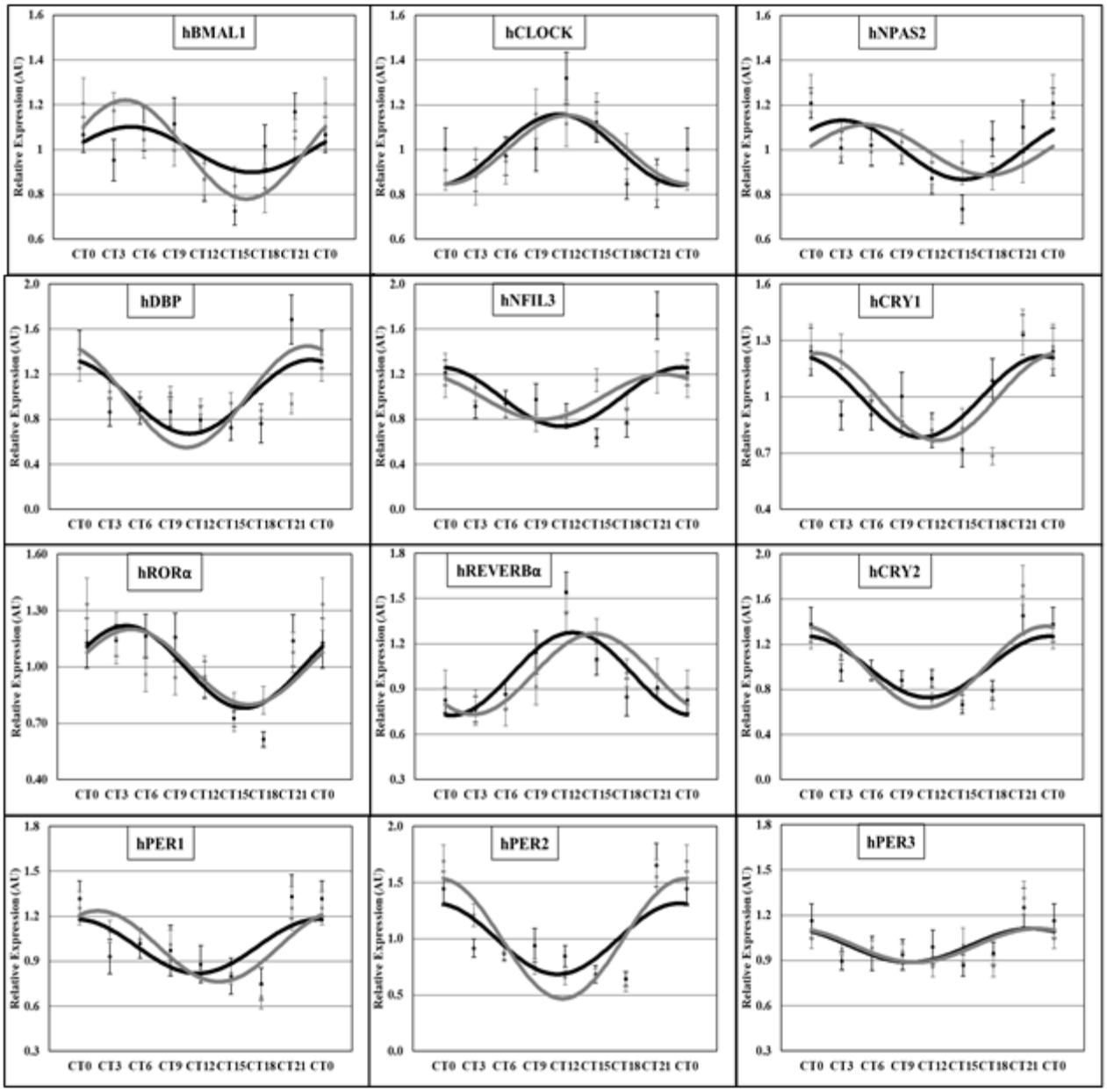

Figure 4.2: Circadian profiles of circadian clock genes. Sterile-cultured adipose tissue was collected every three hours at baseline (●, black) and post-surgery (● , grey). Mesor for each subject and biopsy was adjusted to one arbitrary unit (AU) (N = 10) . Estimated rhythms were fit using a unimodal cosinor algorithm (CircWave) with phase of twenty-four hours. The estimated rhythms are shown as solid lines. Raw experimental derived data is displayed as discrete points ± SEM. The profiles are shown against 24-hour clock time (CT).

the estimated profile resulting from the parameter estimates output from the model (Figure 4.2).

There were no phase differences detected between baseline and post-surgery (Figure 4.3A). In alignment with prior reports, positive arm (*hBMAL1, hCLOCK, hNPAS2*) were anti-phase to negative arm elements of the circadian clock (*hPER1/2/3, hCRY1/2*). There was also a notable phase difference between *hRORα* and *hREVERBα*, which is known to be associated with establishment of *hBMAL1* oscillation. The amplitude of the rhythm of *hBMAL1* increased from

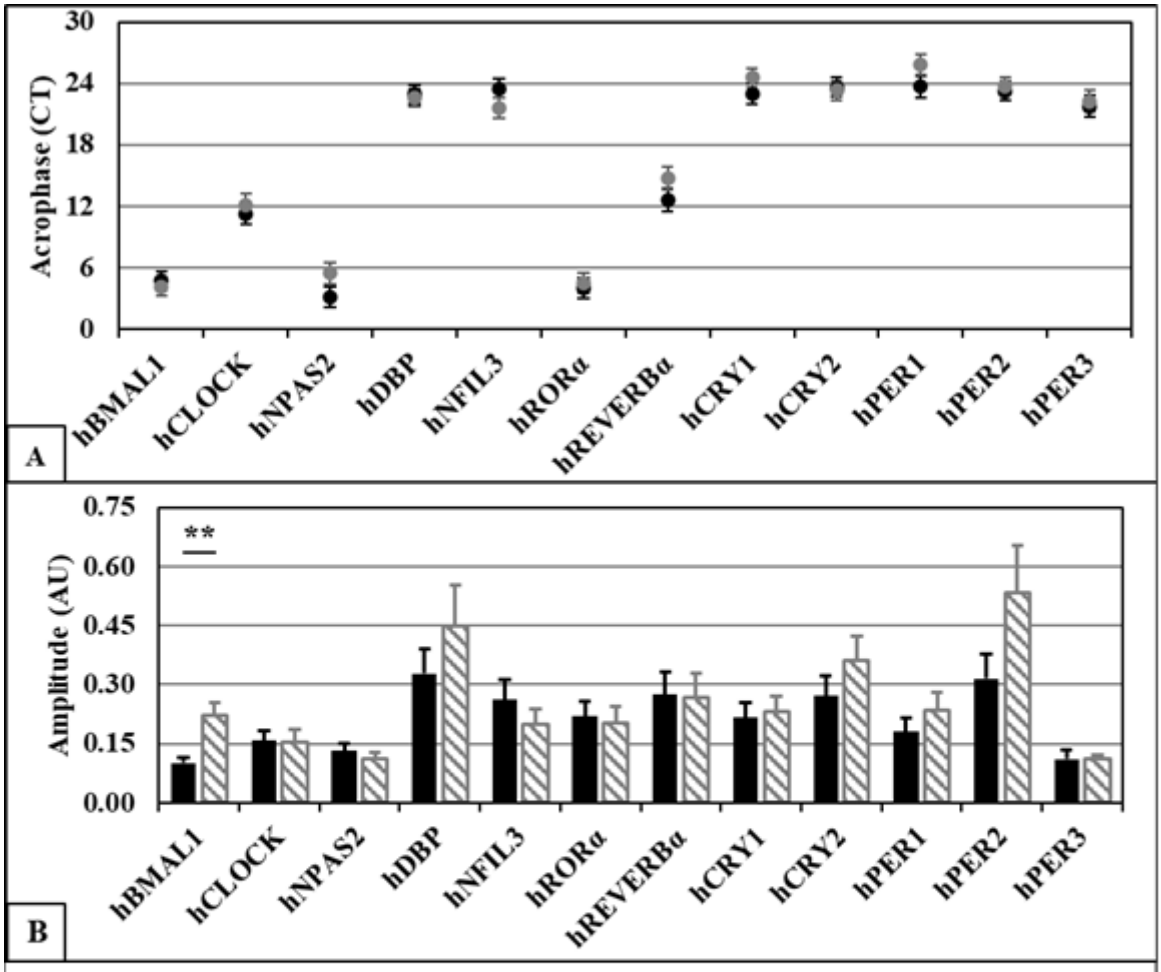

Figure 4.3: Analysis of circadian mRNA rhythm characteristics of clock genes. Sterile-cultured subcutaneous adipose tissue was collected (n=10) at baseline (black) and twelve weeks following surgery (grey). Relative expression was fit to a unimodal cosinor algorithm (CircWave) with phase of twenty-four hours. Characteristics of the fit rhythm were defined for each gene. **A) Acrophase (τ)**, the time of highest expression, is shown (●) ± SEM of τ. **B) Amplitude** of estimated rhythm was shown ± SEM of mean expression. Significance was determined by two-tailed t-test. P-values: ** < 0.01.

10.2 ± 1.3% to 22.1 ± 3.5% (p = 1.91e-3) (Figure 4.3B). No other genes exhibited a significant change to amplitude of the rhythm.

Total Gene Expression

Alterations in average expression (MESOR) from baseline to post-surgery was assessed through mixed linear modeling. Data was corrected before modeling to exclude non-linearity from the circadian oscillation. Corrections made during modeling included: 1) expression drift during the time series experiment, 2) weight loss before surgery, 3) weight loss after surgery, and 4) age. Factors that did not improve model fit were not included in the surgery effect model. All values are adjusted to a baseline intercept of one. The surgery effect for each gene was reported in Figure 4.4. Two genes were estimated to have decreased expression following surgery: *hNFIL3* (-40.5 ± 13.5 %, p = 3.2e-3), and *hREVERBα* (-44.8 ± 15.9%, p= 5.2e-3). Seven genes were estimated to have increased expression following surgery: *hNPAS2* (238 ± 89%, p = 7.7e-3), *hDBP* (417 ± 121%, p = 7.1e-4), *PER1* (375 ± 130%, p = 8.6e-3), *hPER2* (553 ± 184%, p = 3.0e-3), *hPER3* (76 ± 30%, p = 5.4e-3), *hCRY1* (158 ± 70%, p = 0.013), and *hCRY2* (218 ± 76%, p = 2.2e-3).

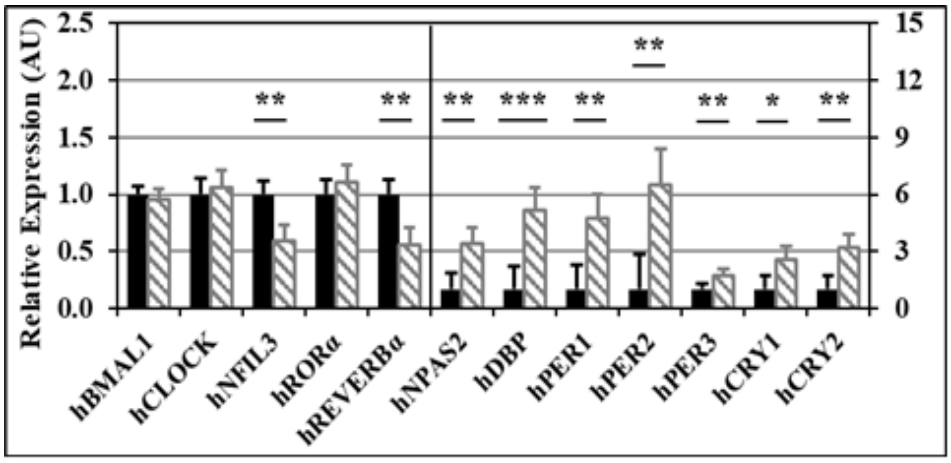

Figure 4.4: Analysis of gene expression level changes after sleeve gastrectomy surgery. Subcutaneous adipose tissue (n=10) was collected from sterile culture at baseline (black) and at post-surgery (grey). Mixed linear modeling was used to estimate the effect of surgery after correction for weight loss and subject baseline expression. Significance was determined by a two-sided t-test. P-values were, respectively: * < 0.05, ** < 0.01 and *** < 0.001.

Association of gene expression with weight loss

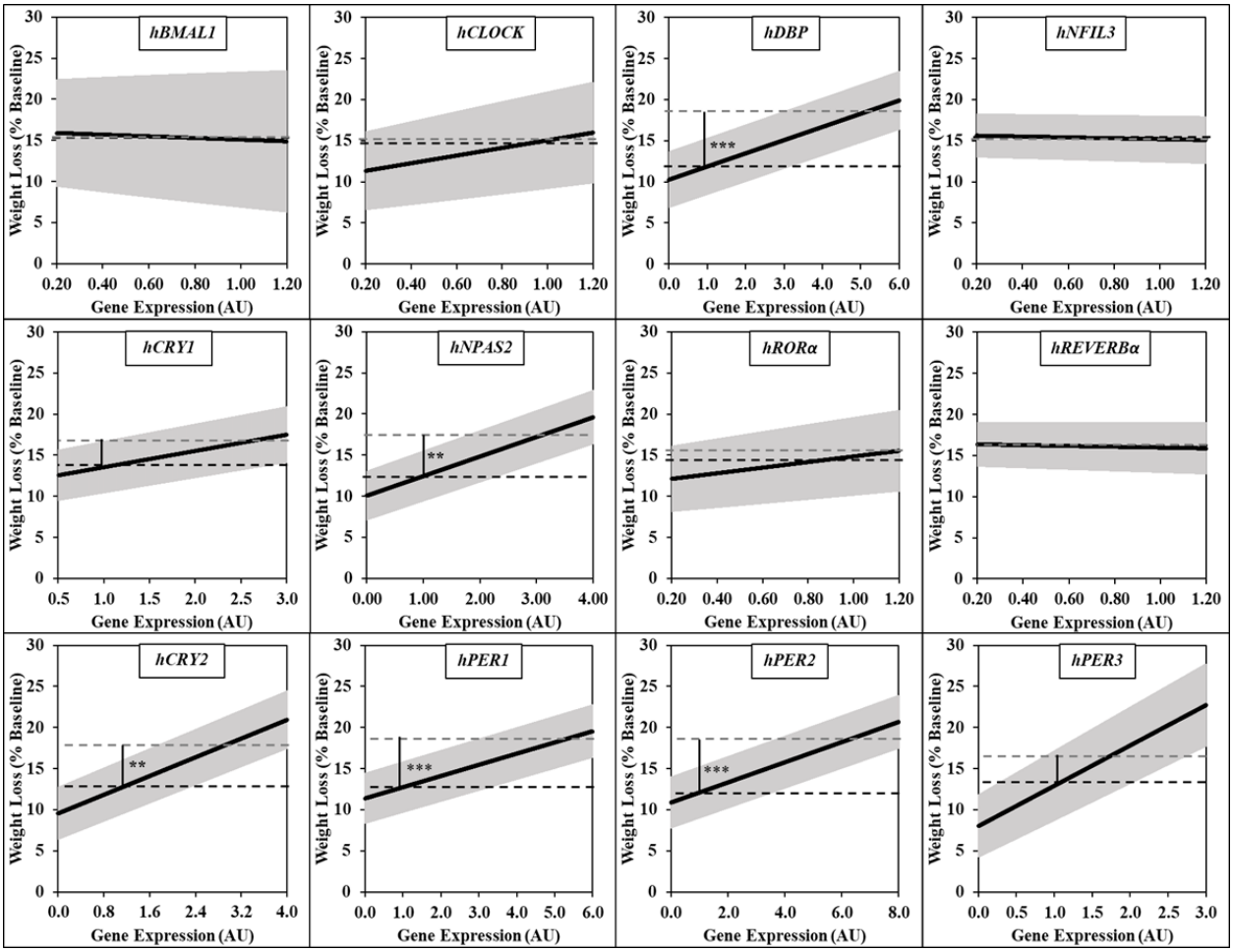

Figure 4.5: Analysis of clock gene expression on percent weight loss from baseline. Subcutaneous adipose tissue (n=10) was collected from sterile culture at baseline and at post-surgery. Mixed linear modeling was used to estimate the effect of each gene expression on weight loss achieved. 95% confidence interval is shown. Comparison is between estimated weight loss given average expression of each gene at baseline (black) or post-surgery (grey). Significance was determined by a two-sided t-test. P-values were, respectively: ** < 0.01 and *** < 0.001.

Post-surgery weight loss (surgery intake to post-surgery session) averaged 15.5% and ranged between [9.9%, 18.9%]. We tested whether there was an association of changes to gene expression with changes to weight loss after surgery. Five genes were associated with significantly increased weight loss at post-surgery gene expression as compared to pre-surgery gene expression. The genes were: *hNPAS2* (12.47 ± 1.57% [BL g.e.], 17.52 ± 1.64 % [PS], p = 2.4e-3), *hDBP* (12.18

± 1.75% [BL], 18.47 ± 1.80% [PS], p = 5.9e-4), *hCRY2* (12.46 ± 1.67% [BL], 18.02 ± 1.75 % [PS], p = 1.8e-3), *hPER1* (12.78 ± 1.58% [BL], 18.24 ± 1.63 % [PS], p = 9.9e-4), *hCRY2* (12.13 ± 1.60% [BL], 18.47 ± 1.64 % [PS], p = 1.6e-4). Weight loss is associated with several metabolic alterations after surgery. We tested whether the changes in the gene expression are also associated with changes to metabolic parameters from glucose management, decreases caloric consumption directly, or changes to fatty acid metabolism.

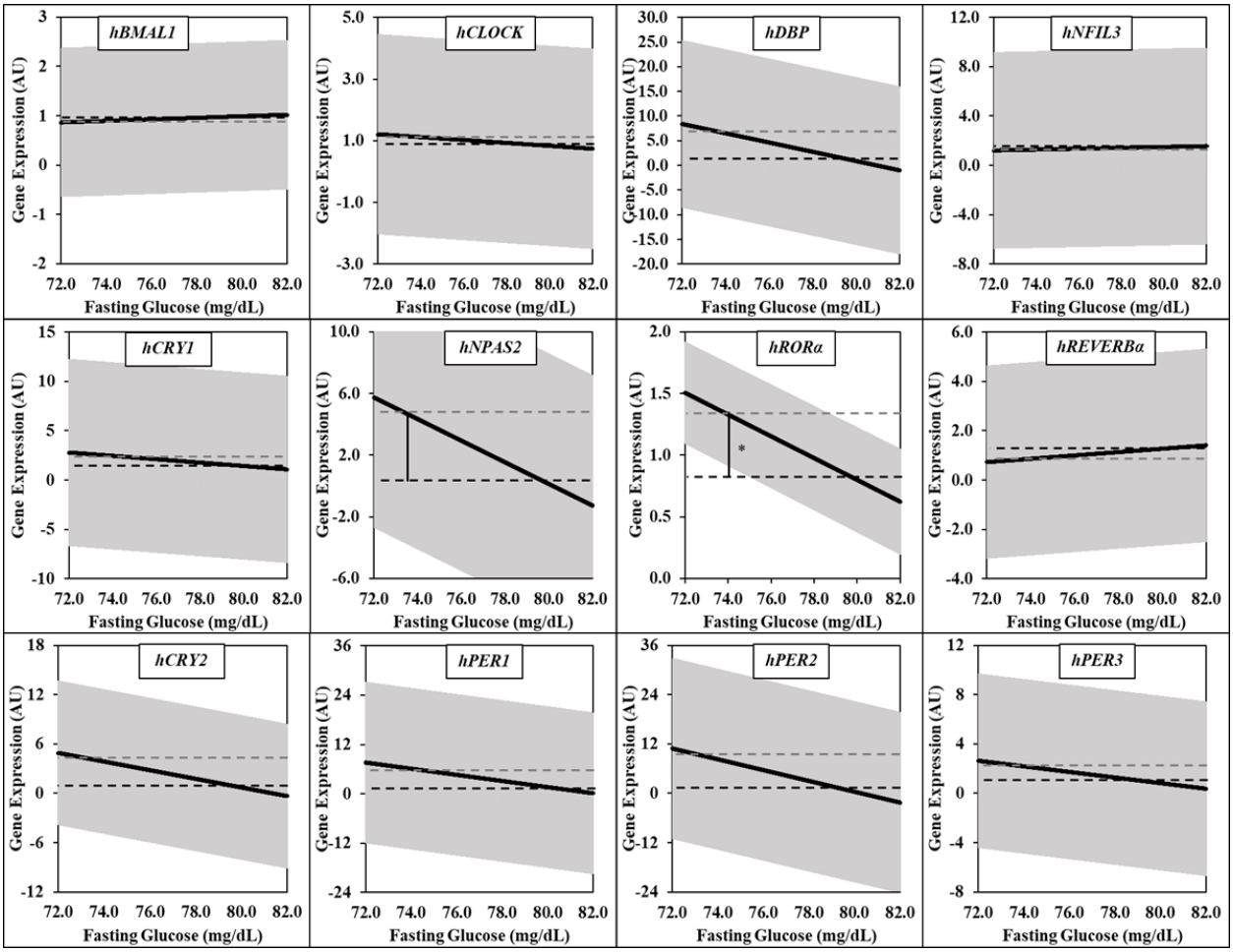

Figure 4.6: Association of circadian clock gene expression with fasting glucose. Subcutaneous adipose tissue (N = 7) was collected from sterile culture at baseline and twelve weeks following surgery. Fasting blood glucose was determined by ELISA. Mixed linear modeling was used to estimate the effect of each gene expression on weight loss achieved. 95% confidence interval is shown. Comparison is between estimated weight loss given average expression of each gene at baseline (black) or post-surgery (grey). Significance was determined by a two-sided t-test. Significance was determined by a two-sided t-test. P-values were, respectively: * < 0.05.

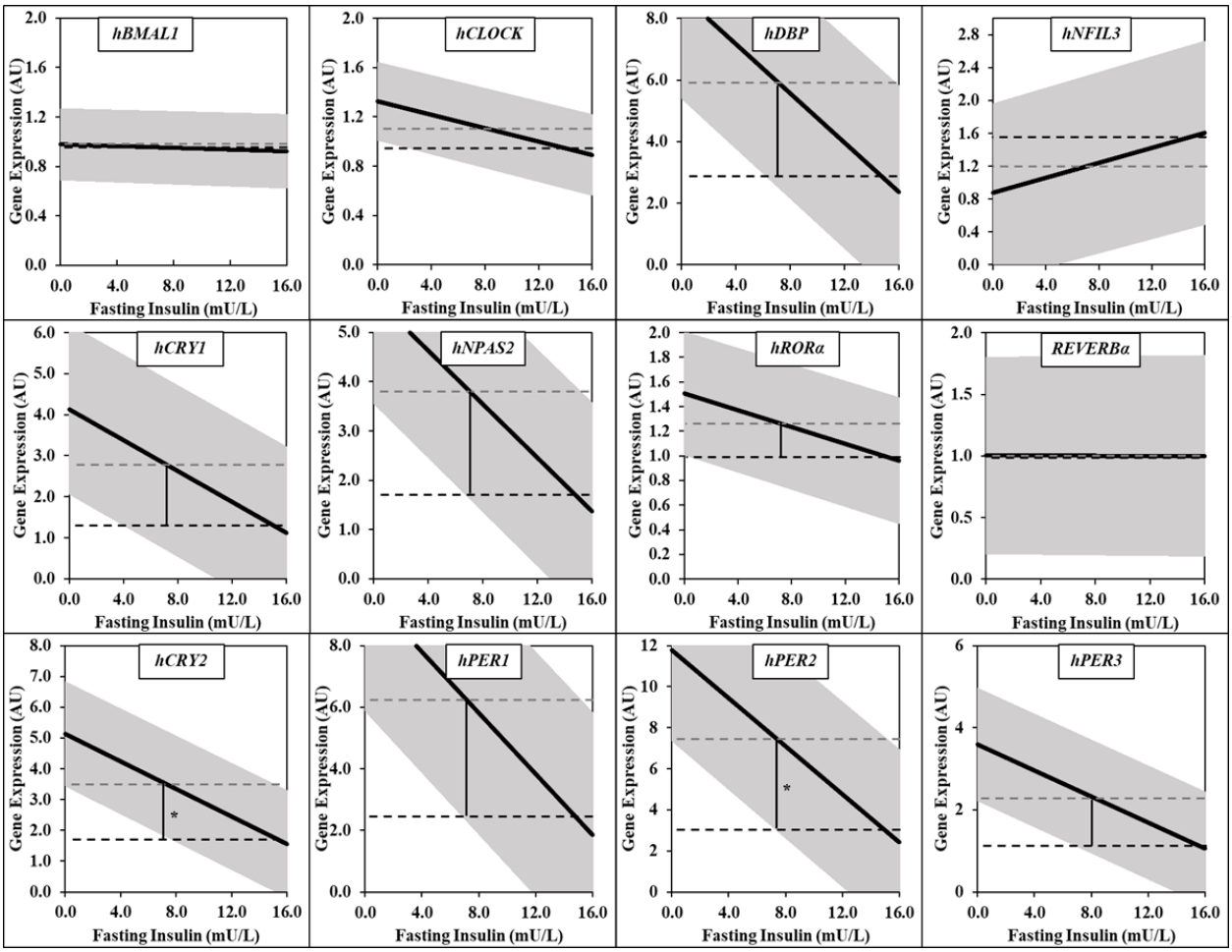

Figure 4.7: Association of circadian clock gene expression with fasting insulin. Subcutaneous adipose tissue (N = 7) was collected from sterile culture at baseline and twelve weeks following surgery. Fasting blood insulin was determined by ELISA. Mixed linear modeling was used to estimate the effect of each gene expression on weight loss achieved. 95% confidence interval is shown. Comparison is between estimated weight loss given average expression of each gene at baseline (black) or post-surgery (grey). Significance was determined by a two-sided t-test. Significance was determined by a two-sided t-test. P-values were, respectively: * < 0.05.

Association of glucose management with gene expression

Parameters of glucose management were derived from MINMOD Millenium software analysis of raw fsIV-GTT results. We modeled the association of differences in fasting glucose, fasting insulin, insulin sensitivity, beta cell function, and disposition index on differences in the gene expression of each clock gene. No significant effect on gene expression were found with disposition index or beta cell function. Despite the unchanged *hRORα* expression following

surgery, the decline in fasting glucose (82.5 [BL], 78.4 mg/dL [PS]) was associated with a significant increase in hRORα expression (0.84 ± 0.21 [BL], 1.39 ± 0.21 [PS], p = 0.01) (Figure 4.6). The decline in fasting plasma insulin (was associated with increased *hCRY2* and *hPER2* expression (Figure 4.7). The increase in systemic insulin sensitivity was associated with increased *hNPAS2* expression (Figure 4.8).

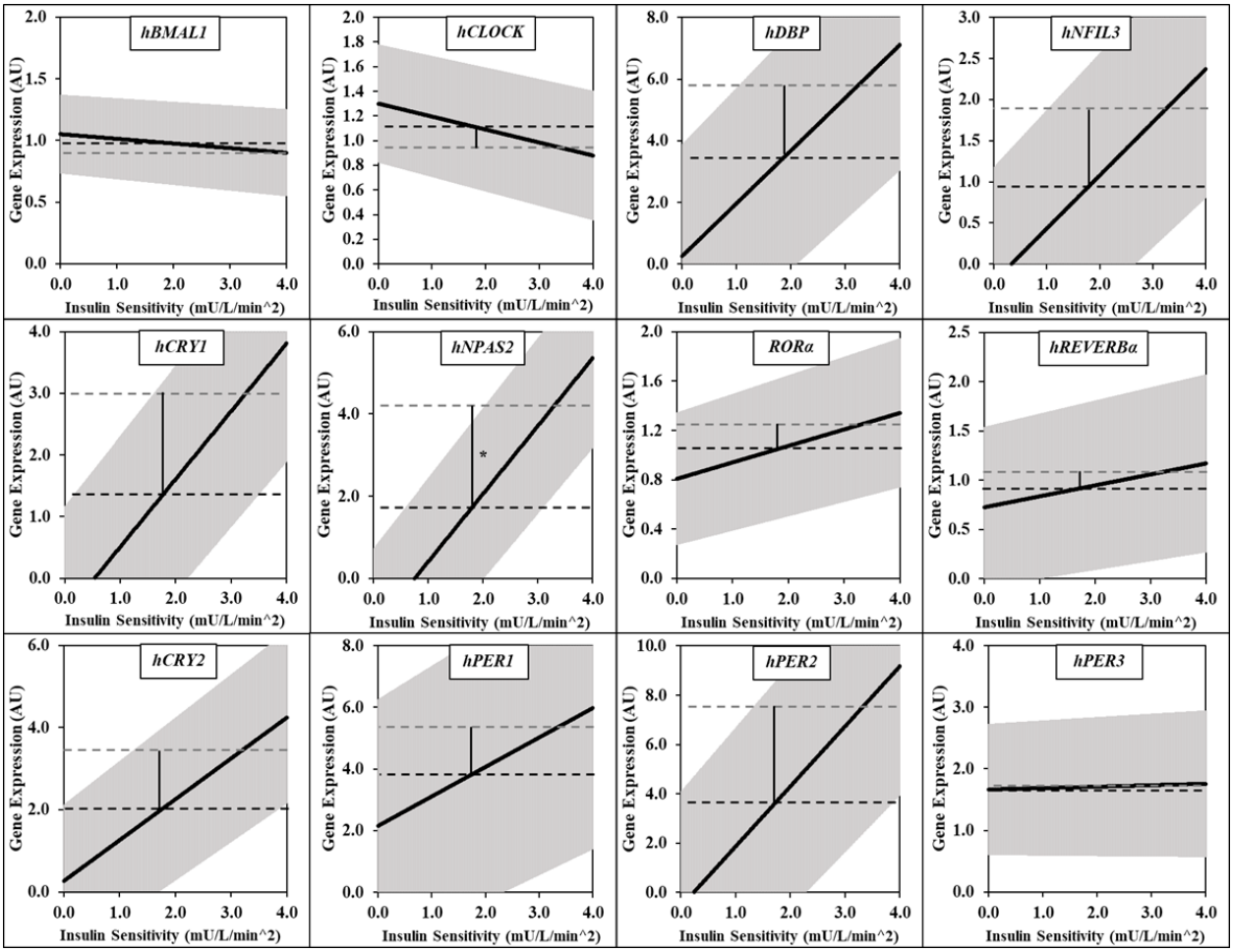

Figure 4.8: Association of circadian clock gene expression with insulin sensitivity. Subcutaneous adipose tissue (N = 7) was collected from sterile culture at baseline and twelve weeks following surgery. Insulin sensitivity was computed using MINMOD Millenium software on fsIV-GTT results. Mixed linear modeling was used to estimate the effect of each gene expression on weight loss achieved. 95% confidence interval is shown. Comparison is between estimated weight loss given average expression of each gene at baseline (black) or post-surgery (grey). Significance was determined by a two-sided t-test. Significance was determined by a two-sided t-test. P-values were, respectively: * < 0.05.

Association of calories consumed with gene expression

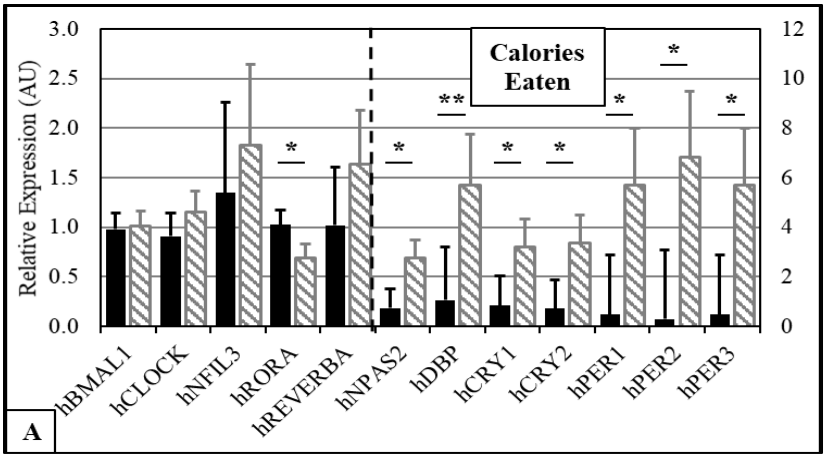

Figure 4.9: Effect of calories eaten on gene expression of clock genes. Subcutaneous adipose tissue (n=10) was collected from sterile culture at baseline (black) and at post-surgery (grey). Mixed linear modeling was used to estimate gene expression of each gene using: four meal average calories eaten during each lab session. Significance was determined by two-tailed t-tests. P-values were: * < 0.05, ** < 0.01, *** < 0.001.

Four-meal average of calories consumed during respective laboratory sessions was used to model gene expression. The decline in calories consumed ((2223 [BL], 591 [PS]) was associated with a change in eight genes (Figure 4.9). There was a significant decrease in hRORα expression (1.02 ± 0.15 [BL], 0.69 ± 0.14 [PS], p = 0.02). There was a significant increase in seven genes: hNPAS2 (0.75 ± 0.77 [BL], 2.75 ± 0.74 [PS], p = 0.008), hDBP (1.07 ± 2.13 [BL], 5.71 ± 2.03 [PS], p = 0.02), hCRY1 (0.84 ± 1.19 [BL], 3.20 ± 1.12 [PS], p = 0.04), hCRY2 (0.71 ± 1.17 [BL], 3.38 ± 1.12 [PS], p = 0.02), hPER1 (0.48 ± 2.39 [BL], 5.72 ± 2.29 [PS], p = 0.02), hPER2 (0.30 ± 0.21 [BL], 6.82 ± 0.21 [PS], p = 0.02), and hPER3 (0.79 ± 0.49 [BL], 2.06 ± 0.48 [PS], p = 0.009).

Association of fatty acid secretion and fasting serum FFA level with gene expression

Systemic fatty acids can be measured by serum fasting free fatty acid levels and adipose tissue lipolysis was measured by glycerol secretion rate. Increased glycerol secretion rate (30.7 [BL], 51.4 ng/hr [PS]) was associated with increased expression of hCRY1 (0.58 ± 1.14 [BL], 3.64 ± 1.16 [PS], p = 0.01) and hPER3 (1.00 ± 0.39 [BL], 2.12 ± 0.40 [PS], p = 0.006) (Figure 4.10).

Free fatty acid levels (498 [BL], 367 μM [PS]) did not significantly associate with changes to gene expression of any of the circadian clock genes (Figure 4.11).

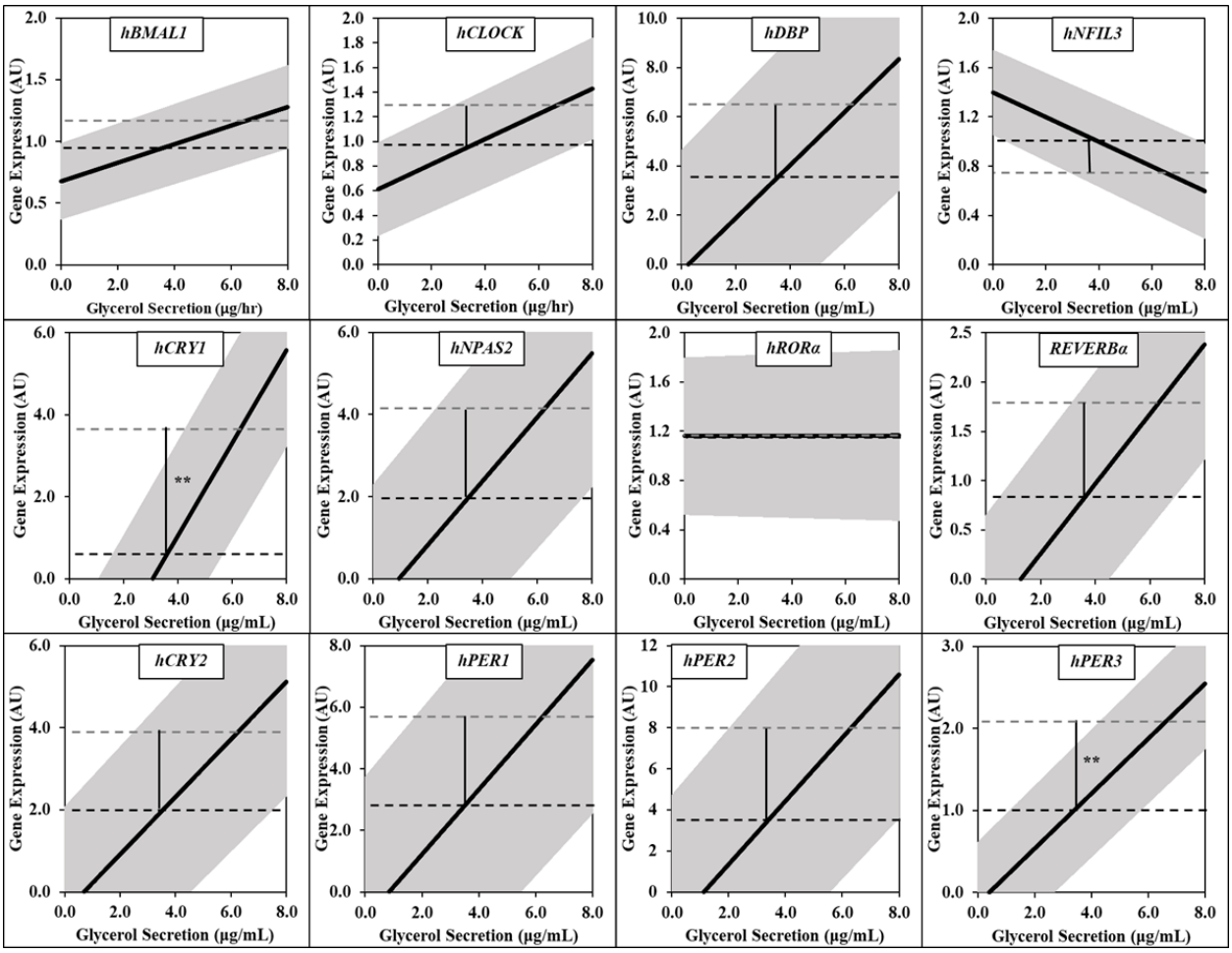

Figure 4.10: Association of circadian clock gene expression with adipose tissue lipolysis. Subcutaneous adipose tissue (N = 8) was collected from sterile culture at baseline and twelve weeks following surgery. Glycerol secretion rate was computed colorimetric assay on conditioned media. Mixed linear modeling was used to estimate the effect of each gene expression on weight loss achieved. 95% confidence interval is shown. Comparison is between estimated weight loss given average expression of each gene at baseline (black) or post-surgery (grey). Significance was determined by a two-sided t-test. Significance was determined by a two-sided t-test. P-values were, respectively: ** < 0.01.

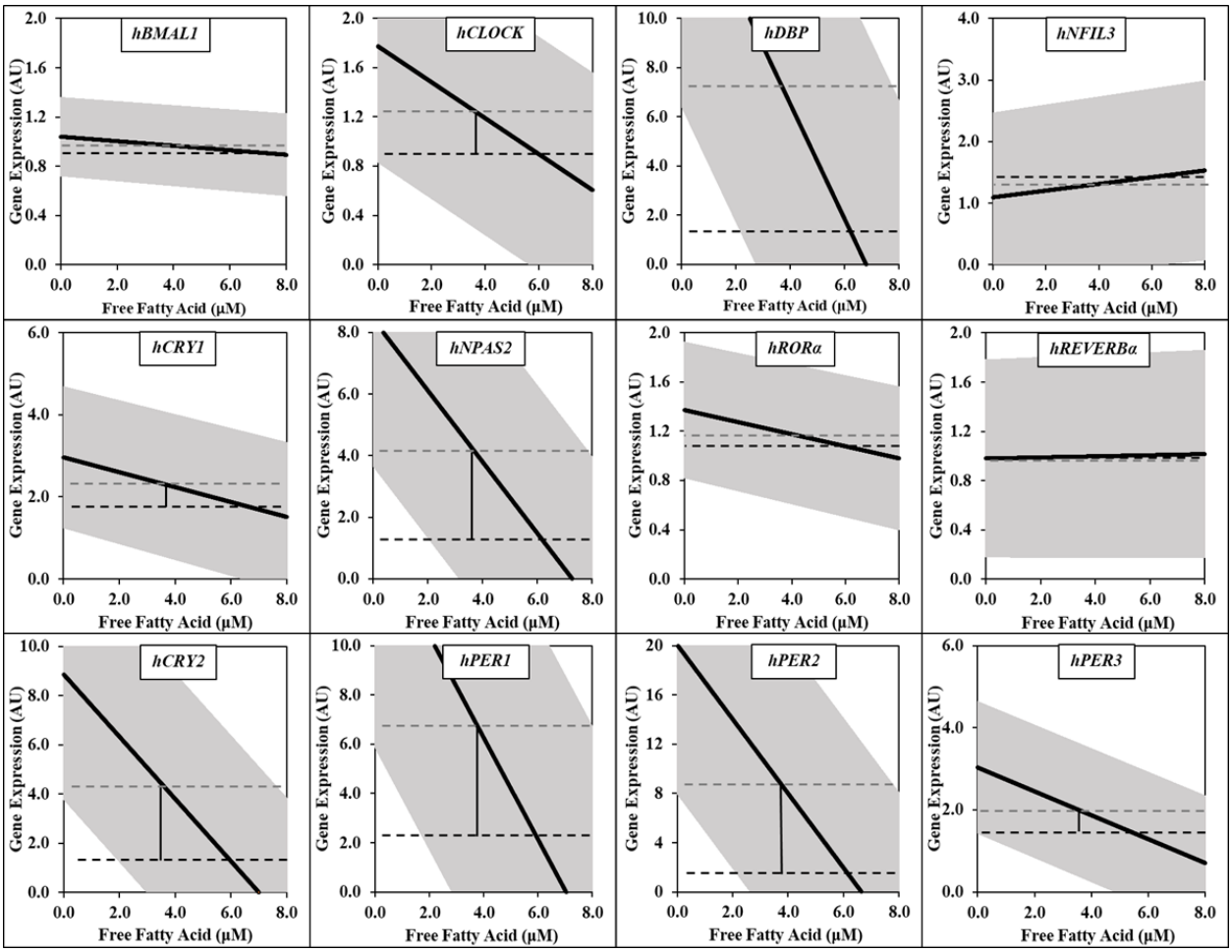

Figure 4.11: Association of circadian clock gene expression with blood free fatty acid levels. Subcutaneous adipose tissue (N = 7) was collected from sterile culture at baseline and twelve weeks following surgery. Fasting free fatty acid levels were computed colorimetric assay on blood. Mixed linear modeling was used to estimate the effect of each gene expression on weight loss achieved. 95% confidence interval is shown. Comparison is between estimated weight loss given average expression of each gene at baseline (black) or post-surgery (grey). Significance was determined by a two-sided t-test. Significance was determined by a two-sided t-test. P-values were, respectively: * < 0.05.

Association of internal clock expression association

To assess whether internal regulation could explain the observed changes seen in expression between baseline and post-surgery, we constructed models to use elements interacting with each transcriptional promoter region. Similar to the surgery model, there was no change in the overall

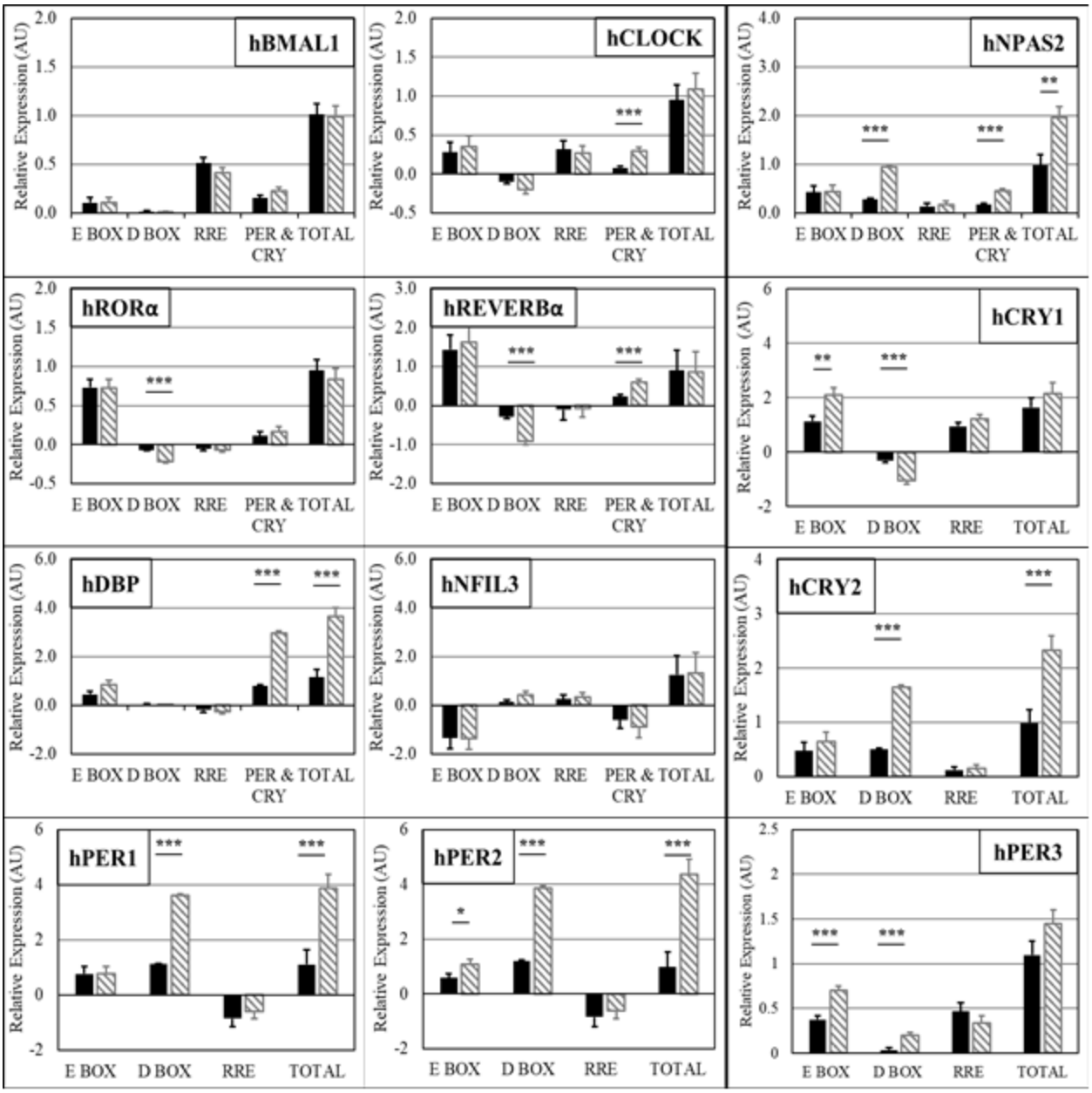

Figure 4.12: Association of clock gene expression to expression of other clock genes. Each clock gene was modeled with a simple intercept set to the subject ID. Additionally, each model contained at least on element that acted on E-box promoter, D-box promoter, and RRE promoter regions. The total estimated difference in gene expression between baseline (black) and post-surgery (grey) is shown as total. Significance was determined by a two-tailed t-test which compared the total modeled effect of each promoter region on respective expression between baseline and post-surgery.

expression of hBMAL1, hCLOCK, hRORα. hCLOCK was associated with the change to hPER1 (p = 3.9e-5). Alterations in DBP-acting genes were highly associated with changes to: hRORα (p = 1.1e-12), hREVERBα (p = 1.6e-7), hCRY2 (p = 1.3e-44), hPER1 (p = 1.2e-70), hPER2 (p = 7.2e-48), hPER3 (p = 1.6e-4), and hNPAS2 (p = 9.1e-40). E-box acting genes were also significantly associated with the change in gene expression of hPER2 (p = 0.049), hPER3 (p = 5.2e-6) and hCRY1 (p = 3.8e-4). However, the model for hCRY1 did not explain the increase in gene expression between baseline and post-surgery. Additionally, gene expression of clock elements failed to explain the decrease in gene expression of *hREVERBα* and *hNFIL3* at post-surgery.

Discussion

The overall results show an upregulation in several genes in the subcutaneous adipose tissue circadian clock. The overt results suggest a shift towards positive regulation at D-box promoter regions via *hDBP* and E-promoter region via *hNPAS2*. The consequent apparent upregulation in the negative limb elements of the circadian clock lends evidence to support this claim. The undeniable association of the changes of *hPER1, hPER2, hCRY2* with *hDBP* solidifies the connection. The connection of *hNPAS2* with hCRY1 and hPER3 are distinct from the effect of *hDBP*. Prior literature on the effects of these clocks is not inconsistent with a metabolic profile of improved glucose homeostasis, lower insulin levels, increased insulin sensitivity, decreased lipogenesis, and decreased adipogenesis.

A major known factor in the result of bariatric surgery is significant caloric restriction. This report on clock gene expression twelve weeks after bariatric surgery supports the role of significant caloric restriction. Firstly, hDBP These two effects are able to exert an effect on the function of

the circadian clock. Circadian clock expression in adipose tissue was measured in individuals with obesity who were put on an eight week very-low calorie diet. (Pivovarova et al. 2016) Subjects lost around ten kilograms of weight. hPER2 was found to increase in overall expression in proportion to weight loss. This finding is congruent with the present study. However, hREVERBα was indicated to increase rather than decrease as seen in this study. Yet, the isolated effect could be consistent with the trend seen in Figure 4.6A. In a caloric restriction study in mice mPER1, mPER2, and mDBP were each upregulated. (Patel et al. 2016) Each effect is congruent with the present study. Yet, the increase in mCLOCK, the lack of change in mNFIL3, and the increase in mBMAL1 contrasted with the present study. These results would suggest that there may be improvements to circadian clock function that are related to caloric restriction. Yet, it is clear that it is not the whole story of what is occurring.

Each of the three period genes was shown to be upregulated at post-surgery as compared to baseline. Yet, *hPER3* was notably less elevated than *hPER1* and *hPER2*. Low caloric consumption may partially explain the difference. *mPER1* and *mPER2* promoter regions are shown to have cAMP response elements, while *mPER3* does not. (Travnickova-Bendova et al. 2002). The common factor that associates *hNPAS2, hCRY1,* and *hPER3* and improved glucose metabolism is a promising step in understanding the effects driving the differences.

In this study, we showed that there are not significant changes to the phase of the adipose tissue clock. However, the average expression of several clock genes was increased in association with caloric restriction and systemic metabolic improvements. The caloric restriction effects seem to be mediated with upregulation of *hDBP*, while the metabolic effects appear to be affecting the expression of *hNPAS2*. The implications of these changes can be explored in the future.

Chapter 5: Adipose Tissue Metabolic Gene Expression is Highly Associated with Caloric Restriction Twelve Weeks following Sleeve Gastrectomy

Abstract

In humans with morbid obesity, there is a significant trend for the attenuation of systemic circadian rhythms and a deterioration of metabolic health. Bariatric surgery has been shown to improve several systemic and adipose tissue metabolic health parameters. We tested the hypothesis that laparoscopic sleeve gastrectomy (LSG) would regulate adipose tissue metabolic genes to resist caloric-restriction-mediated lipolysis. We recruited ten women with morbid obesity who had been scheduled for LSG. We collected a peri-umbilical fat biopsy at baseline and twelve weeks following surgery. The tissue was minced and sterile cultured in separate wells for approximately twenty-four hours. A well of fat was collected every three hours and flash frozen. To assess changes in gene expression of components of adipose tissue metabolic control, reverse-transcriptase qPCR was conducted from each tissue section on twelve genes. Fourier-based bimodal cosinor regression was conducted (CircWave) to estimate parameters of the respective biological rhythm profiles assuming 24-hr phase duration. We showed phase delay of insulin signaling genes (*INSR, IRS1, PIK3.CA*) and lipid regulatory gene *INSIG2*. Further, we showed down regulation in adipokine genes (*LEPTIN, ADIPOQ)* and lipolysis gene (*ATGL*), and upregulation of master transcription factor genes (*SREBP1* and *PGC1α)* and insulin pathway genes (*INSR, IRS1, GLUT4, SOCS3)*. A majority of the changes could be explained by caloric restriction with expected declines in fasting insulin and systemic insulin sensitivity. Surgery did not associate with change to *INSIG2*, but caloric restriction and upregulated lipolysis were significantly associated.

Introduction

Adipose tissue may not be a major site of glucose uptake, but the loss of insulin-mediated inhibition of lipolysis contributes significantly to systemic insulin resistance, ectopic lipid deposition, and lipotoxicity. (Angelini et al. 2019, Ye et al. 2019, Morigny et al. 2016) Traditional lifestyle modification has resulted in short-term improvements to obesity comorbidities but has also been inconsistent as a long-term intervention strategy. (Unick et al. 2013, van Baak and Mariman 2019, Crowe et al. 2015) However, dramatic long-term improvements have been achieved through LSG surgeries. Beyond maintenance of weight loss, risk of metabolic disease has been reduced dramatically while endocrine dysfunction and resistances have been resolved. (Fischer et al. 2012, Adams et al. 2007, Basso et al. 2011, Ashrafian et al. 2011, Casella et al. 2016) Impressively, these effects have been shown to occur beyond the expectation by weight loss alone. (Chambers et al. 2011, Longo 2014)

Our inquiry was focused on the human subcutaneous adipose tissue clock in time-relation to LSG surgery. We conducted time-series experiments on sterile-cultured adipose tissue derived from peri-umbilical aspiratory biopsies at baseline prior to surgery and at twelve weeks following surgery from women with morbid obesity. At this time following surgery, reports indicate that weight loss and metabolic improvements have begun but have yet to stabilize. Our hypothesis is that the adipose tissue gene expression will reflect improved insulin signaling but also be reflective of the negative energy balance by the promotion of lipolysis, and suppression of adipogenesis and lipogenesis. The particular effects will provide insight into how adipose tissue is involved in the systemic metabolic changes.

Materials and Methods

Subject characteristics

Screening of potential subjects and the process of enrollment into the clinical study was conducted as previously described (University of Chicago IRB 14-0984). (White et al. 2020) Ten women with morbid obesity were voluntarily enrolled with informed, written consent following approval and scheduling for LSG surgery.

Laboratory Sessions

In-laboratory sessions were structured as previously reported. (White et al. 2020) Identical sessions were conducted at baseline one-to-two weeks prior to the scheduled surgery date and twelve-to-thirteen weeks following the surgery date.

qRT-PCR

Experimental design and execution of qRT-PCR runs were as previously described. (White et al. 2020) The runs were prepared on ice with SYBR green chemistry in low-profile 96-well plates with melt curve calculation, three technical replicates, and inter-plate calibration on CFX Connect Real-time PCR Detection systems (40 cycles, 1000 fixed fluorescent unit threshold). Reference gene normalization was conducted as previously described with three reference genes using geometrically-averaged Cq, as previously described. (Vandesompele et al. 2002a, White et al. 2020) Circadian clock gene primers were purchased from Qiagen with a documented guarantee for high efficiency and broad dynamic range but without a precise sequence. The list of primers used were: *LEPTIN* (PPH00581F), *ADIPOQ* (PPH00441F), *LIPE (HSL)* (PPH02383A), *PNPLA2* (*ATGL*) (PPH11403B), *LPL* (PPH00023C), *FASN* (PPH01012B), *PPARG* (PPH02291G), *PPARGC1A* (PPH00461F), *INSIG2* (PPH07473A), *SREBF1* (PPH00393A), *INSR* (PPH02324A),

IRS1 (PPH02328A), *PIK3CA* (PPH01355A), *AKT2* (PPH00289F), *SLC2A4 (GLUT4)* (PPH02326A), *SOCS3* (PPH00763A).

Rhythm and Expression Analysis

To robustly identify alterations in gene expression of the metabolic genes a time series experiment was conducted on minced sterile-cultured peri-umbilical subcutaneous adipose tissue at baseline and post-surgery as previously described. (White et al. 2020) This experimental design allows the ability to interrogate alterations in both the twenty-four-hour rhythms in time proximity to surgery and to leverage the power of the repeated measures design of the time series experiment to increase confidence of overall gene expression levels.

Quantitative characteristics of each gene rhythm were obtained from parameter estimation of Fourier-based cosinor regression software (CircWave version 1.4). (Costa et al. 2013) One harmonic was utilized with phase set to twenty-four hours to allow for testing and regression to a circadian profile. The experimental delta Cq measurements were formatted in two steps: 1) conversion to relative expression, and 2) average twenty-four-hour expression for each subject was adjusted to one. The second adjustment was necessary to treat each subject identically for the regression, which was conducted once including all ten subject profiles. The set of estimated parameters were used to create a profile for a twenty-four-hour rhythm with a data interval of three minutes. The estimated rhythm profile was created for both the baseline measurements and the post-surgery measurements. The acrophase was the estimated clock time of maximal expression. The amplitude was defined as half the difference between the point of lowest expression, the nadir, and the point of maximal expression, the peak. Significance of difference in profiles were compared using two-tailed t-tests.

Mixed Model Construction

Mixed modeling was utilized to estimate the degree of difference in gene expression levels between baseline and post-surgery. Model fitting was conducted by R package (lme4). In order to ensure that the dependence derived from time series collection was accounted for in the statistics, the random vector was a simple intercept set as the subject identification number (SID). Experimental expression level was prepared according to the equation below.

$$E_{SID,\ TP} = 2^{-\Delta C_{q,TP}} \div R_{CT}$$

Relative expression (2^-ΔCq) was adjusted for estimated circadian rhythm (R_{CT}) at the clock time (CT) corresponding to that time point to yield gene expression estimates specific for each subject (SID) and time point (TP). The sinusoidal 24-hr rhythms would have violated the linearity assumed in the modeling leading to distorted estimated factor effects and increased variance.

The surgery-associated parsimonious model was calculated by using surgery as a binomial variable (Pre [0], Post [1]) and iterative inclusion of factors representing potential corrections for: 1) age (integer, years), 2) pre-surgery weight loss, 3) post-surgery weight loss, or 4) expression drift across time (time point = integer: $\{1, 2, \ldots, n\}$). This was enabled by holding each potential correction factor constant for all respective points of a given subject. An enhanced model was chosen by: 1) an improved Akaike Information Criterion of the N+1 model (compared to N model without the addition of the factor), 2) each factor effect has low Type S error rate ($p < 0.05$), and low inflation of standard error of estimation (< 50%).

Additional models were made to identify any associations of gene expression with the changes to metabolic parameters. Weight loss after surgery is a primary outcome variable that is

collected. Therefore, given that there is weight loss after surgery, we constructed a univariate fixed model to estimate the weight loss after surgery (float, 5 digits) given no change in gene expression (float, 5 digits) from baseline or the average change in gene expression observed in this study from baseline to post-surgery. Yet, we also wanted to provide insight into which metabolic changes were associated with the changes to clock gene expression. Therefore, we estimated baseline and post-surgery gene expression (float, 4 digits) by: 1) fasting glucose (float, 0.01 mg/dL precision), 2) fasting insulin (float, 0.01 mU/L precision), insulin sensitivity (float, 0.01 mU/L*min^-2 precision), four meal laboratory session calories consumed (float, 1e-4 [kCal] precision), glycerol secretion rate (float, 0.01 ng/hr precision), fasting serum FFA (float, 0.001 [100 μM] precision). Disposition Index and beta cell function were run in models, but yielded no significant associations.

Lastly, models were set up to identify whether the changes in one clock gene was associated with the change to other clock genes. A complete model was formed to explain the expression of each gene. Clock elements were excluded that notably increased unexplained variance and that did not notably decrease AIC. Multiple negative arm clock elements *(hPER1/2/3, hCRY1/2*) were not included in the same model due to collinearity of regulation. A parsimonious model was completed when there was at least one D-box acting, E-box acting, and RRE-acting element as well as a negative arm element. This allowed comparison of the degree of association between changes to each element and the association with internal clock transcriptional regulation.

Results

Twenty-four-hour Rhythm Analysis

Metabolism in adipose tissue is known to have a distinct circadian profile. And, the regulation and expression of metabolic genes are also known to be circadian. Therefore, the first step in observing the gene expression was to identify whether there was a difference in the phase and amplitude of gene expression. There were four genes with significant phase delays: *INSIG2* acrophase (22:45 [BL], 6:33 [PS], p = 6.8e-6), *INSR* (22:06 [BL], 2:09 [PS], p = 4.7e-3), *IRS1* (20:33 [BL], 2:15 [PS], p = 1.5e-4), *PIK3.CA* (22:30 [BL], 4:03 [PS], p = 5.7e-4) (Figure 5.1A, 5.1B). Three genes had significant alterations to the 24-hr rhythm amplitude: *IRS1* (21.9 [BL],

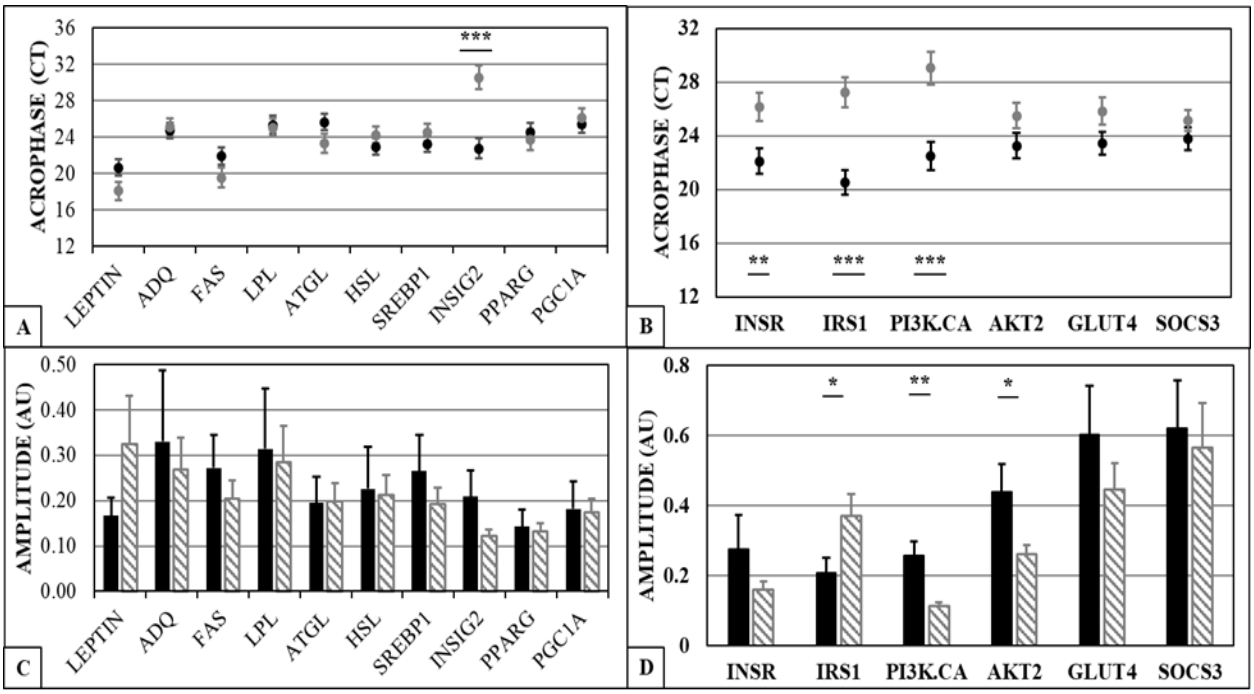

Figure 5.1: Analysis of circadian mRNA rhythm characteristics of metabolic genes. Sterile-cultured subcutaneous adipose tissue was collected (n=10) at baseline (black) and twelve weeks following surgery (grey). Relative expression was fit to a unimodal cosinor algorithm (CircWave) with phase of twenty-four hours. Characteristics of the fit rhythm were defined for each gene. **A) Acrophase (τ)**, the time of highest expression, is shown (●) ± SEM of τ. **B) Amplitude** of estimated rhythm was shown ± SEM of mean expression. Significance was determined by two-tailed t-test. P-values: * < 0.05, ** < 0.01, *** < 0.001.

37.0%, p= 0.02), *PIK3.CA* (25.7 [BL], 11.4% [PS], 1.1e-3), *AKT2* (43.9 [BL], 26.2% [PS], p = 0.04). (Figure 5.1C, 5.1D)

Total Gene Expression

With the 24-hr rhythm subtracted from the gene expression data, the subjects were analyzed by mixed modeling if expression levels were different from baseline to post-surgery (Figure 5.2). Three genes were down-regulated following surgery: *LEPTIN* (1.00 [BL], 0.48 [PS], p = 0.03), *ADIPOQ* (1.11 [BL], 0.72 [PS], p = 0.03), and *ATGL* (1.02 [BL], 0.73 [PS], p = 7.9e-3). Six genes were up-regulated after surgery: *SREBP1* (0.82 [BL], 4.15 [PS], p = 5.7e-3)., *PGC1α* (1.09 [BL], 4.80 [PS], p = 1.5e-4)., *INSR* (0.90 [BL], 4.49 [PS], p = 0.01)., *IRS1* (0.92 [BL], 4.93 [PS], p = 2.2e-3), *GLUT4* (0.92 [BL], 11.4 [PS], p = 0.01), *SOCS3* (0.87 [BL], 5.16 [PS], p = 3.7e-3).

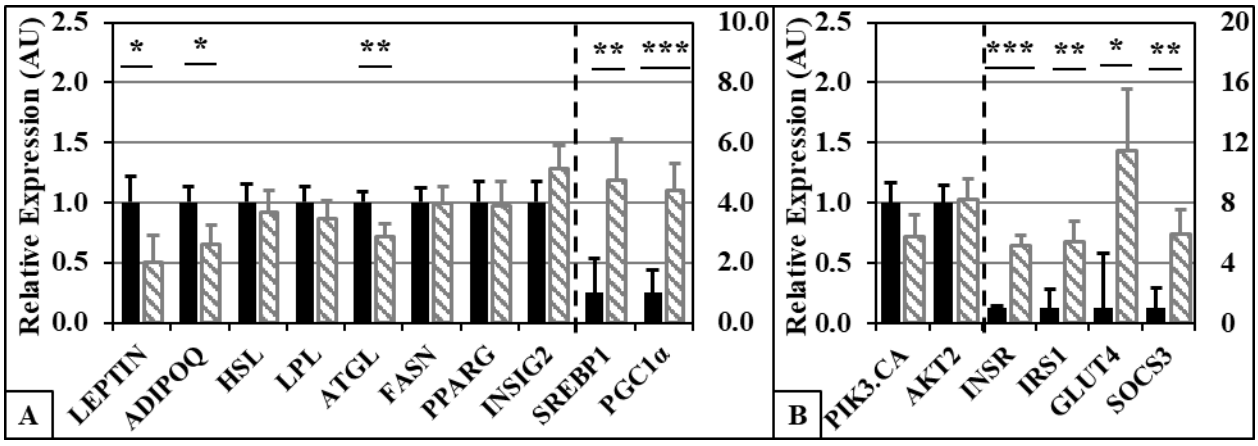

Figure 5.2: Analysis of gene expression level changes after sleeve gastrectomy surgery. Subcutaneous adipose tissue (n=10) was collected from sterile culture at baseline (black) and at post-surgery (grey). Mixed linear modeling was used to estimate the effect of surgery after correction for weight loss and subject baseline expression. Significance was determined by a two-sided t-test. P-values were, respectively: * < 0.05, ** < 0.01 and *** < 0.001.

Association of gene expression with weight loss

Post-surgery weight loss (surgery intake to post-surgery session) averaged 15.5% and ranged between [9.9%, 18.9%]. We tested whether there was an association of changes to gene expression with changes to weight loss after surgery (Figure 5.3). Six genes were associated with significantly increased weight loss at post-surgery gene expression as compared to pre-surgery gene expression. The genes were: *LEPTIN* (9.81 ± 2.63% [BL], 19.86 ± 2.24 % [PS], p = 1.2e-5), *SREBP1* (13.02 ± 1.61% [BL], 17.49 ± 1.66% [PS], p = 7.7e-3), *PGC1α* (10.92 ± 1.38% [BL], 17.81 ± 1.45 % [PS], p = 4.0e-6), *INSR* (14.24 ± 1.43% [BL], 19.22 ± 1.49 % [PS], p = 1.5e-3), *IRS1* (13.64 ± 1.80% [BL], 20.69 ± 1.86 % [PS], p = 2.1e-4), and *SOCS3* (13.29 ± 1.24% [BL], 17.24 ± 1.28 % [PS], p = 2.4e-3).

Association of glucose management with gene expression

Parameters of glucose management were derived from MINMOD Millenium software analysis of raw fsIV-GTT results. We modeled the association of differences in fasting glucose, fasting insulin, insulin sensitivity, beta cell function, and disposition index on differences in the gene expression of each clock gene. No significant effect on gene expression were found with disposition index or beta cell function. Decline in fasting insulin were associated with less expression of *LEPTIN* (0.91 ± 0.13 [BL], 0.56 ± 0.13 [PS], p = 6.4e-3) (Figure 5.5) and increased expression of *IRS1* (2.89 ± 1.39 [BL], 6.06 ± 1.36 [PS], p = 0.02) and *SOCS3* (3.44 ± 1.93 [BL], 7.26 ± 1.88 [PS], p = 0.046). The increase in systemic insulin sensitivity was associated with decreased *ADIPOQ* (1.13 ± 0.15 [BL], 0.62 ± 0.16 [PS], p = 1.5e-3) and increased *INSR* (2.13 ± 2.44 [BL], 7.15 ± 2.49 [PS], p = 0.046) (Figure 5.6).

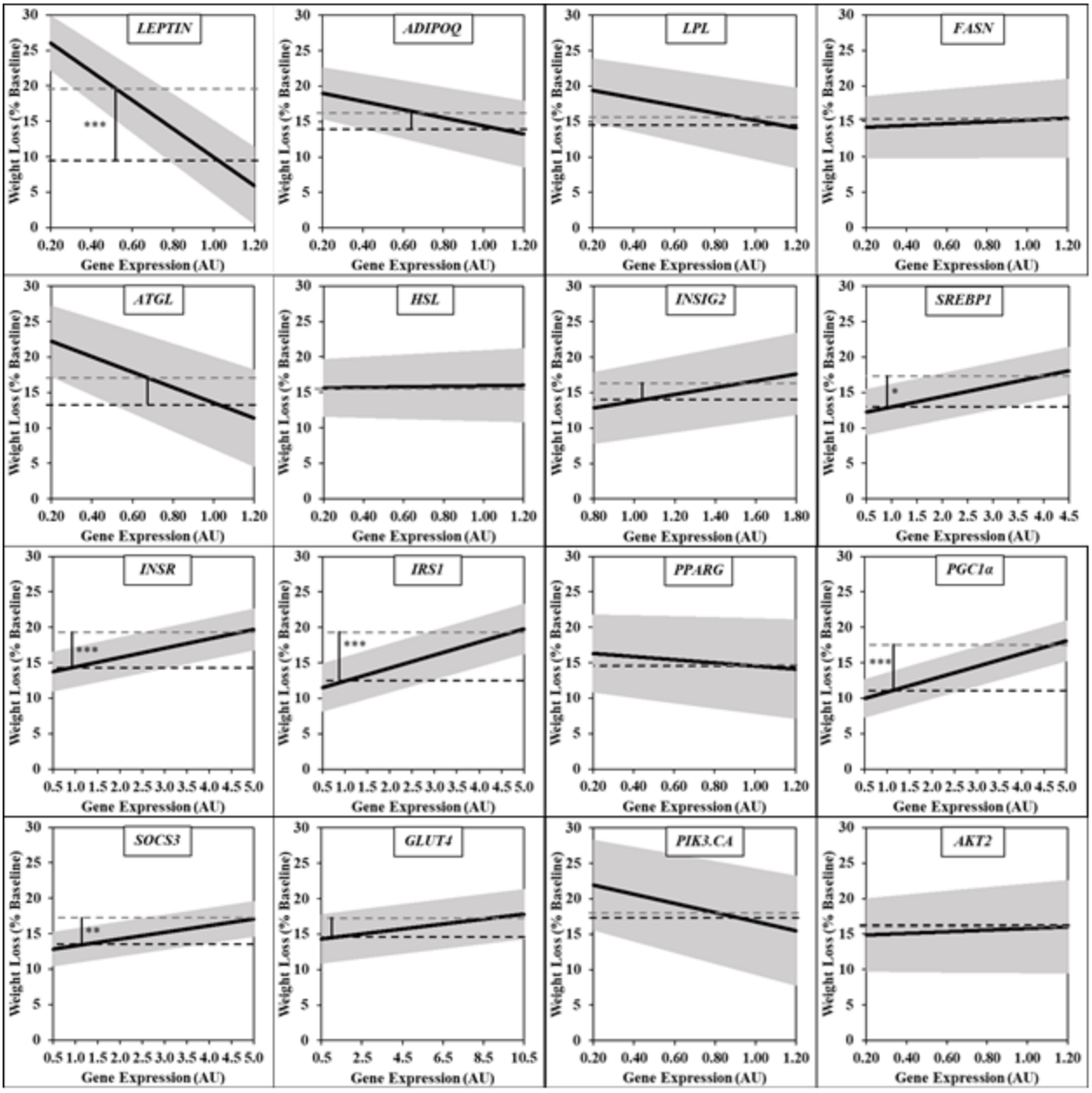

Figure 5.3: Analysis of adipose tissue metabolic gene expression on percent weight loss from baseline. Subcutaneous adipose tissue (n= 10) was collected from sterile culture at baseline and at post-surgery. Mixed linear modeling was used to estimate the effect of each gene expression on weight loss achieved. 95% confidence interval is shown. Comparison is between estimated weight loss given average expression of each gene at baseline (black) or post-surgery (grey). Significance was determined by a two-sided t-test. P-values were, respectively: * < 0.05, ** < 0.01 and *** < 0.001.

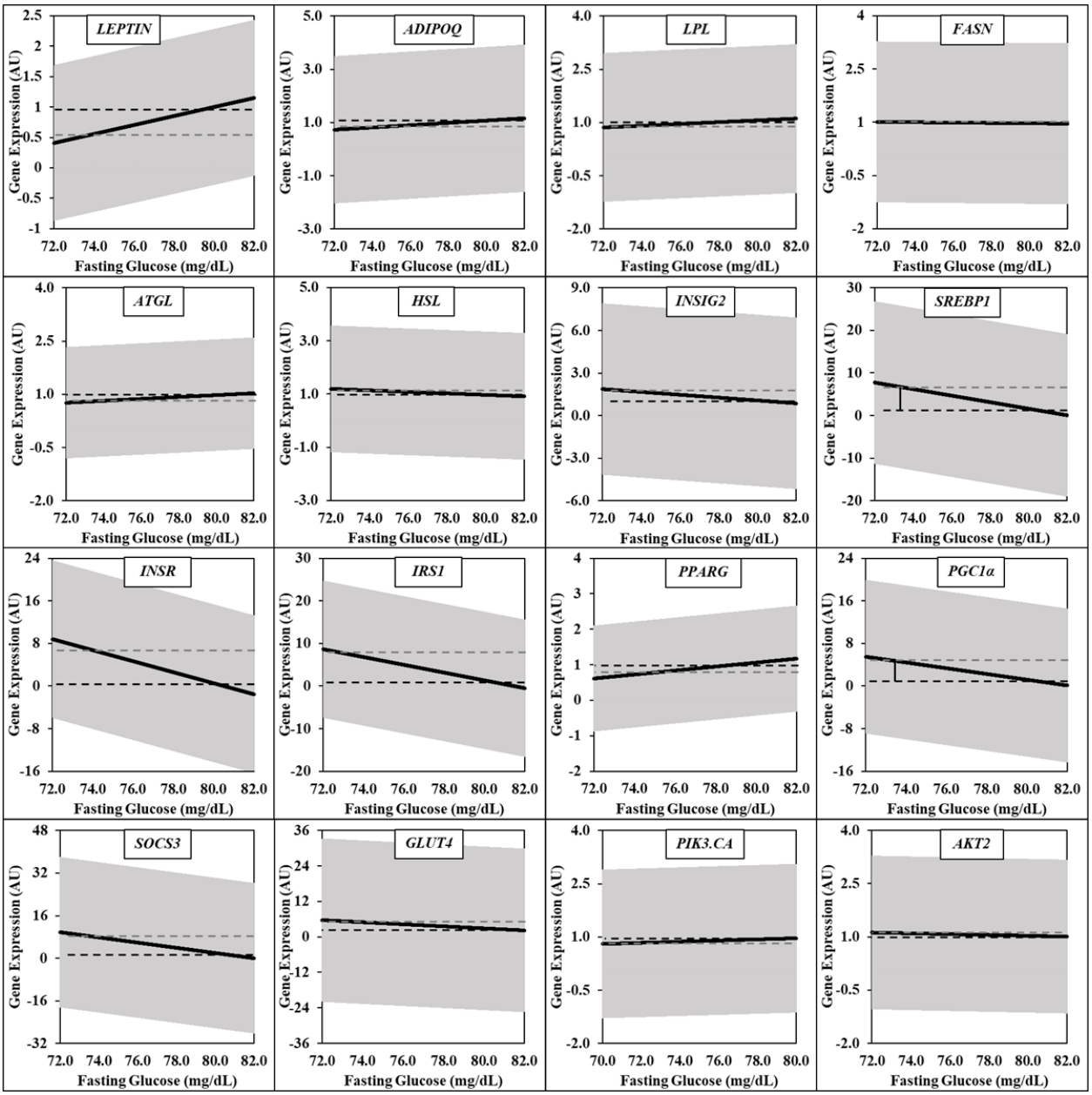

Figure 5.4: Association of circadian clock gene expression with fasting glucose. Subcutaneous adipose tissue (N = 7) was collected from sterile culture at baseline and twelve weeks following surgery. Fasting blood glucose was determined by ELISA. Mixed linear modeling was used to estimate the effect of each gene expression on weight loss achieved. 95% confidence interval is shown. Comparison is between estimated weight loss given average expression of each gene at baseline (black) or post-surgery (grey). Significance was determined by a two-sided t-test. Significance was determined by a two-sided t-test. P-values were all non-significant.

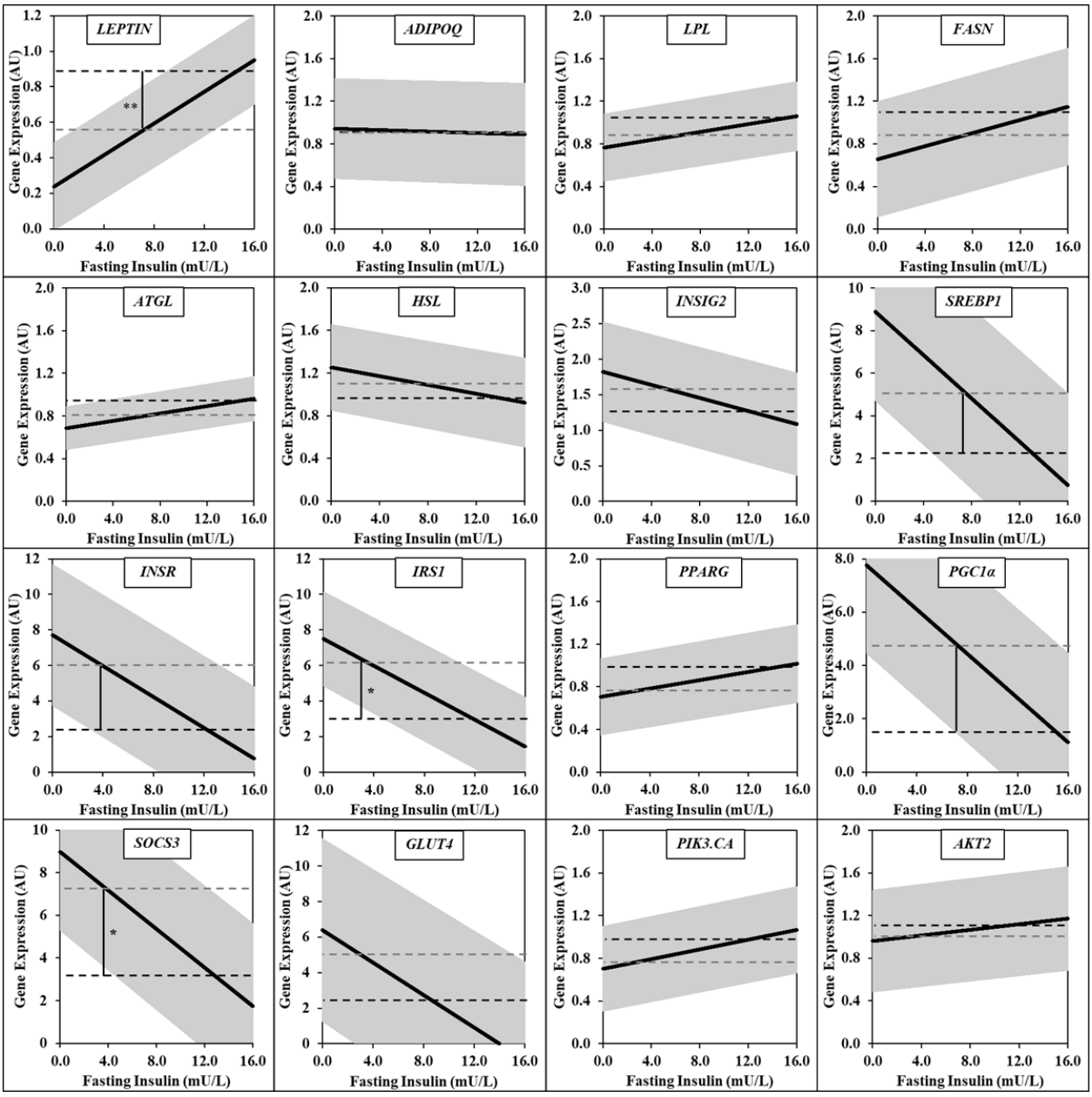

Figure 5.5: Association of circadian clock gene expression with fasting insulin. Subcutaneous adipose tissue (N = 7) was collected from sterile culture at baseline and twelve weeks following surgery. Fasting blood insulin was determined by ELISA. Mixed linear modeling was used to estimate the effect of each gene expression on weight loss achieved. 95% confidence interval is shown. Comparison is between estimated weight loss given average expression of each gene at baseline (black) or post-surgery (grey). Significance was determined by a two-sided t-test. Significance was determined by a two-sided t-test. P-values were, respectively: * < 0.05, ** < 0.01.

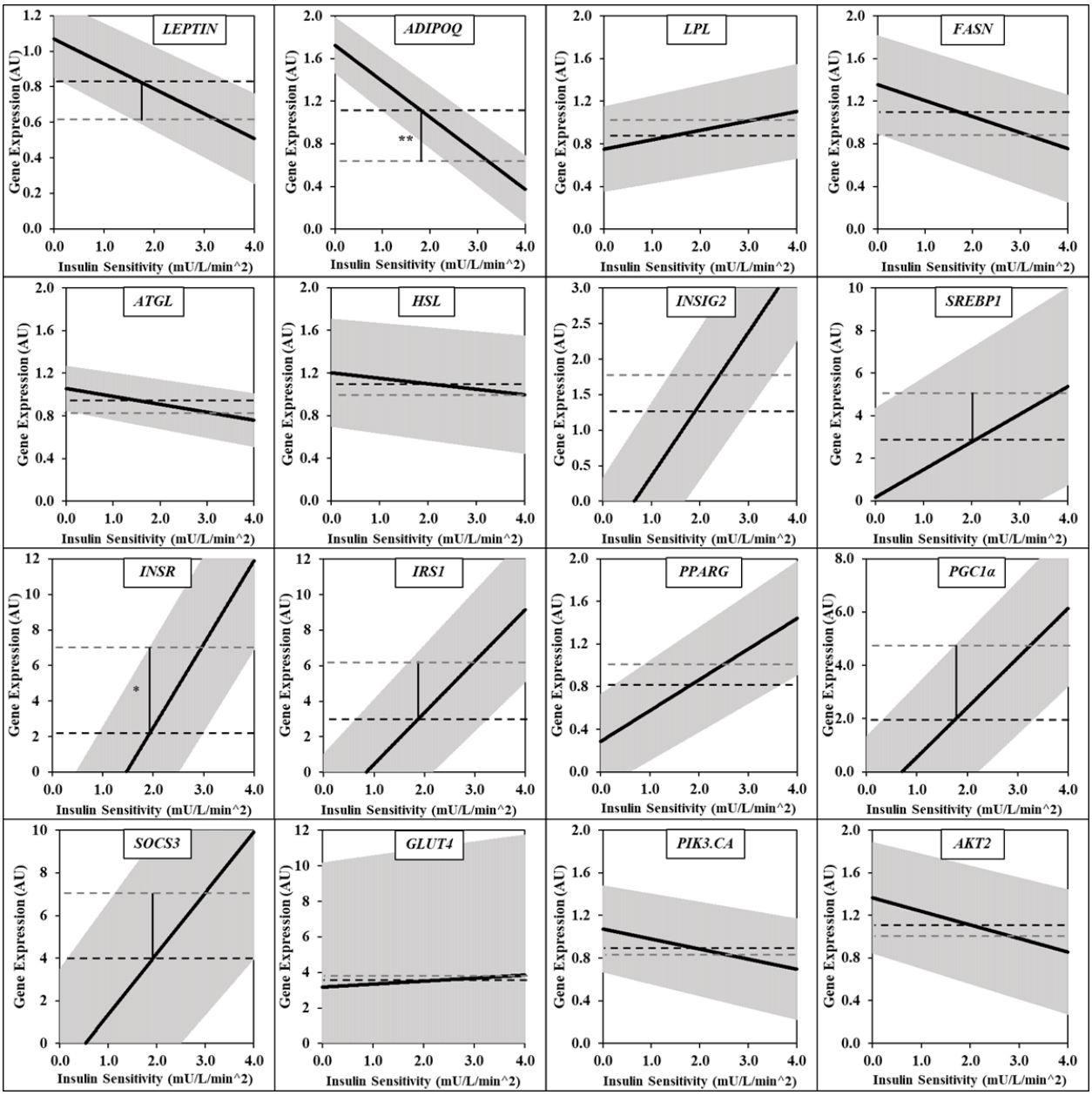

Figure 5.6: Association of adipose tissue metabolic gene expression with insulin sensitivity. Subcutaneous adipose tissue (N = 7) was collected from sterile culture at baseline and twelve weeks following surgery. Insulin sensitivity was computed using MINMOD Millenium software on fsIV-GTT results. Mixed linear modeling was used to estimate the effect of each gene expression on weight loss achieved. 95% confidence interval is shown. Comparison is between estimated weight loss given average expression of each gene at baseline (black) or post-surgery (grey). Significance was determined by a two-sided t-test. Significance was determined by a two-sided t-test. P-values were, respectively: * < 0.05, ** < 0.01.

Association of calories consumed and fatty acids with metabolic gene expression

Weight loss is associated with several metabolic alterations. We tested whether the changes in the gene expression are also associated could predict the degree of change in serum free fatty acids, adipose tissue lipolysis, and caloric consumption. The decline in calories eaten is associated with decreased *LEPTIN* (1.05 ± 0.11 [BL], 0.50 ± 0.12 [PS], p = 1.4E-5) and increased: *INSIG2* (1.00 ± 0.34 [BL], 1.96 ± 0.37 [PS], p = 0.01); *SREBP1* (0.35 ± 2.03 [BL], 6.40 ± 2.13 [PS], p = 5.3e-3); *PGC1α* (0.79 ± 1.29 [BL], 5.46 ± 1.37 [PS], p = 8.0e-4); *INSR* (1.01 ± 1.96 [BL], 6.27 ± 2.07 [PS], p = 0.01); *IRS1* (0.77 ± 1.78 [BL], 7.16 ± 1.88 [PS], p = 9.6E-4); *GLUT4* (0.26 ± 2.75 [BL], 6.17 ± 2.91 [PS], p = 0.045); *SOCS3* (0.53 ± 2.25 [BL], 7.56 ± 2.41 [PS], p = 4.3E-3) (Figure 5.7).

The change in serum free fatty acids was not associated with any of the metabolic genes (Figure 5.8). However, the increase in adipose tissue lipolysis was associated with decreased *LEPTIN* (0.92 ± 0.13 [BL], 0.56 ± 0.14 [PS], p = 0.009) and *ADIPOQ* (0.93 ± 0.19 [BL], 0.54 ± 0.19 [PS], p = 0.049) and increased *INSIG2* (1.01 ± 0.39 [BL], 2.22 ± 0.39 [PS], p = 3.0e-3) and *PGC1α* (0.99 ± 1.68 [BL], 6.43 ± 1.70 [PS], p = 1.9e-3) (Figure 5.9).

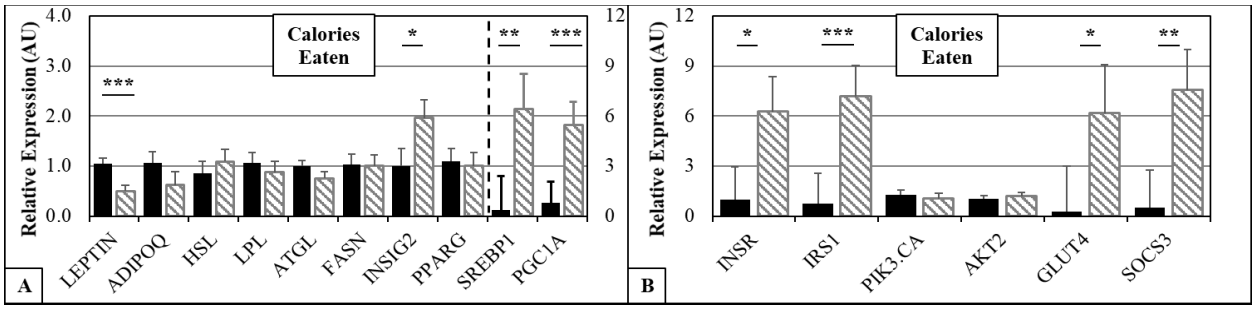

Figure 5.7: Effect of calories eaten on gene expression of metabolic genes. Subcutaneous adipose tissue (n=10) was collected from sterile culture at baseline (black) and at post-surgery (grey). Mixed linear modeling was used to estimate gene expression of each gene using: four meal average calories eaten during each lab session, Comparison is estimated expression at calories eaten at baseline or post-surgery. Significance was determined by a two-sided t-test. P-values were, respectively: * < 0.05, ** < 0.01 and *** < 0.001.

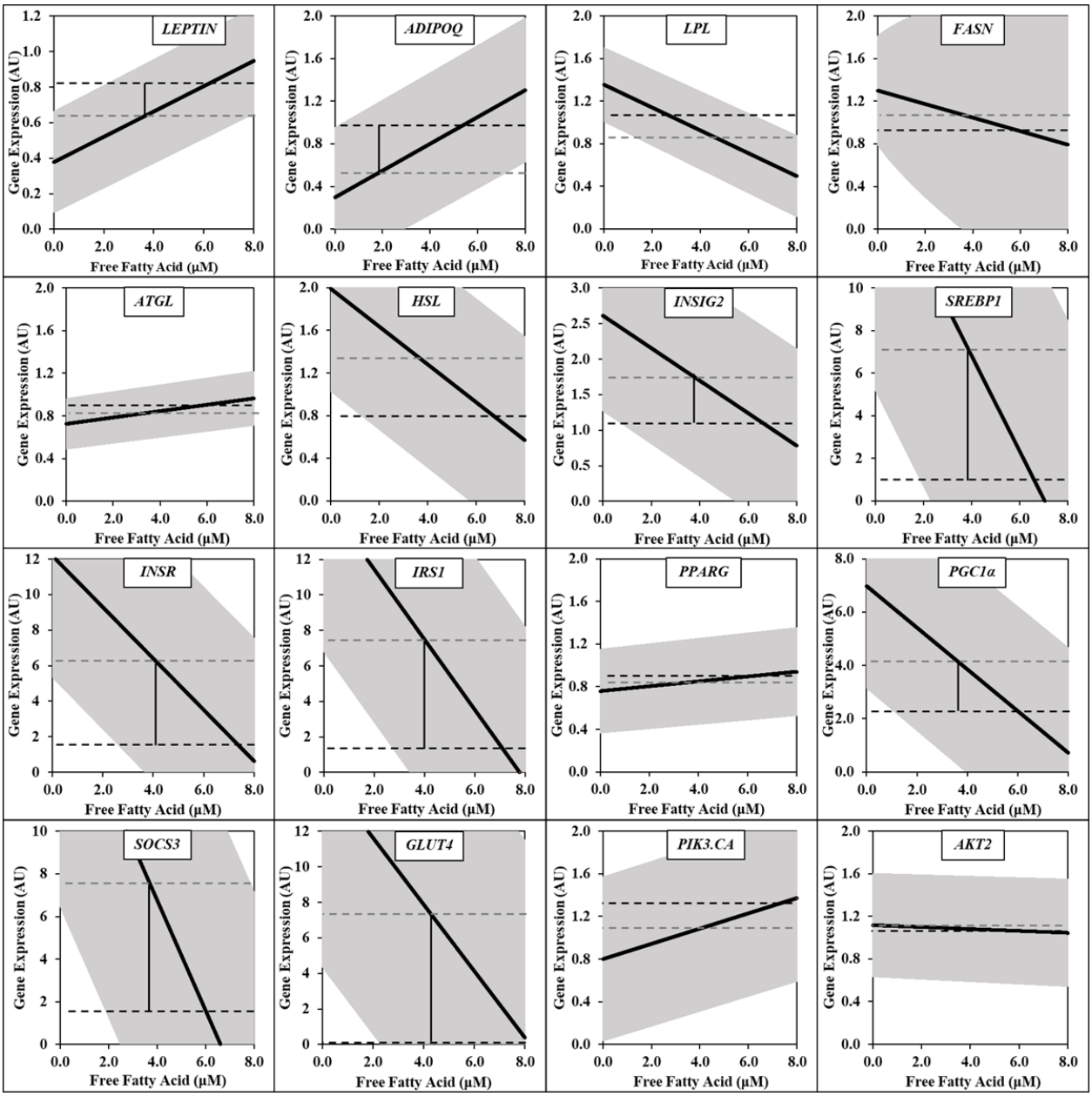

Figure 5.8: Association of adipose tissue metabolic gene expression with serum free fatty acid levels. Subcutaneous adipose tissue (N = 8) was collected from sterile culture at baseline and twelve weeks following surgery. Free fatty acid levels were determined by a colorimetric assay on blood. Mixed linear modeling was used to estimate the effect of each gene expression on weight loss achieved. 95% confidence interval is shown. Comparison is between estimated weight loss given average expression of each gene at baseline (black) or post-surgery (grey). Significance was determined by a two-sided t-test. Significance was determined by a two-sided t-test. P-values were not significant.

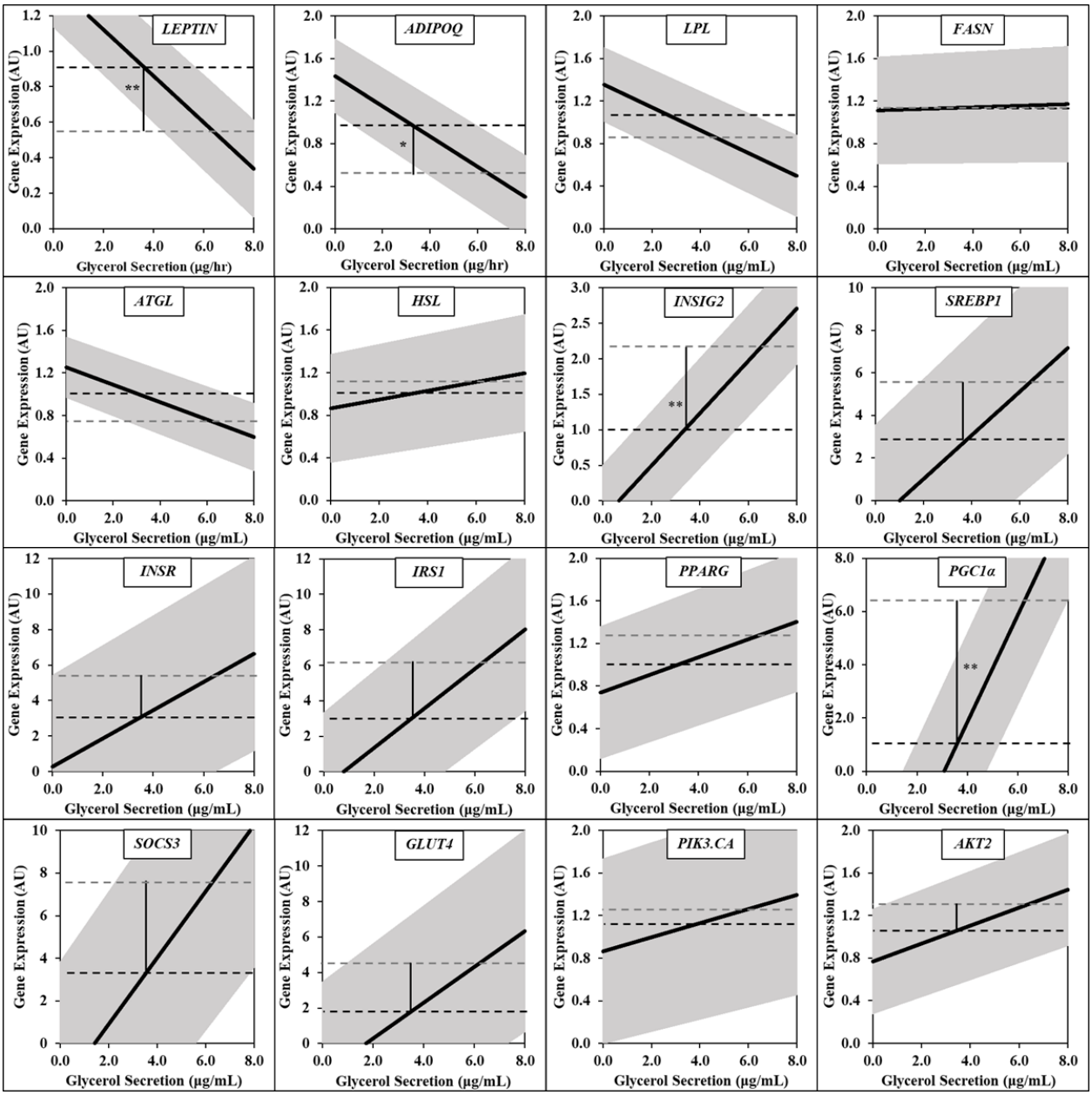

Figure 5.9: Association of adipose tissue metabolic gene expression with adipose tissue lipolysis. Subcutaneous adipose tissue (N = 8) was collected from sterile culture at baseline and twelve weeks following surgery. Glycerol secretion rate was computed colorimetric assay on conditioned media. Mixed linear modeling was used to estimate the effect of each gene expression on weight loss achieved. 95% confidence interval is shown. Comparison is between estimated weight loss given average expression of each gene at baseline (black) or post-surgery (grey). Significance was determined by a two-sided t-test. Significance was determined by a two-sided t-test. P-values were, respectively: * < 0.05, and ** < 0.01.

Discussion

It is clear that there are metabolic improvements that are occurring post-surgery. The weight loss after twelve weeks is not different from the degree of weight loss that has been shown from previous bariatric surgery trials. The alignment of the degree of improvements to fasting glucose, fasting insulin and systemic insulin sensitivity are more difficult to place next to other literature. Yet, the direction of the changes to these variables is in agreement with prior reports.

Two changes to gene expression are unsurprising given the nature of the caloric restriction that the patients were under: *LEPTIN* and *PGC1α.* It is therefore, then unsurprising, that these genes were highly associated with the weight loss achieved and specifically the difference in calories consumed per day at baseline and post-surgery. However, a decrease would be expected to *PPARG* under fasting conditions, which was absent.

It is of interest that the transcriptional balance that occurred as a result of surgery would appear to support lipogenesis over lipolysis. Yet, it is also clear that lipolysis as measured by glycerol secretion rate is elevated from baseline at this point following surgery. It is perhaps not hard to explain that *INSIG2* is elevated in association with a greater decline in calories eaten. However, the upregulation of *SREBP1* would only be expected to be present in the context of a fasting-refeeding paradigm. *ATGL/PNPLA2* did appear to be down-regulated following surgery. However, caloric restriction nor systemic metabolism effectively modelled the effect. It would be interesting to see if mTORC1-Egr-ATGL axis was responsible. A closer look at downstream insulin-mediated effect would be warranted.

There is little controversial of the changes to the insulin signaling genes. *SOCS3* upregulation can be easily explained by caloric restriction. *INSR* and *IRS1* are well explained by

the association of the highly colinear variables of insulin sensitivity and fasting insulin levels. It would be interesting to see if the is any differences in the propensity for degradation or overall levels of INSR and IRS1 in relation to the weight loss and improvements to insulin sensitivity. It would also be interesting to know whether there are differences in insulin action under repeated stimulation at baseline and post-surgery.

Overall, these results indicate that the adipose tissue is responding to the systemic caloric restriction by increasing the degree of lipolysis. However, from a gene expression standpoint, it would appear that lipolysis would be supported (SREBP1) while lipolysis is inhibited (ATGL). Gene expression changes are clearly favoring an increase in insulin action in parallel with the increased systemic insulin sensitivity (increased INSR, IRS1, SOCS3).

Chapter 6: Conclusions and Future Directions

During the conduct of this thesis project there were a few conclusions that were reached. Firstly, following laparoscopic sleeve gastrectomy in women with morbid obesity, there were systemic improvements to fasting glucose, fasting insulin, and insulin sensitivity. Additionally, there was a trend for a decrease in global fasting free fatty acid levels despite a subcutaneous adipose tissue increase in lipolysis. There was not a change in rhythms of melatonin or cortisol, nor was there significant sleep-related improvements. Overall, appetite decreased on several parameters while hormonally the total ghrelin was unchanged while active ghrelin-to-total-ghrelin increased and leptin decreased. In the adipose tissue there was no change in the phase of the circadian clock, but there was an overall upregulation in the several elements apparently in association with *hDBP* and *hNPAS2*. The changes were associated with the degree of caloric restriction and weight loss, and *hNPAS2*-related changes also associated with systemic insulin sensitivity. Several genes related to adipose tissue metabolism also exhibited altered gene expression. Adipokine genes were down-regulated in parallel with caloric restriction, while insulin signaling was upregulated. There was a phase delay in maximal gene expression of several metabolic genes (*INSR, IRS1, SOCS3,* and *INSIG2*) from near sleep onset to early morning.

It is clear that there is a caloric restriction aspect to what is occurring in adipose tissue and systemically in the period twelve weeks following surgery. We showed that the levels of serum free fatty acids are trending downward despite significantly elevated free fatty acid release from adipose tissue. This raises questions regarding the regulation of the lipoprotein system after surgery. It is known that there is a period shortly after surgery whereby the caloric deficit results in excess free fatty acid release from adipose tissue. However, it is not clear which organ is mostly responsible for the disposal of the free fatty acids by later times post-surgery. Under the hypothesis

of increased bile acid production, it is possible that the liver is responsible for upregulating the bile acid production from ectopically stored free fatty acids. It is also possible that the adipose tissue is undergoing significant changes that increase the caloric expenditure. For example, there is very little thermogenesis that occurs in severe obesity. However, it is possible that the adipocytes are: 1) undergoing more lipogenesis-lipolysis futile cycling, 2) there is increased recruitment of the thermogenic capacity from resident adipose tissue beige adipocytes.

I believe that targeted metabolic studies monitoring the distribution in metabolite flux through different organs would be beneficial. The simplest of the metabolic studies would be to use hyperinsulinemic-euglycemic clamps studies to measure the estimated contribution of the liver, skeletal muscle, and adipose tissue. An interesting follow-up would be to look at DEXA scan quantification of subcutaneous-to-visceral fat loss relative to the metabolic improvements that are being seen. In a slightly different angle, subjects could be monitored for truncal fat loss versus gynoid fat loss as it relates to the improvements seen in metabolic health. The combination of clamp studies with DEXA scans and blood measure of metabolic health could yield useful associations for understanding the implications of certain types of adipose-tissue-associated weight loss. An inclusion of longitudinal tracking may contribute to creation of different profiles of weight loss and how each contributes to the stability and magnitude of metabolic health improvements.

Yet, I would like to know the difference in caloric expenditure following surgery beyond just adipose tissue. I would especially like to know how the differences following bariatric surgery relate to the differences seen in individuals on a lowered (500 kcal deficit) and very low-calorie diet (1000 kcal deficit). If I were to design a clinical study, I would like to measure the changes in fasting morning and post-breakfast levels of appetite regulating hormones. The hormones that I

think are highly relevant to the discussion of appetite are: 1) leptin, 2) total and active ghrelin, 3) PYY, 4) GLP-1, 5) orexin, and 6) NPY. In addition, I would be highly interested in nutritional screening for: 1) iron, 2) zinc, 3) folic acid, 4) cobalamin (B12), 5) vitamin D and calcium, and 6) copper. Lastly, I would screen for metabolic variables: glucose and insulin. In coordination, I would like to see the subjective hunger and appetite ratings. More resolution would be beneficial to further identify differences across the day, but two ratings are the minimum resolution necessary to gauge the fasting and prandial effects. The blood could be obtained by a phlebotomist could take two-to-four vials of blood at baseline and two vials at thirty minutes following a meal, which could then be treated as necessary to ensure acute quantitation. The low-calorie diets would be measured once-a-week for up to a year under nutritionist supervision and verified diet compliance. For the bariatric surgery arm of the study, I would prefer to monitor them at baseline two weeks before surgery, within a day prior to surgery, one week following surgery, two weeks following surgery, 1 month following surgery, and then once a month (± 1 week) until 6 months, and then every three months for up to five years. The outputs from this study would be the alignment of longitudinal appetite changes across time with appetite regulating hormones. Given the vital data collected, I could identify whether there is a type of appetite or appetite regulatory hormones differences that are associated with the transition from weight-loss-to-weight-maintenance, and weight-maintenance-to-weight-gain. Importantly for patient quality of life, the same metrics could be assessed for the degree of nutritional deficiencies.

The alteration in the phase of the subcutaneous adipose tissue gene expression of the metabolic genes: *INSIG2, INSR, IRS1,* and *SOCS3* has not been clarified. The first step would be to identify if there is a change in the protein levels of these genes and if those changes are at certain times during the day. These changes could be observed in parallel with morning and evening

insulin action in adipose tissue. Importantly, these results of short-term and intermediate-term insulin response could be compared to the insulin action of non-obese individuals. These results could answer question of chronotype alignment of metabolism during the resolution of severe obesity to milder classes of obesity as it compares to physiology in non-obese individuals.

Regarding the circadian clock function, it would be interesting to see the results of knock-down of mBMAL1, mNPAS2, or mDBP, globally or in adipose tissue, on the magnitude of the weight loss and metabolic improvements seen in post-surgery. Obviously, these experiments would need to be conducted in mice or rats. While the phase was not changed post-surgery, there is an open question of whether the oscillation of the circadian clock is necessary for the improvements seen post-surgery. The knock-down of mBMAL1 could evince whether it is the global expression or the MESOR-driven accentuation in the circadian clock that is responsible for the changes seen post-surgery. Knock-down of mNPAS2 or mDBP could help to explain whether the metabolic improvements are partially dependent on the altered circadian clock expression.

In a converse fashion, there is justification to identify further the proteins responsible for the changes to circadian clock gene expression. One approach could be to use functional genomics to identify the gene regions that are differentially regulated. Next, the potential genes suspected to regulate those regions could be tested for differential DNA residence. Following, the pathways that regulate the differential binding could be modulated to identify if they are able to lead to a regulatory profile consistent with the post-surgery profile without surgery, or are able to accentuate or attenuate the changes seen post-surgery. The systemic metabolic consequence could be observed to see to what extent the specific pathway is involved in mediating the overall changes.

There are unanswered questions regarding the stromal vascular fraction of the adipose tissue. It would be beneficial to know the differences in the types of immune cells that were present

after bariatric surgery. Further, it would be beneficial to look at the markers of the macrophages in adipose tissue to identify polarization. If these studies were conducted in longitudinal studies it could point to a point whereby the macrophages switch from predominately metabolically-activated to a M2 polarization. With experiments that have lipolysis and insulin action measured, it could tie macrophages partially to the metabolic differences seen in adipose tissue.

There is no doubt that the systemic insulin sensitivity and glucose tolerance are associated with the changes in adipose tissue, but there is still a need to improve the picture of how adipose tissue is changing across time and to what degree adipose tissue is reacting to metabolic changes or contributing to them. Future projects could shed light on these questions so that it is clear how to support the beneficial effects of bariatric surgery while limiting the detrimental side effects. And, in the future, a clearer picture of the cascade of metabolic changes can be leveraged to eliminate the need for surgical intervention.

References

(2010) Diagnosis and Classification of Diabetes Mellitus. *Diabetes Care,* 33**,** S62.

Abbatini, F., M. Rizzello, G. Casella, G. Alessandri, D. Capoccia, F. Leonetti & N. Basso (2010) Long-term effects of laparoscopic sleeve gastrectomy, gastric bypass, and adjustable gastric banding on type 2 diabetes. *Surg Endosc,* 24**,** 1005-10.

Adams, T. D., L. E. Davidson, S. E. Litwin, J. Kim, R. L. Kolotkin, M. N. Nanjee, J. M. Gutierrez, S. J. Frogley, A. R. Ibele, E. A. Brinton, P. N. Hopkins, R. McKinlay, S. C. Simper & S. C. Hunt (2017) Weight and Metabolic Outcomes 12 Years after Gastric Bypass. *New England Journal of Medicine,* 377**,** 1143-1155.

Adams, T. D., R. E. Gress, S. C. Smith, R. C. Halverson, S. C. Simper, W. D. Rosamond, M. J. LaMonte, A. M. Stroup & S. C. Hunt (2007) Long-term mortality after gastric bypass surgery. *New England Journal of Medicine,* 357**,** 753-761.

Albers, P. H., K. N. Bojsen-Moller, C. Dirksen, A. K. Serup, D. E. Kristensen, J. Frystyk, T. R. Clausen, B. Kiens, E. A. Richter, S. Madsbad & J. F. P. Wojtaszewski (2015) Enhanced insulin signaling in human skeletal muscle and adipose tissue following gastric bypass surgery. *American Journal of Physiology-Regulatory Integrative and Comparative Physiology,* 309**,** R510-R524.

Amable, P. R., M. V. T. Teixeira, R. B. V. Carias, J. M. Granjeiro & R. Borojevic (2013) Identification of Appropriate Reference Genes for Human Mesenchymal Cells during Expansion and Differentiation. *Plos One,* 8**,** 9.

Angelini, G., L. Castagneto Gissey, G. Del Corpo, C. Giordano, B. Cerbelli, A. Severino, M. Manco, N. Basso, A. L. Birkenfeld, S. R. Bornstein, A. Genco, G. Mingrone & G. Casella (2019) New insight into the mechanisms of ectopic fat deposition improvement after bariatric surgery. *Scientific Reports,* 9**,** 17315.

Asada, S., H. Daitoku, H. Matsuzaki, T. Saito, T. Sudo, H. Mukai, S. Iwashita, K. Kako, T. Kishi, Y. Kasuya & A. Fukamizu (2007) Mitogen-activated protein kinases, Erk and p38, phosphorylate and regulate Foxo1. *Cell Signal,* 19**,** 519-27.

Asher, G., D. Gatfield, M. Stratmann, H. Reinke, C. Dibner, F. Kreppel, R. Mostoslavsky, F. W. Alt & U. Schibler (2008) SIRT1 regulates circadian clock gene expression through PER2 deacetylation. *Cell,* 134**,** 317-28.

Ashrafian, H., T. Athanasiou, J. V. Li, M. Bueter, K. Ahmed, K. Nagpal, E. Holmes, A. Darzi & S. R. Bloom (2011) Diabetes resolution and hyperinsulinaemia after metabolic Roux-en-Y gastric bypass. *Obesity Reviews,* 12**,** e257-e272.

Atri, C., F. Z. Guerfali & D. Laouini (2018) Role of Human Macrophage Polarization in Inflammation during Infectious Diseases. *Int J Mol Sci,* 19.

Aubin, K., M. Safoine, M. Proulx, M.-A. Audet-Casgrain, J.-F. Côté, F.-A. Têtu, A. Roy & J. Fradette (2015) Characterization of In Vitro Engineered Human Adipose Tissues: Relevant Adipokine Secretion and Impact of TNF-α. *PloS one,* 10**,** e0137612-e0137612.

Avgerinos, K. I., N. Spyrou, C. S. Mantzoros & M. Dalamaga. 2019. Obesity and cancer risk: Emerging biological mechanisms and perspectives. In *Metabolism*, 121-135. United States: © 2018 Elsevier Inc.

Bae, K., X. Jin, E. S. Maywood, M. H. Hastings, S. M. Reppert & D. R. Weaver (2001) Differential functions of mPer1, mPer2, and mPer3 in the SCN circadian clock. *Neuron,* 30**,** 525-536.

Barakat, R., O. Oakley, H. Kim, J. Jin & C. J. Ko (2016) Extra-gonadal sites of estrogen biosynthesis and function. *BMB Rep,* 49**,** 488-96.

Barthel, A. & D. Schmoll (2003) Novel concepts in insulin regulation of hepatic gluconeogenesis. *American Journal of Physiology-Endocrinology and Metabolism,* 285**,** E685-E692.

Bartness, T. J., Y. Liu, Y. B. Shrestha & V. Ryu (2014) Neural innervation of white adipose tissue and the control of lipolysis. *Front Neuroendocrinol,* 35**,** 473-93.

Basso, N., D. Capoccia, M. Rizzello, F. Abbatini, P. Mariani, C. Maglio, F. Coccia, G. Borgonuovo, M. L. De Luca, R. Asprino, G. Alessandri, G. Casella & F. Leonetti (2011) First-phase insulin secretion, insulin sensitivity, ghrelin, GLP-1, and PYY changes 72 h after sleeve gastrectomy in obese diabetic patients: the gastric hypothesis. *Surgical Endoscopy and Other Interventional Techniques,* 25**,** 3540-3550.

Berson, D. M., F. A. Dunn & M. Takao (2002) Phototransduction by Retinal Ganglion Cells That Set the Circadian Clock. *Science,* 295**,** 1070.

Blagojevic, M., C. Jinks, A. Jeffery & K. P. Jordan (2010) Risk factors for onset of osteoarthritis of the knee in older adults: a systematic review and meta-analysis. *Osteoarthritis Cartilage,* 18**,** 24-33.

Bohdjalian, A., F. B. Langer, S. Shakeri-Leidenmuhler, L. Gfrerer, B. Ludvik, J. Zacherl & G. Prager (2010) Sleeve Gastrectomy as Sole and Definitive Bariatric Procedure: 5-Year Results for Weight Loss and Ghrelin. *Obesity Surgery,* 20**,** 535-540.

Bonnet, M. H. & D. L. Arand (2005) Impact of Motivation on Multiple Sleep Latency Test and Maintenance of Wakefulness Test Measurements. *Journal of Clinical Sleep Medicine,* 1**,** 386-390.

Boston, R. C., D. Stefanovski, P. J. Moate, A. E. Sumner, R. M. Watanabe & R. N. Bergman (2003) MINMOD Millennium: a computer program to calculate glucose effectiveness and insulin sensitivity from the frequently sampled intravenous glucose tolerance test. *Diabetes Technol Ther,* 5**,** 1003-15.

Broussard, J. L., D. A. Ehrmann, E. Van Cauter, E. Tasali & M. J. Brady (2012) Impaired insulin signaling in human adipocytes after experimental sleep restriction: a randomized, crossover study. *Annals of internal medicine,* 157**,** 549-557.

Brown, S. A., E. Kowalska & R. Dallmann. 2012. (Re)inventing the circadian feedback loop. In *Dev Cell*, 477-87. United States: Â© 2012 Elsevier Inc.

Bunger, M. K., L. D. Wilsbacher, S. M. Moran, C. Clendenin, L. A. Radcliffe, J. B. Hogenesch, M. C. Simon, J. S. Takahashi & C. A. Bradfield (2000) Mop3 is an essential component of the master circadian pacemaker in mammals. *Cell,* 103**,** 1009-1017.

Bustin, S. A., V. Benes, J. Garson, J. Hellemans, J. Huggett, M. Kubista, R. Mueller, T. Nolan, M. W. Pfaffl, G. Shipley, C. T. Wittwer, P. Schjerling, P. J. Day, M. Abreu, B. Aguado, J.-F. Beaulieu, A. Beckers, S. Bogaert, J. A. Browne, F. Carrasco-Ramiro, L. Ceelen, K. Ciborowski, P. Cornillie, S. Coulon, A. Cuypers, S. De Brouwer, L. De Ceuninck, J. De Craene, H. De Naeyer, W. De Spiegelaere, K. Deckers, A. Dheedene, K. Durinck, M. Ferreira-Teixeira, A. Fieuw, J. M. Gallup, S. Gonzalo-Flores, K. Goossens, F. Heindryckx, E. Herring, H. Hoenicka, L. Icardi, R. Jaggi, F. Javad, M. Karampelias, F. Kibenge, M. Kibenge, C. Kumps, I. Lambertz, T. Lammens, A. Markey, P. Messiaen, E. Mets, S. Morais, A. Mudarra-Rubio, J. Nakiwala, H. Nelis, P. A. Olsvik, C. Pérez-Novo, M. Plusquin, T. Remans, A. Rihani, P. Rodrigues-Santos, P. Rondou, R. Sanders, K. Schmidt-Bleek, K. Skovgaard, K. Smeets, L. Tabera, S. Toegel, T. Van Acker, W. Van den Broeck, J. Van der Meulen, M. Van Gele, G. Van Peer, M. Van Poucke, N. Van Roy, S. Vergult, J. Wauman, M. Tshuikina-Wiklander, E. Willems, S. Zaccara, F. Zeka & J. Vandesompele (2013) The need for transparency and good practices in the qPCR literature. *Nature Methods,* 10**,** 1063.

Bustin, S. A., V. Benes, J. A. Garson, J. Hellemans, J. Huggett, M. Kubista, R. Mueller, T. Nolan, M. W. Pfaffl, G. L. Shipley, J. Vandesompele & C. T. Wittwer (2009) The MIQE Guidelines: Minimum Information for Publication of Quantitative Real-Time PCR Experiments. *Clinical Chemistry,* 55**,** 611-622.

Camacho, F., M. Cilio, Y. Guo, D. Virshup, K. Patel, O. Khorkova, S. Styren, B. Morse, Z. Yao & G. Keesler (2001) Human casein kinase Iδ phosphorylation of human circadian clock proteins period 1 and 2. *FEBS letters,* 489**,** 159-165.

Cao, Y. (2013) Angiogenesis and vascular functions in modulation of obesity, adipose metabolism, and insulin sensitivity. *Cell metabolism,* 18**,** 478-489.

Carmean, C. M., A. M. Bobe, J. C. Yu, P. A. Volden & M. J. Brady (2013) Refeeding-induced brown adipose tissue glycogen hyper-accumulation in mice is mediated by insulin and catecholamines. *PLoS One,* 8**,** e67807.

Carswell, K. A., M. J. Lee & S. K. Fried. 2012. Culture of Isolated Human Adipocytes and Isolated Adipose Tissue. In *Human Cell Culture Protocols, Third Edition,* eds. R. R. Mitry & R. D. Hughes, 203-214. Totowa: Humana Press Inc.

Carter, M. E., A. Adamantidis, H. Ohtsu, K. Deisseroth & L. de Lecea (2009) Sleep Homeostasis Modulates Hypocretin-Mediated Sleep-to-Wake Transitions. *Journal of Neuroscience,* 29**,** 10939-10949.

Casella, G., E. Soricelli, L. Castagneto-Gissey, A. Redler, N. Basso & G. Mingrone (2016) Changes in insulin sensitivity and secretion after sleeve gastrectomy. *British Journal of Surgery,* 103**,** 242-248.

Castagneto-Gissey, L. & G. Mingrone (2012) Insulin sensitivity and secretion modifications after bariatric surgery. *Journal of Endocrinological Investigation,* 35**,** 692-698.

Castoldi, A., C. Naffah de Souza, N. O. Câmara & P. M. Moraes-Vieira (2015) The Macrophage Switch in Obesity Development. *Front Immunol,* 6**,** 637.

Chakrabarti, P., J. Y. Kim, M. Singh, Y. K. Shin, J. Kim, J. Kumbrink, Y. Wu, M. J. Lee, K. H. Kirsch, S. K. Fried & K. V. Kandror (2013) Insulin inhibits lipolysis in adipocytes via the evolutionarily conserved mTORC1-Egr1-ATGL-mediated pathway. *Mol Cell Biol,* 33**,** 3659-66.

Chambers, A. P., L. Jessen, K. K. Ryan, S. Sisley, H. E. Wilson-Perez, M. A. Stefater, S. G. Gaitonde, J. E. Sorrell, M. Toure, J. Berger, D. A. D'Alessio, S. C. Woods, R. J. Seeley & D. A. Sandoval (2011) Weight-Independent Changes in Blood Glucose Homeostasis After Gastric Bypass or Vertical Sleeve Gastrectomy in Rats. *Gastroenterology,* 141**,** 950-958.

Chan, J. L., E. C. Mun, V. Stoyneva, C. S. Mantzoros & A. B. Goldfine (2006) Peptide YY levels are elevated after gastric bypass surgery. *Obesity (Silver Spring),* 14**,** 194-8.

Chen, S. R., H. Chen, J. J. Zhou, G. Pradhan, Y. Sun, H. L. Pan & D. P. Li (2017) Ghrelin receptors mediate ghrelin-induced excitation of agouti-related protein/neuropeptide Y but not pro-opiomelanocortin neurons. *J Neurochem,* 142**,** 512-520.

Chen, Y., L. Huang, X. Qi & C. Chen (2019) Insulin Receptor Trafficking: Consequences for Insulin Sensitivity and Diabetes. *Int J Mol Sci,* 20.

Choe, S. S., J. Y. Huh, I. J. Hwang, J. I. Kim & J. B. Kim (2016) Adipose Tissue Remodeling: Its Role in Energy Metabolism and Metabolic Disorders. *Front Endocrinol (Lausanne),* 7**,** 30.

Coats, B. R., K. Q. Schoenfelt, V. C. Barbosa-Lorenzi, E. Peris, C. Cui, A. Hoffman, G. Zhou, S. Fernandez, L. Zhai, B. A. Hall, A. S. Haka, A. M. Shah, C. A. Reardon, M. J. Brady, C. J. Rhodes, F. R. Maxfield & L. Becker (2017) Metabolically Activated Adipose Tissue Macrophages Perform Detrimental and Beneficial Functions during Diet-Induced Obesity. *Cell Rep,* 20**,** 3149-3161.

Coelho, M., T. Oliveira & R. Fernandes (2013) Biochemistry of adipose tissue: an endocrine organ. *Arch Med Sci,* 9**,** 191-200.

Coggon, D., I. Reading, P. Croft, M. McLaren, D. Barrett & C. Cooper (2001) Knee osteoarthritis and obesity. *Int J Obes Relat Metab Disord,* 25**,** 622-7.

Coppack, S. W. (2001) Pro-inflammatory cytokines and adipose tissue. *Proc Nutr Soc,* 60**,** 349-56.

Costa, M. J., B. Finkenstädt, V. Roche, F. Lévi, P. D. Gould, J. Foreman, K. Halliday, A. Hall & D. A. Rand (2013) Inference on periodicity of circadian time series. *Biostatistics,* 14**,** 792-806.

Craig M. Hales, M. D., Margaret D. Carroll, M.S.P.H., Cheryl D. Fryar, M.S.P.H., and Cynthia L. Ogden, Ph.D. Feb 2020. Prevalence of Obesity and Severe Obesity Among Adults: United States, 2017-2018.

Crowe, C., I. Gibson, K. Cunningham, C. Kerins, C. Costello, J. Windle, P. M. O. Shea, M. Hynes, B. McGuire, K. Kilkelly, H. Griffin, T. O. Brien, J. Jones & F. M. Finucane (2015) Effects of an eight-week supervised, structured lifestyle modification programme on anthropometric, metabolic and cardiovascular risk factors in severely obese adults. *Bmc Endocrine Disorders,* 15**,** 8.

Cui, X., F. Lu, Y. Li, Y. Xue, Y. Kang, S. Zhang, Q. Qiu, X. Cui, S. Zheng, B. Liu, X. Xu & X. Cao (2013) Ubiquitin-specific proteases UBP12 and UBP13 act in circadian clock and photoperiodic flowering regulation in Arabidopsis. *Plant physiology,* 162**,** 897-906.

Curtis, K. M., L. A. Gomez, C. Rios, E. Garbayo, A. P. Raval, M. A. Perez-Pinzon & P. C. Schiller (2010) EF1 alpha and RPL13a represent normalization genes suitable for RT-qPCR analysis of bone marrow derived mesenchymal stem cells. *Bmc Molecular Biology,* 11**,** 15.

Czeisler, C. A., J. F. Duffy, T. L. Shanahan, E. N. Brown, J. F. Mitchell, D. W. Rimmer, J. M. Ronda, E. J. Silva, J. S. Allan & J. S. Emens (1999a) Stability, precision, and near-24-hour period of the human circadian pacemaker. *Science,* 284**,** 2177-2181.

Czeisler, C. A., J. F. Duffy, T. L. Shanahan, E. N. Brown, J. F. Mitchell, D. W. Rimmer, J. M. Ronda, E. J. Silva, J. S. Allan, J. S. Emens, D.-J. Dijk & R. E. Kronauer (1999b) Stability, Precision, and Near-24-Hour Period of the Human Circadian Pacemaker. *Science,* 284**,** 2177.

Dardente, H., E. E. Fortier, V. Martineau & N. Cermakian (2007) Cryptochromes impair phosphorylation of transcriptional activators in the clock: a general mechanism for circadian repression. *Biochem J,* 402**,** 525-36.

De Pergola, G. & F. Silvestris (2013) Obesity as a major risk factor for cancer. *J Obes,* 2013**,** 291546.

DeBose-Boyd, R. A. & J. Ye (2018) SREBPs in Lipid Metabolism, Insulin Signaling, and Beyond. *Trends Biochem Sci,* 43**,** 358-368.

Debruyne, J. P. (2008) Oscillating perceptions: the ups and downs of the CLOCK protein in the mouse circadian system. *Journal of genetics,* 87**,** 437-446.

DeBruyne, J. P., E. Noton, C. M. Lambert, E. S. Maywood, D. R. Weaver & S. M. Reppert (2006) A clock shock: mouse CLOCK is not required for circadian oscillator function. *Neuron,* 50**,** 465-477.

del Pozo, C. H., R. M. Calvo, G. Vesperinas-Garcia, J. Gomez-Ambrosi, G. Fruhbeck, R. Corripio-Sanchez, M. A. Rubio & M. J. Obregon (2010) IPO8 and FBXL10: New Reference Genes for Gene Expression Studies in Human Adipose Tissue. *Obesity,* 18**,** 897-903.

Denroche, H. C., F. K. Huynh & T. J. Kieffer (2012) The role of leptin in glucose homeostasis. *Journal of Diabetes Investigation,* 3**,** 115-129.

Dodd, A. N., N. Salathia, A. Hall, E. Kévei, R. Tóth, F. Nagy, J. M. Hibberd, A. J. Millar & A. A. R. Webb (2005) Plant Circadian Clocks Increase Photosynthesis, Growth, Survival, and Competitive Advantage. *Science,* 309**,** 630.

Donga, E., M. van Dijk, J. G. van Dijk, N. R. Biermasz, G. J. Lammers, K. van Kralingen, R. P. Hoogma, E. P. Corssmit & J. A. Romijn (2010) Partial sleep restriction decreases insulin sensitivity in type 1 diabetes. *Diabetes Care,* 33**,** 1573-7.

Duez, H. & B. Staels (2010) Nuclear Receptors Linking Circadian Rhythms and Cardiometabolic Control. *Arteriosclerosis, Thrombosis, and Vascular Biology,* 30**,** 1529-1534.

Duncan, R. E., M. Ahmadian, K. Jaworski, E. Sarkadi-Nagy & H. S. Sul (2007) Regulation of lipolysis in adipocytes. *Annu Rev Nutr,* 27**,** 79-101.

Dvornyk, V., O. Vinogradova & E. Nevo (2003) Origin and evolution of circadian clock genes in prokaryotes. *Proceedings of the National Academy of Sciences,* 100**,** 2495.

Ebbert, J. O. & M. D. Jensen (2013) Fat depots, free fatty acids, and dyslipidemia. *Nutrients,* 5**,** 498-508.

Emile, S. & H. Elfeki. 2017. NUTRITIONAL DEFICIENCY AFTER SLEEVE GASTRECTOMY : A COMPREHENSIVE LITERATURE REVIEW *.

Fain, J. N., P. S. Cheema, S. W. Bahouth & M. Lloyd Hiler (2003) Resistin release by human adipose tissue explants in primary culture. *Biochemical and Biophysical Research Communications,* 300**,** 674-678.

Feuerer, M., L. Herrero, D. Cipolletta, A. Naaz, J. Wong, A. Nayer, J. Lee, A. B. Goldfine, C. Benoist, S. Shoelson & D. Mathis (2009) Lean, but not obese, fat is enriched for a unique population of regulatory T cells that affect metabolic parameters. *Nature Medicine,* 15**,** 930-939.

Fiaschi, T. (2019) Mechanisms of Adiponectin Action. *Int J Mol Sci,* 20.

Fink, T., P. Lund, L. Pilgaard, J. G. Rasmussen, M. Duroux & V. Zachar (2008) Instability of standard PCR reference genes in adipose-derived stem cells during propagation, differentiation and hypoxic exposure. *Bmc Molecular Biology,* 9**,** 9.

Finkelstein, E. A., J. G. Trogdon, J. W. Cohen & W. Dietz (2009) Annual medical spending attributable to obesity: payer-and service-specific estimates. *Health Aff (Millwood),* 28**,** w822-31.

Fischer, L., C. Hildebrandt, T. Bruckner, H. Kenngott, G. R. Linke, T. Gehrig, M. W. Büchler & B. P. Müller-Stich (2012) Excessive weight loss after sleeve gastrectomy: a systematic review. *Obesity surgery,* 22**,** 721-731.

Flaherty, S. E., A. Grijalva, X. Xu, E. Ables, A. Nomani & A. W. Ferrante (2019) A lipase-independent pathway of lipid release and immune modulation by adipocytes. *Science,* 363**,** 989.

Flegal, K. M., M. D. Carroll, B. K. Kit & C. L. Ogden (2012) Prevalence of Obesity and Trends in the Distribution of Body Mass Index Among US Adults, 1999-2010. *Jama-Journal of the American Medical Association,* 307**,** 491-497.

Flegal, K. M., B. K. Kit, H. Orpana & B. I. Graubard (2013) Association of all-cause mortality with overweight and obesity using standard body mass index categories: a systematic review and meta-analysis. *Jama,* 309**,** 71-82.

Foldager, C. B., S. Munir, M. Ulrik-Vinther, K. Soballe, C. Bunger & M. Lind (2009) Validation of suitable house keeping genes for hypoxia-cultured human chondrocytes. *Bmc Molecular Biology,* 10**,** 8.

Frayn, K. N., P. Arner & H. Yki-Järvinen (2006) Fatty acid metabolism in adipose tissue, muscle and liver in health and disease. *Essays in Biochemistry,* 42**,** 89-103.

Fu, Y., N. Luo, R. L. Klein & W. T. Garvey (2005) Adiponectin promotes adipocyte differentiation, insulin sensitivity, and lipid accumulation. *Journal of Lipid Research,* 46**,** 1369-1379.

Galanakis, C. G., M. Daskalakis, A. Manios, A. Xyda, A. H. Karantanas & J. Melissas (2015) Computed Tomography-Based Assessment of Abdominal Adiposity Changes and Their Impact on Metabolic Alterations Following Bariatric Surgery. *World Journal of Surgery,* 39**,** 417-423.

Ganz, M. L., N. Wintfeld, Q. Li, V. Alas, J. Langer & M. Hammer (2014) The association of body mass index with the risk of type 2 diabetes: a case-control study nested in an electronic health records system in the United States. *Diabetol Metab Syndr,* 6**,** 50.

Garaulet, M., J. M. Ordovás, P. Gómez-Abellán, J. A. Martínez & J. A. Madrid (2011) An approximation to the temporal order in endogenous circadian rhythms of genes implicated in human adipose tissue metabolism. *Journal of cellular physiology,* 226**,** 2075-2080.

Garrido-Sanchez, L., M. Murri, J. Rivas-Becerra, L. Ocana-Wilhelmi, R. V. Cohen, E. Garcia-Fuentes & F. J. Tinahones (2012) Bypass of the duodenum improves insulin resistance much more rapidly than sleeve gastrectomy. *Surgery for Obesity and Related Diseases,* 8**,** 145-150.

Gekakis, N., D. Staknis, H. B. Nguyen, F. C. Davis, L. D. Wilsbacher, D. P. King, J. S. Takahashi & C. J. Weitz (1998) Role of the CLOCK protein in the mammalian circadian mechanism. *Science,* 280**,** 1564-1569.

Goldberg, I. J., R. H. Eckel & N. A. Abumrad (2009) Regulation of fatty acid uptake into tissues: lipoprotein lipase- and CD36-mediated pathways. *J Lipid Res,* 50 Suppl**,** S86-90.

Gottlieb, D. J., N. M. Punjabi, A. B. Newman, H. E. Resnick, S. Redline, C. M. Baldwin & F. J. Nieto (2005) Association of sleep time with diabetes mellitus and impaired glucose tolerance. *Archives of Internal Medicine,* 165**,** 863-868.

Griffin, E. A., D. Staknis & C. J. Weitz (1999) Light-independent role of CRY1 and CRY2 in the mammalian circadian clock. *Science,* 286**,** 768-771.

Gómez-Abellán, P., A. Díez-Noguera, J. A. Madrid, J. A. Luján, J. M. Ordovás & M. Garaulet (2012) Glucocorticoids Affect 24 h Clock Genes Expression in Human Adipose Tissue Explant Cultures. *PLOS ONE,* 7**,** e50435.

Gómez-Santos, C., P. Gómez-Abellán, J. A. Madrid, J. J. Hernández-Morante, J. A. Lujan, J. M. Ordovas & M. Garaulet (2009) Circadian Rhythm of Clock Genes in Human Adipose Explants. *Obesity,* 17**,** 1481-1485.

Hatcher, K. M., S. E. Royston & M. M. Mahoney (2020) Modulation of circadian rhythms through estrogen receptor signaling. *European Journal of Neuroscience,* 51**,** 217-228.

Hatori, M., C. Vollmers, A. Zarrinpar, L. DiTacchio, E. A. Bushong, S. Gill, M. Leblanc, A. Chaix, M. Joens, J. A. J. Fitzpatrick, M. H. Ellisman & S. Panda (2012) Time-Restricted Feeding without Reducing Caloric Intake Prevents Metabolic Diseases in Mice Fed a High-Fat Diet. *Cell Metabolism,* 15**,** 848-860.

Herder, C., S. Schneitler, W. Rathmann, B. Haastert, H. Schneitler, H. Winkler, R. Bredahl, E. Hahnloser & S. Martin (2007) Low-Grade Inflammation, Obesity, and Insulin Resistance in Adolescents. *The Journal of Clinical Endocrinology & Metabolism,* 92**,** 4569-4574.

Hertzel, A. V., B. R. Thompson, B. M. Wiczer & D. A. Bernlohr. 2008. CHAPTER 10 - Lipid metabolism in adipose tissue. In *Biochemistry of Lipids, Lipoproteins and Membranes (Fifth Edition),* eds. D. E. Vance & J. E. Vance, 277-304. San Diego: Elsevier.

Hetemäki, N., H. Savolainen-Peltonen, M. J. Tikkanen, F. Wang, H. Paatela, E. Hämäläinen, U. Turpeinen, M. Haanpää, V. Vihma & T. S. Mikkola (2017) Estrogen Metabolism in Abdominal Subcutaneous and Visceral Adipose Tissue in Postmenopausal Women. *The Journal of Clinical Endocrinology & Metabolism,* 102**,** 4588-4595.

Horton, J. D., J. L. Goldstein & M. S. Brown (2002) SREBPs: activators of the complete program of cholesterol and fatty acid synthesis in the liver. *J Clin Invest,* 109**,** 1125-31.

Hutch, C. R. & D. Sandoval (2017) The Role of GLP-1 in the Metabolic Success of Bariatric Surgery. *Endocrinology,* 158**,** 4139-4151.

Ikeda, K., P. Maretich & S. Kajimura (2018) The Common and Distinct Features of Brown and Beige Adipocytes. *Trends in Endocrinology & Metabolism,* 29**,** 191-200.

Inagaki, T., J. Sakai & S. Kajimura (2016) Transcriptional and epigenetic control of brown and beige adipose cell fate and function. *Nat Rev Mol Cell Biol,* 17**,** 480-95.

Iwabu, M., T. Yamauchi, M. Okada-Iwabu, K. Sato, T. Nakagawa, M. Funata, M. Yamaguchi, S. Namiki, R. Nakayama, M. Tabata, H. Ogata, N. Kubota, I. Takamoto, Y. K. Hayashi, N. Yamauchi, H. Waki, M. Fukayama, I. Nishino, K. Tokuyama, K. Ueki, Y. Oike, S. Ishii, K. Hirose, T. Shimizu, K. Touhara & T. Kadowaki (2010) Adiponectin and AdipoR1 regulate PGC-1alpha and mitochondria by Ca(2+) and AMPK/SIRT1. *Nature,* 464**,** 1313-9.

Izquierdo, A. G., A. B. Crujeiras, F. F. Casanueva & M. C. Carreira (2019) Leptin, Obesity, and Leptin Resistance: Where Are We 25 Years Later? *Nutrients,* 11.

Jacob, F., R. Guertler, S. Naim, S. Nixdorf, A. Fedier, N. F. Hacker & V. Heinzelmann-Schwarz (2013) Careful Selection of Reference Genes Is Required for Reliable Performance of RT-qPCR in Human Normal and Cancer Cell Lines. *Plos One,* 8**,** 8.

Jin, X., L. P. Shearman, D. R. Weaver, M. J. Zylka, G. J. De Vries & S. M. Reppert (1999) A molecular mechanism regulating rhythmic output from the suprachiasmatic circadian clock. *Cell,* 96**,** 57-68.

John, S. & C. Hoegerl (2009) Nutritional Deficiencies After Gastric Bypass Surgery. *The Journal of the American Osteopathic Association,* 109**,** 601-604.

Jordan, S. D., A. Kriebs, M. Vaughan, D. Duglan, W. Fan, E. Henriksson, A. L. Huber, S. J. Papp, M. Nguyen, M. Afetian, M. Downes, R. T. Yu, A. Kralli, R. M. Evans & K. A. Lamia (2017) CRY1/2 Selectively Repress PPARδ and Limit Exercise Capacity. *Cell Metab,* 26**,** 243-255.e6.

Kaczmarek, J. L., S. V. Thompson & H. D. Holscher (2017) Complex interactions of circadian rhythms, eating behaviors, and the gastrointestinal microbiota and their potential impact on health. *Nutrition reviews,* 75**,** 673-682.

Kang, S., R. Dahl, W. Hsieh, A. Shin, K. M. Zsebo, C. Buettner, R. J. Hajjar & D. Lebeche (2016) Small Molecular Allosteric Activator of the Sarco/Endoplasmic Reticulum Ca2+-ATPase (SERCA) Attenuates Diabetes and Metabolic Disorders. *J Biol Chem,* 291**,** 5185-98.

Keesler, G. A., F. Camacho, Y. Guo, D. Virshup, C. Mondadori & Z. Yao (2000) Phosphorylation and destabilization of human period I clock protein by human casein kinase Iε. *Neuroreport,* 11**,** 951-955.

Kennaway, D. J., J. A. Owens, A. Voultsios, M. J. Boden & T. J. Varcoe (2007) Metabolic homeostasis in mice with disrupted Clock gene expression in peripheral tissues. *American Journal of Physiology-Regulatory, Integrative and Comparative Physiology,* 293**,** R1528-R1537.

Kershaw, E. E. & J. S. Flier (2004) Adipose Tissue as an Endocrine Organ. *The Journal of Clinical Endocrinology & Metabolism,* 89**,** 2548-2556.

King, L., L. March & A. Anandacoomarasamy (2013) Obesity & osteoarthritis. *Indian Journal of Medical Research,* 138**,** 185-193.

Knutson, K. L., K. Spiegel, P. Penev & E. Van Cauter (2007) The metabolic consequences of sleep deprivation. *Sleep medicine reviews,* 11**,** 163-178.

Kohlgruber, A. & L. Lynch (2015) Adipose Tissue Inflammation in the Pathogenesis of Type 2 Diabetes. *Current Diabetes Reports,* 15**,** 11.

Kriebs, A., S. D. Jordan, E. Soto, E. Henriksson, C. R. Sandate, M. E. Vaughan, A. B. Chan, D. Duglan, S. J. Papp & A.-L. Huber (2017) Circadian repressors CRY1 and CRY2 broadly interact with nuclear receptors and modulate transcriptional activity. *Proceedings of the National Academy of Sciences,* 114**,** 8776-8781.

Kumari, M., E. Badrick, J. Ferrie, A. Perski, M. Marmot & T. Chandola (2009) Self-Reported Sleep Duration and Sleep Disturbance Are Independently Associated with Cortisol Secretion in the Whitehall II Study. *Journal of Clinical Endocrinology & Metabolism,* 94**,** 4801-4809.

Kume, K., M. J. Zylka, S. Sriram, L. P. Shearman, D. R. Weaver, X. Jin, E. S. Maywood, M. H. Hastings & S. M. Reppert (1999) mCRY1 and mCRY2 are essential components of the negative limb of the circadian clock feedback loop. *Cell,* 98**,** 193-205.

Kwon, I., J. Lee, S. H. Chang, N. C. Jung, B. J. Lee, G. H. Son, K. Kim & K. H. Lee (2006) BMAL1 shuttling controls transactivation and degradation of the CLOCK/BMAL1 heterodimer. *Molecular and cellular biology,* 26**,** 7318-7330.

Kwon, Y., H. J. Kim, E. Lo Menzo, S. Park, S. Szomstein & R. J. Rosenthal (2014) Anemia, iron and vitamin B12 deficiencies after sleeve gastrectomy compared to Roux-en-Y gastric bypass: a meta-analysis. *Surg Obes Relat Dis,* 10**,** 589-97.

Lam, V. H., Y. H. Li, X. Liu, K. A. Murphy, J. S. Diehl, R. S. Kwok & J. C. Chiu (2018) CK1α collaborates with DOUBLETIME to regulate PERIOD function in the Drosophila circadian clock. *The Journal of Neuroscience*.

Lamia, K. A., U. M. Sachdeva, L. DiTacchio, E. C. Williams, J. G. Alvarez, D. F. Egan, D. S. Vasquez, H. Juguilon, S. Panda, R. J. Shaw, C. B. Thompson & R. M. Evans (2009) AMPK Regulates the Circadian Clock by Cryptochrome Phosphorylation and Degradation. *Science,* 326**,** 437.

Lamia, K. A., K.-F. Storch & C. J. Weitz (2008) Physiological significance of a peripheral tissue circadian clock. *Proceedings of the national academy of sciences,* 105**,** 15172-15177.

Lazar, D. F. & A. R. Saltiel (2006) Lipid phosphatases as drug discovery targets for type 2 diabetes. *Nat Rev Drug Discov,* 5**,** 333-42.

Leonhardt, W., M. Hanefeld & H. Haller (1978) The adipocyte volume in human adipose tissue: 1. Lipid space, normal and maximum values, and the relation to body weight index. *Int J Obes,* 2**,** 33-45.

Leproult, R., G. Copinschi, O. Buxton & E. VanCauter (1997) Sleep loss results in an elevation of cortisol levels the next evening. *Sleep,* 20**,** 865-870.

Li, P., W. Fan, J. Xu, M. Lu, H. Yamamoto, J. Auwerx, D. D. Sears, S. Talukdar, D. Oh & A. Chen (2011) Adipocyte NCoR knockout decreases PPARγ phosphorylation and enhances PPARγ activity and insulin sensitivity. *Cell,* 147**,** 815-826.

Lizcano, J. M. & D. R. Alessi (2002) The insulin signalling pathway. *Curr Biol,* 12**,** R236-8.

Lobo, S. & D. A. Bernlohr (2007) Fatty acid transport in adipocytes and the development of insulin resistance. *Novartis Found Symp,* 286**,** 113-21; discussion 121-6, 162-3, 196-203.

Longo, C. M. (2014) Bariatric Surgery versus intensive medical therapy in diabetes: results of 3 years. *Revista Clinica Espanola,* 214**,** 417-417.

Longo, V. D. & S. Panda (2016) Fasting, Circadian Rhythms, and Time-Restricted Feeding in Healthy Lifespan. *Cell metabolism,* 23**,** 1048-1059.

Magee, C. A., X. F. Huang, D. C. Iverson & P. Caputi (2009) Acute sleep restriction alters neuroendocrine hormones and appetite in healthy male adults. *Sleep and Biological Rhythms,* 7**,** 125-127.

Mahawar, K. K., A. G. Bhasker, V. Bindal, Y. Graham, U. Dudeja, M. Lakdawala & P. K. Small (2017) Zinc Deficiency after Gastric Bypass for Morbid Obesity: a Systematic Review. *Obes Surg,* 27**,** 522-529.

Makki, K., P. Froguel & I. Wolowczuk (2013) Adipose tissue in obesity-related inflammation and insulin resistance: cells, cytokines, and chemokines. *ISRN Inflamm,* 2013**,** 139239.

Manna, P. & S. K. Jain (2015) Obesity, Oxidative Stress, Adipose Tissue Dysfunction, and the Associated Health Risks: Causes and Therapeutic Strategies. *Metabolic Syndrome and Related Disorders,* 13**,** 423-444.

Mans, E., M. Serra-Prat, E. Palomera, X. Suñol & P. Clavé (2015) Sleeve gastrectomy effects on hunger, satiation, and gastrointestinal hormone and motility responses after a liquid meal test. *Am J Clin Nutr,* 102**,** 540-7.

Martyniak, K. & M. M. Masternak (2017) Changes in adipose tissue cellular composition during obesity and aging as a cause of metabolic dysregulation. *Exp Gerontol,* 94**,** 59-63.

Matsuda, M., B. S. Korn, R. E. Hammer, Y. A. Moon, R. Komuro, J. D. Horton, J. L. Goldstein, M. S. Brown & I. Shimomura (2001) SREBP cleavage-activating protein (SCAP) is required for increased lipid synthesis in liver induced by cholesterol deprivation and insulin elevation. *Genes Dev,* 15**,** 1206-16.

McGown, C., A. Birerdinc & Z. M. Younossi (2014) Adipose Tissue as an Endocrine Organ. *Clinics in Liver Disease,* 18**,** 41-58.

McNamara, P., S.-b. Seo, R. D. Rudic, A. Sehgal, D. Chakravarti & G. A. FitzGerald (2001) Regulation of CLOCK and MOP4 by nuclear hormone receptors in the vasculature: a humoral mechanism to reset a peripheral clock. *Cell,* 105**,** 877-889.

Mehta, R., A. Birerdinc, N. Hossain, A. Afendy, V. Chandhoke, Z. Younossi & A. Baranova (2010) Validation of endogenous reference genes for qRT-PCR analysis of human visceral adipose samples. *BMC Molecular Biology,* 11**,** 39-39.

Mendoza, M. C., E. E. Er & J. Blenis (2011) The Ras-ERK and PI3K-mTOR pathways: cross-talk and compensation. *Trends Biochem Sci,* 36**,** 320-8.

Meng, Q. J., A. McMaster, S. Beesley, W. Q. Lu, J. Gibbs, D. Parks, J. Collins, S. Farrow, R. Donn & D. Ray (2008) Ligand modulation of REV-ERBα function resets the peripheral circadian clock in a phasic manner. *Journal of cell science,* 121**,** 3629-3635.

Miller, M. A. & F. P. Cappuccio (2007) Inflammation, sleep, obesity and cardiovascular disease. *Current vascular pharmacology,* 5**,** 93-102.

Min, T., S. L. Prior, R. Churm, G. Dunseath, J. D. Barry & J. W. Stephens (2020) Effect of Laparoscopic Sleeve Gastrectomy on Static and Dynamic Measures of Glucose Homeostasis and Incretin Hormone Response 4-Years Post-Operatively. *Obesity Surgery,* 30**,** 46-55.

Miyamoto, J., R. Ohue-Kitano, H. Mukouyama, A. Nishida, K. Watanabe, M. Igarashi, J. Irie, G. Tsujimoto, N. Satoh-Asahara, H. Itoh & I. Kimura (2019) Ketone body receptor GPR43 regulates lipid metabolism under ketogenic conditions. *Proceedings of the National Academy of Sciences,* 116**,** 23813.

Monteiro, R. & I. Azevedo (2010) Chronic inflammation in obesity and the metabolic syndrome. *Mediators Inflamm,* 2010.

Morigny, P., M. Houssier, E. Mouisel & D. Langin (2016) Adipocyte lipolysis and insulin resistance. *Biochimie,* 125**,** 259-66.

Mottillo, E. P., V. D. Ramseyer & J. G. Granneman (2018) SERCA2b Cycles Its Way to UCP1-Independent Thermogenesis in Beige Fat. *Cell Metabolism,* 27**,** 7-9.

Muir, L. A., N. A. Baker, A. R. Washabaugh, C. K. Neeley, C. G. Flesher, J. B. DelProposto, L. M. Geletka, A. A. Ghaferi, J. F. Finks, K. Singer, O. A. Varban, C. N. Lumeng & R. W. O'Rourke (2017) Adipocyte hypertrophy-hyperplasia balance contributes to weight loss after bariatric surgery. *Adipocyte,* 6**,** 134-140.

Muratani, M. & W. P. Tansey (2003) How the ubiquitin–proteasome system controls transcription. *Nature reviews Molecular cell biology,* 4**,** 192-201.

Naimark, A. & R. M. Cherniack (1960) Compliance of the respiratory system and its components in health and obesity. *J Appl Physiol,* 15**,** 377-82.

Nakahata, Y., M. Kaluzova, B. Grimaldi, S. Sahar, J. Hirayama, D. Chen, L. P. Guarente & P. Sassone-Corsi (2008) The NAD+-dependent deacetylase SIRT1 modulates CLOCK-mediated chromatin remodeling and circadian control. *Cell,* 134**,** 329-40.

Neovius, M., G. Bruze, P. Jacobson, K. Sjöholm, K. Johansson, F. Granath, J. Sundström, I. Näslund, C. Marcus, J. Ottosson, M. Peltonen & L. M. S. Carlsson (2018) Risk of suicide and non-fatal self-harm after bariatric surgery: results from two matched cohort studies. *Lancet Diabetes Endocrinol,* 6**,** 197-207.

Newton, A. C. & L. C. Trotman (2014) Turning off AKT: PHLPP as a drug target. *Annu Rev Pharmacol Toxicol,* 54**,** 537-58.

Nikolaeva, S., S. Pradervand, G. Centeno, V. Zavadova, N. Tokonami, M. Maillard, O. Bonny & D. Firsov (2012) The circadian clock modulates renal sodium handling. *Journal of the American Society of Nephrology,* 23**,** 1019-1026.

Nishimura, S., I. Manabe, M. Nagasaki, K. Eto, H. Yamashita, M. Ohsugi, M. Otsu, K. Hara, K. Ueki, S. Sugiura, K. Yoshimura, T. Kadowaki & R. Nagai (2009) CD8+ effector T cells contribute to macrophage recruitment and adipose tissue inflammation in obesity. *Nat Med,* 15**,** 914-20.

Nunes, J., G. Jean-Louis, F. Zizi, G. J. Casimir, H. von Gizycki, C. D. Brown & S. I. McFarlane (2008) Sleep duration among black and white Americans: Results of the National Health Interview Survey. *Journal of the National Medical Association,* 100**,** 317-322.

O'Sullivan, T. E., M. Rapp, X. Fan, O. E. Weizman, P. Bhardwaj, N. M. Adams, T. Walzer, A. J. Dannenberg & J. C. Sun (2016) Adipose-Resident Group 1 Innate Lymphoid Cells Promote Obesity-Associated Insulin Resistance. *Immunity,* 45**,** 428-41.

Ogden, C. L., M. D. Carroll, B. K. Kit & K. M. Flegal (2014) Prevalence of Childhood and Adult Obesity in the United States, 2011-2012. *Jama-Journal of the American Medical Association,* 311**,** 806-814.

Osland, E., R. M. Yunus, S. Khan, B. Memon & M. A. Memon (2017) Diabetes improvement and resolution following laparoscopic vertical sleeve gastrectomy (LVSG) versus laparoscopic Roux-en-Y gastric bypass (LRYGB) procedures: a systematic review of randomized controlled trials. *Surg Endosc,* 31**,** 1952-1963.

Ouyang, Y., C. R. Andersson, T. Kondo, S. S. Golden & C. H. Johnson (1998) Resonating circadian clocks enhance fitness in cyanobacteria. *Proceedings of the National Academy of Sciences of the United States of America,* 95**,** 8660-8664.

Pacini, G. & R. N. Bergman (1986) MINMOD - A COMPUTER-PROGRAM TO CALCULATE INSULIN SENSITIVITY AND PANCREATIC RESPONSIVITY FROM THE FREQUENTLY SAMPLED INTRAVENOUS GLUCOSE-TOLERANCE TEST. *Computer Methods and Programs in Biomedicine,* 23**,** 113-122.

Panda, S., J. B. Hogenesch & S. A. Kay (2002) Circadian rhythms from flies to human. *Nature,* 417**,** 329.

Park, D., J. A. Spencer, B. I. Koh, T. Kobayashi, J. Fujisaki, T. L. Clemens, C. P. Lin, H. M. Kronenberg & D. T. Scadden (2012) Endogenous bone marrow MSCs are dynamic, fate-restricted participants in bone maintenance and regeneration. *Cell Stem Cell,* 10**,** 259-72.

Park, J., D. M. Euhus & P. E. Scherer (2011) Paracrine and endocrine effects of adipose tissue on cancer development and progression. *Endocr Rev,* 32**,** 550-70.

Park, Y. M. (2014) CD36, a scavenger receptor implicated in atherosclerosis. *Experimental & Molecular Medicine,* 46**,** e99-e99.

Patel, S. A., N. Velingkaar, K. Makwana, A. Chaudhari & R. Kondratov (2016) Calorie restriction regulates circadian clock gene expression through BMAL1 dependent and independent mechanisms. *Scientific reports,* 6**,** 25970.

Peppard, P. E., T. Young, M. Palta, J. Dempsey & J. Skatrud (2000) Longitudinal Study of Moderate Weight Change and Sleep-Disordered Breathing. *JAMA,* 284**,** 3015-3021.

Peterli, R., R. E. Steinert, B. Woelnerhanssen, T. Peters, C. Christoffel-Courtin, M. Gass, B. Kern, M. von Fluee & C. Beglinger (2012) Metabolic and Hormonal Changes After Laparoscopic Roux-en-Y Gastric Bypass and Sleeve Gastrectomy: a Randomized, Prospective Trial. *Obesity Surgery,* 22**,** 740-748.

Phillips, S. A., T. P. Ciaraldi, D. K. Oh, M. K. Savu & R. R. Henry (2008) Adiponectin secretion and response to pioglitazone is depot dependent in cultured human adipose tissue. *American journal of physiology. Endocrinology and metabolism,* 295**,** E842-E850.

Pischon, T. & K. Nimptsch (2016) Obesity and Risk of Cancer: An Introductory Overview. *Recent Results Cancer Res,* 208**,** 1-15.

Pittendrigh, C. S. (1954) ON TEMPERATURE INDEPENDENCE IN THE CLOCK SYSTEM CONTROLLING EMERGENCE TIME IN DROSOPHILA. *Proceedings of the National Academy of Sciences of the United States of America,* 40**,** 1018-1029.

Pivovarova, O., Ö. Gögebakan, S. Sucher, J. Groth, V. Murahovschi, K. Kessler, M. Osterhoff, N. Rudovich, A. Kramer & A. F. Pfeiffer (2016) Regulation of the clock gene expression in human adipose tissue by weight loss. *International Journal of Obesity,* 40**,** 899-906.

Prachand, V. N., R. T. DaVee & J. C. Alverdy (2006) Duodenal switch provides superior weight loss in the super-obese (BMI >= 50kg/m(2)) compared with gastric bypass. *Annals of Surgery,* 244**,** 611-619.

Quail, D. F. & A. J. Dannenberg (2019) The obese adipose tissue microenvironment in cancer development and progression. *Nature Reviews Endocrinology,* 15**,** 139-154.

Radonić, A., S. Thulke, I. M. Mackay, O. Landt, W. Siegert & A. Nitsche (2004) Guideline to reference gene selection for quantitative real-time PCR. *Biochemical and Biophysical Research Communications,* 313**,** 856-862.

Radziuk, J. M. (2013) The suprachiasmatic nucleus, circadian clocks, and the liver. *Diabetes,* 62**,** 1017-1019.

Ramadan, M., M. Loureiro, K. Laughlan, R. Caiazzo, A. Iannelli, L. Brunaud, S. Czernichow, M. Nedelcu & D. Nocca (2016) Risk of Dumping Syndrome after Sleeve Gastrectomy and Roux-en-Y Gastric Bypass: Early Results of a Multicentre Prospective Study. *Gastroenterol Res Pract,* 2016**,** 2570237.

Ripperger, J. A., L. P. Shearman, S. M. Reppert & U. Schibler (2000) CLOCK, an essential pacemaker component, controls expression of the circadian transcription factor DBP. *Genes & development,* 14**,** 679-689.

Rogers, P. M., N. Mashtalir, M. A. Rathod, O. Dubuisson, Z. Wang, K. Dasuri, S. Babin, A. Gupta, N. Markward, W. T. Cefalu & N. V. Dhurandhar (2008) Metabolically favorable remodeling of human adipose tissue by human adenovirus type 36. *Diabetes,* 57**,** 2321-2331.

Romero-Corral, A., S. M. Caples, F. Lopez-Jimenez & V. K. Somers (2010) Interactions between obesity and obstructive sleep apnea: implications for treatment. *Chest,* 137**,** 711-9.

Rosen, E. D. & B. M. Spiegelman (2006) Adipocytes as regulators of energy balance and glucose homeostasis. *Nature,* 444**,** 847-53.

Rothschild, J., K. K. Hoddy, P. Jambazian & K. A. Varady (2014) Time-restricted feeding and risk of metabolic disease: a review of human and animal studies. *Nutrition Reviews,* 72**,** 308-318.

Rubinow, K. B. (2018) An intracrine view of sex steroids, immunity, and metabolic regulation. *Mol Metab,* 15**,** 92-103.

Rudic, R. D., P. McNamara, A.-M. Curtis, R. C. Boston, S. Panda, J. B. Hogenesch & G. A. FitzGerald (2004) BMAL1 and CLOCK, Two Essential Components of the Circadian Clock, Are Involved in Glucose Homeostasis. *PLOS Biology,* 2**,** e377.

Rui, L. (2014) Energy metabolism in the liver. *Compr Physiol,* 4**,** 177-97.

Rutter, J., M. Reick, L. C. Wu & S. L. McKnight (2001) Regulation of clock and NPAS2 DNA binding by the redox state of NAD cofactors. *Science,* 293**,** 510-4.

Sakurai, T. (2007) The neural circuit of orexin (hypocretin): maintaining sleep and wakefulness. *Nature Reviews Neuroscience,* 8**,** 171-181.

Salans, L. B., J. L. Knittle & J. Hirsch (1968) The role of adipose cell size and adipose tissue insulin sensitivity in the carbohydrate intolerance of human obesity. *The Journal of Clinical Investigation,* 47**,** 153-165.

Saltiel, A. R. & J. E. Pessin (2002) Insulin signaling pathways in time and space. *Trends in Cell Biology,* 12**,** 65-71.

SCHMID, S. M., M. HALLSCHMID, K. JAUCH-CHARA, J. BORN & B. SCHULTES (2008) A single night of sleep deprivation increases ghrelin levels and feelings of hunger in normal-weight healthy men. *Journal of Sleep Research,* 17**,** 331-334.

Schwab, R. J., M. Pasirstein, R. Pierson, A. Mackley, R. Hachadoorian, R. Arens, G. Maislin & A. I. Pack (2003) Identification of upper airway anatomic risk factors for obstructive sleep apnea with volumetric magnetic resonance imaging. *Am J Respir Crit Care Med,* 168**,** 522-30.

Shan, T., X. Liang, P. Bi, P. Zhang, W. Liu & S. Kuang (2013) Distinct populations of adipogenic and myogenic Myf5-lineage progenitors in white adipose tissues. *J Lipid Res,* 54**,** 2214-24.

Shan, Z., H. Ma, M. Xie, P. Yan, Y. Guo, W. Bao, Y. Rong, C. L. Jackson, F. B. Hu & L. Liu (2015) Sleep Duration and Risk of Type 2 Diabetes: A Meta-analysis of Prospective Studies. *Diabetes Care,* 38**,** 529.

Shearman, L. P., S. Sriram, D. R. Weaver, E. S. Maywood, I. Chaves, B. Zheng, K. Kume, C. C. Lee, M. H. Hastings & S. M. Reppert (2000) Interacting molecular loops in the mammalian circadian clock. *Science,* 288**,** 1013-1019.

Shelton, K. E., H. Woodson, S. Gay & P. M. Suratt (1993) Pharyngeal fat in obstructive sleep apnea. *Am Rev Respir Dis,* 148**,** 462-6.

Shi, X., S. Karmali, A. M. Sharma & D. W. Birch (2010) A review of laparoscopic sleeve gastrectomy for morbid obesity. *Obesity surgery,* 20**,** 1171-1177.

Shimano, H. & R. Sato (2017) SREBP-regulated lipid metabolism: convergent physiology — divergent pathophysiology. *Nature Reviews Endocrinology,* 13**,** 710-730.

Singhal, A. (2005) Endothelial dysfunction: role in obesity-related disorders and the early origins of CVD. *Proceedings of the Nutrition Society,* 64**,** 15-22.

Sjöström, L., A. Gummesson, C. D. Sjöström, K. Narbro, M. Peltonen, H. Wedel, C. Bengtsson, C. Bouchard, B. Carlsson, S. Dahlgren, P. Jacobson, K. Karason, J. Karlsson, B. Larsson, A. K. Lindroos, H. Lönroth, I. Näslund, T. Olbers, K. Stenlöf, J. Torgerson & L. M. Carlsson (2009) Effects of bariatric surgery on cancer incidence in obese patients in Sweden (Swedish Obese Subjects Study): a prospective, controlled intervention trial. *Lancet Oncol,* 10**,** 653-62.

Smith, R. E., Jr. (2010) The clinical and economic burden of anemia. *Am J Manag Care,* 16 Suppl Issues**,** S59-66.

Solt, L. A., D. J. Kojetin & T. P. Burris (2011) The REV-ERBs and RORs: molecular links between circadian rhythms and lipid homeostasis. *Future medicinal chemistry,* 3**,** 623-638.

Spiegel, K., K. Knutson, R. Leproult, E. Tasali & E. Van Cauter (2005) Sleep loss: a novel risk factor for insulin resistance and Type 2 diabetes. *Journal of Applied Physiology,* 99**,** 2008-2019.

Spiegel, K., R. Leproult, M. L'Hermite-Baleriaux, G. Copinschi, P. D. Penev & E. Van Cauter (2004) Leptin levels are dependent on sleep duration: Relationships with sympathovagal balance, carbohydrate regulation, cortisol, and thyrotropin. *Journal of Clinical Endocrinology & Metabolism,* 89**,** 5762-5771.

Spittal, M. J. & G. Frühbeck (2018) Bariatric surgery: many benefits, but emerging risks. *The Lancet Diabetes & Endocrinology,* 6**,** 161-163.

Spoelstra, K., M. Wikelski, S. Daan, A. S. I. Loudon & M. Hau (2016) Natural selection against a circadian clock gene mutation in mice. *Proceedings of the National Academy of Sciences,* 113**,** 686.

Steinberg, G. R. & D. Carling (2019) AMP-activated protein kinase: the current landscape for drug development. *Nature Reviews Drug Discovery,* 18**,** 527-551.

Steinert, R. E., R. Peterli, S. Keller, A. C. Meyer-Gerspach, J. Drewe, T. Peters & C. Beglinger (2013) Bile acids and gut peptide secretion after bariatric surgery: A 1-year prospective randomized pilot trial. *Obesity,* 21**,** E660-E668.

Stenberg, E., Y. Cao, R. Marsk, M. Sundbom, T. Jernberg & E. Näslund (2020) Association between metabolic surgery and cardiovascular outcome in patients with hypertension: A nationwide matched cohort study. *PLoS Med,* 17**,** e1003307.

Stroh, C., T. Manger & F. Benedix (2017) Metabolic surgery and nutritional deficiencies. *Minerva Chir,* 72**,** 432-441.

Strzyz, P. (2020) NAD+ keeps the clock young. *Nature Reviews Molecular Cell Biology,* 21**,** 360-361.

Sturniolo, G. C., M. C. Montino, L. Rossetto, A. Martin, R. D'Inca, A. D'Odorico & R. Naccarato (1991) Inhibition of gastric acid secretion reduces zinc absorption in man. *J Am Coll Nutr,* 10**,** 372-5.

Sztalryd, C. & D. L. Brasaemle (2017) The perilipin family of lipid droplet proteins: Gatekeepers of intracellular lipolysis. *Biochim Biophys Acta Mol Cell Biol Lipids,* 1862**,** 1221-1232.

Taheri, S., L. Lin, D. Austin, T. Young & E. Mignot (2004) Short sleep duration is associated with reduced leptin, elevated ghrelin, and increased body mass index. *Plos Medicine,* 1**,** 210-217.

Takahashi, J. S. (2017) Transcriptional architecture of the mammalian circadian clock. *Nature reviews. Genetics,* 18**,** 164-179.

Takeda, Y., H. S. Kang, M. Angers & A. M. Jetten (2011) Retinoic acid-related orphan receptor γ directly regulates neuronal PAS domain protein 2 transcription in vivo. *Nucleic acids research,* 39**,** 4769-4782.

Thomas Svava, N., J. Niels, L. J. Jens Otto, M. Niels & L. Sten (2014) Dissecting adipose tissue lipolysis: molecular regulation and implications for metabolic disease. *Journal of Molecular Endocrinology,* 52**,** R199-R222.

Tiwari, P., A. Blank, C. Cui, K. Q. Schoenfelt, G. Zhou, Y. Xu, G. Khramtsova, F. Olopade, A. M. Shah, S. A. Khan, M. R. Rosner & L. Becker (2019) Metabolically activated adipose tissue macrophages link obesity to triple-negative breast cancer. *J Exp Med,* 216**,** 1345-1358.

Travnickova-Bendova, Z., N. Cermakian, S. M. Reppert & P. Sassone-Corsi (2002) Bimodal regulation of mPeriod promoters by CREB-dependent signaling and CLOCK/BMAL1 activity. *Proceedings of the National Academy of Sciences,* 99**,** 7728-7733.

Trogdon, J. G., E. A. Finkelstein, T. Hylands, P. S. Dellea & S. J. Kamal-Bahl (2008) Indirect costs of obesity: a review of the current literature. *Obes Rev,* 9**,** 489-500.

Turek, F. W., C. Joshu, A. Kohsaka, E. Lin, G. Ivanova, E. McDearmon, A. Laposky, S. Losee-Olson, A. Easton, D. R. Jensen, R. H. Eckel, J. S. Takahashi & J. Bass (2005) Obesity and metabolic syndrome in circadian Clock mutant mice. *Science (New York, N.Y.),* 308**,** 1043-1045.

Um, J. H., S. Yang, S. Yamazaki, H. Kang, B. Viollet, M. Foretz & J. H. Chung (2007) Activation of 5'-AMP-activated kinase with diabetes drug metformin induces casein kinase Iepsilon (CKIepsilon)-dependent degradation of clock protein mPer2. *J Biol Chem,* 282**,** 20794-8.

Unick, J. L., D. Beavers, D. S. Bond, J. M. Clark, J. M. Jakicic, A. E. Kitabchi, W. C. Knowler, T. A. Wadden, L. E. Wagenknecht & R. R. Wing (2013) The long-term effectiveness of a lifestyle intervention in severely obese individuals. *The American journal of medicine,* 126**,** 236-242. e2.

Valadan, R., O. Amjadi, M. Tehrani, A. Rafiei, A. Hedayatizadeh-Omran & R. Alizadeh-Navaei (2015) Pseudogene-free amplification of HPRT1 in quantitative reverse transcriptase polymerase chain reaction. *Analytical Biochemistry,* 485**,** 46-48.

van Baak, M. A. & E. C. Mariman (2019) Mechanisms of weight regain after weight loss—the role of adipose tissue. *Nature Reviews Endocrinology,* 15**,** 274-287.

Van Cauter, E., K. Spiegel, E. Tasali & R. Leproult (2008) Metabolic consequences of sleep and sleep loss. *Sleep medicine,* 9 Suppl 1**,** S23-S28.

Van Der Horst, G. T., M. Muijtjens, K. Kobayashi, R. Takano, S.-i. Kanno, M. Takao, J. de Wit, A. Verkerk, A. P. Eker & D. van Leenen (1999) Mammalian Cry1 and Cry2 are essential for maintenance of circadian rhythms. *Nature,* 398**,** 627-630.

Vandesompele, J., K. De Preter, F. Pattyn, B. Poppe, N. Van Roy, A. De Paepe & F. Speleman (2002a) Accurate normalization of real-time quantitative RT-PCR data by geometric averaging of multiple internal control genes. *Genome biology,* 3**,** RESEARCH0034-RESEARCH0034.

--- (2002b) Accurate normalization of real-time quantitative RT-PCR data by geometric averaging of multiple internal control genes. *Genome Biology,* 3**,** research0034.1.

Varela, L. & T. L. Horvath (2012) AgRP neurons: a switch between peripheral carbohydrate and lipid utilization. *The EMBO Journal,* 31**,** 4252-4254.

Vieira, E., E. C. Nilsson, A. Nerstedt, M. Ormestad, Y. C. Long, P. M. Garcia-Roves, J. R. Zierath & M. Mahlapuu (2008) Relationship between AMPK and the transcriptional balance of clock-related genes in skeletal muscle. *Am J Physiol Endocrinol Metab,* 295**,** E1032-7.

Vielhaber, E., E. Eide, A. Rivers, Z.-H. Gao & D. M. Virshup (2000) Nuclear entry of the circadian regulator mPER1 is controlled by mammalian casein kinase I ε. *Molecular and cellular biology,* 20**,** 4888-4899.

Vitaterna, M. H., C. P. Selby, T. Todo, H. Niwa, C. Thompson, E. M. Fruechte, K. Hitomi, R. J. Thresher, T. Ishikawa & J. Miyazaki (1999) Differential regulation of mammalian period genes and circadian rhythmicity by cryptochromes 1 and 2. *Proceedings of the National Academy of Sciences,* 96**,** 12114-12119.

Wadden, T. A., M. L. Butryn & C. Wilson (2007) Lifestyle modification for the management of obesity. *Gastroenterology,* 132**,** 2226-2238.

Wang, H., L. Shen, X. Sun, F. Liu, W. Feng, C. Jiang, X. Chu, X. Ye, C. Jiang, Y. Wang, P. Zhang, M. Zang, D. Zhu & Y. Bi (2019) Adipose group 1 innate lymphoid cells promote adipose tissue fibrosis and diabetes in obesity. *Nature Communications,* 10**,** 3254.

Wang, X., T. You, K. Murphy, M. F. Lyles & B. J. Nicklas (2015) Addition of Exercise Increases Plasma Adiponectin and Release from Adipose Tissue. *Medicine and science in sports and exercise,* 47**,** 2450-2455.

Wang, Y., P. M. Nishina & J. K. Naggert (2009) Degradation of IRS1 leads to impaired glucose uptake in adipose tissue of the type 2 diabetes mouse model TALLYHO/Jng. *J Endocrinol,* 203**,** 65-74.

Weiss, E. C., D. A. Galuska, L. K. Khan, C. Gillespie & M. K. Serdula (2007) Weight regain in US adults who experienced substantial weight loss, 1999–2002. *American journal of preventive medicine,* 33**,** 34-40.

Wheaton, A. G., Y. Liu, G. S. Perry & J. B. Croft (2011) Effect of Short Sleep Duration on Daily Activities-United States, 2005-2008 (Reprinted from MMWR, vol 60, pg 239-242, 2011). *Jama-Journal of the American Medical Association,* 305**,** 1956-1958.

White, J. M., M. J. Piron, V. R. Rangaraj, E. C. Hanlon, R. N. Cohen & M. J. Brady (2020) Reference Gene Optimization for Circadian Gene Expression Analysis in Human Adipose Tissue. *J Biol Rhythms,* 35**,** 84-97.

Wolk, R., S. M. Shamsuzzaman Abu & K. Somers Virend (2003) Obesity, Sleep Apnea, and Hypertension. *Hypertension,* 42**,** 1067-1074.

Wu, H., S. Ghosh, X. D. Perrard, L. Feng, G. E. Garcia, J. L. Perrard, J. F. Sweeney, L. E. Peterson, L. Chan, C. W. Smith & C. M. Ballantyne (2007) T-cell accumulation and regulated on activation, normal T cell expressed and secreted upregulation in adipose tissue in obesity. *Circulation,* 115**,** 1029-38.

Wu, Q., A. M. Ortegon, B. Tsang, H. Doege, K. R. Feingold & A. Stahl (2006) FATP1 Is an Insulin-Sensitive Fatty Acid Transporter Involved in Diet-Induced Obesity. *Molecular and Cellular Biology,* 26**,** 3455.

Wu, Y., M. A. Kinnebrew, V. I. Kutyavin & A. Chawla (2020) Distinct signaling and transcriptional pathways regulate peri-weaning development and cold-induced recruitment of beige adipocytes. *Proceedings of the National Academy of Sciences,* 117**,** 6883.

Wu, Y. C., M. Zhu & D. M. Robertson (2012) Novel nuclear localization and potential function of insulin-like growth factor-1 receptor/insulin receptor hybrid in corneal epithelial cells. *PLoS One,* 7**,** e42483.

Yamaguchi, S., S. Mitsui, L. Yan, K. Yagita, S. Miyake & H. Okamura (2000) Role of DBP in the circadian oscillatory mechanism. *Molecular and cellular biology,* 20**,** 4773-4781.

Yamajuku, D., Y. Shibata, M. Kitazawa, T. Katakura, H. Urata, T. Kojima, S. Takayasu, O. Nakata & S. Hashimoto (2011) Cellular DBP and E4BP4 proteins are critical for determining the period length of the circadian oscillator. *FEBS letters,* 585**,** 2217-2222.

Yang, X., M. Downes, T. Y. Ruth, A. L. Bookout, W. He, M. Straume, D. J. Mangelsdorf & R. M. Evans (2006) Nuclear receptor expression links the circadian clock to metabolism. *Cell,* 126**,** 801-810.

Ye, R., T. Onodera & P. E. Scherer (2019) Lipotoxicity and β Cell Maintenance in Obesity and Type 2 Diabetes. *Journal of the Endocrine Society,* 3**,** 617-631.

Zhao, X., H. Cho, T. Y. Ruth, A. R. Atkins, M. Downes & R. M. Evans (2014) Nuclear receptors rock around the clock. *EMBO reports,* 15**,** 518-528.

Zheng, B., D. W. Larkin, U. Albrecht, Z. S. Sun, M. Sage, G. Eichele, C. C. Lee & A. Bradley (1999) The mPer2 gene encodes a functional component of the mammalian circadian clock. *Nature,* 400**,** 169-173.

Zvonic, S., A. A. Ptitsyn, S. A. Conrad, L. K. Scott, Z. E. Floyd, G. Kilroy, X. Wu, B. C. Goh, R. L. Mynatt & J. M. Gimble (2006) Characterization of peripheral circadian clocks in adipose tissues. *Diabetes,* 55**,** 962-970.